PROJECT ADMINISTRATION DATA SHEET

[x] ORIGINAL [ ] REVISION NO. _____

oject No. A-3157 DATE 6/28/82

oject Director: R. N. Trebits ~~School~~/Lab RAIL/RAD

ponsor: General Electric Co., Armament Systems Dept., VT

ype Agreement: Purchase Order No. 024-SJ350K

ward Period: From 2/2/82 To 6/15/82 (Performance) _____ (Reports)

ponsor Amount: $47,745 Contracted through:

ost Sharing: None ~~GTRI~~/GIT

itle: Performance Evaluation of AN/VP-2 Radar for Light DIVADS Utilization - Task II

ADMINISTRATIVE DATA

OCA Contact William F. Brown x4820

1) Sponsor Technical Contact:

Mr. E. R. Carlson
Aircraft Equipment Div.
General Electric Co.
Armament Sys. Dept.
Burlington, VT 05402
(802) 657-7224

2) Sponsor Admin/Contractual Matters:

Mr. G. D. Baron, Buyer
General Electric Co.
Armament Sys. Dept.
Burlington, VT 05402
(802) 657-6676

Defense Priority Rating: none

Security Classification: none

RESTRICTIONS

See Attached - Supplemental Information Sheet for Additional Requirements.

Travel: Foreign travel must have prior approval — Contact OCA in each case. Domestic travel requires sponsor approval where total will exceed greater of $500 or 125% of approved proposal budget category.

Equipment: Title vests with none proposed or anticipated

COMMENTS:

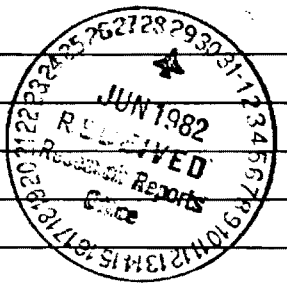

COPIES TO:

Administrative Coordinator
Research Property Management
Accounting
Procurement/EES Supply Services
Research Security Services
Reports Coordinator (OCA)
~~Legal Services (OCA)~~
Library
EES Public Relations (2)
~~Computer Input~~
Project File
Other GTRI

FORM OCA 4:781

GEORGIA INSTITUTE OF TECHNOLOGY OFFICE OF CONTRACT ADMINISTRATION

SPONSORED PROJECT TERMINATION SHEET

Date 8/3/82

Project Title: Performance Evaluation of the AN/VPS-2 Radar For Light DIVIDS Utilization - Task II
Project No: A-3157

Project Director: R.N. Trebits

Sponsor: General Electric Co., Armament Sys. Dept., VT

Effective Termination Date: 6/15/82

Clearance of Accounting Charges: 6/15/82

Grant/Contract Closeout Actions Remaining:

- [x] Final Invoice ~~and Closing Documents~~
- [ ] Final Fiscal Report
- [ ] Final Report of Inventions
- [ ] Govt. Property Inventory & Related Certificate
- [ ] Classified Material Certificate
- [ ] Other _____

Assigned to: RAIL/RAD (~~School~~/Laboratory)

COPIES TO:

Administrative Coordinator	Research Security Services	EES Public Relations (2)
Research Property Management	~~Reports Coordinator~~ (OCA)	Computer Input
Accounting	Legal Services (OCA)	Project File
Procurement/EES Supply Services	Library	Other _____

ENGINEERING EXPERIMENT STATION
Georgia Institute of Technology
A Unit of the University System of Georgia
Atlanta, Georgia 30332

February 22, 1982

General Electric
Armament Systems Department
Lakeside Avenue
Burlington, Vermont 05401

Attention: Mr. Ernie Carlson

Dear Mr. Carlson:

Georgia Tech was tasked to determine the detection performance of the VPS-2 range tracking radar modified for continuous 360 degree search over a 30 degree elevation sector. The Georgia Tech RANGE computer program was utilized to compute the maximum detection range of the VPS-2, with antenna, transmitter, and receiver head end "as is," but in a full scanning mode. Pertinent radar system parameters and designated operational parameters were obtained from the radar manufacturer and General Electric, respectively.

The output of this task is a set of detection probabilities versus range for a scanning VPS-2 radar and a 1 square meter cross section aircraft approaching the radar at constant altitude. Probability of detection is plotted versus range in the accompanying figures, depicting radar detection performance for two aircraft altitudes, two range offsets, and clear air/4 mm/hr rainfall conditions. Maximally efficient signal integration in the radar signal processor during the dwell time of the antenna beam on the aircraft was assumed. In addition, a trapezoidal MTI response function was assumed, with no signal processing loss within the MTI passband. Only the lowest position antenna beam performance was addressed, in a benign multipath interference environment.

The figures indicate a free space detection range of approximately 9 kilometers, as shown in the top graph of each figure. Detection criteria are 90 percent probability of detection and 10^{-6} false alarm rate. The first set of four figures depicts detection performance against an aircraft approaching the radar straight ahead, at a constant 100 foot altitude. In clear air the detection range is 7 to 10 kilometers, where the plateau of the detection curve is a manifestation of multipath interference. A rainfall rate of 4 mm/hr does not significantly degrade detection performance at these ranges. Aircraft approaching within 600 lateral feet lateral displacement of the radar location are detected at virtually the same range as when approaching head on.

The second set of figures depicts detection probability versus range for an aircraft altitude of 500 feet. Comparison with the previous set of figures demonstrates that at the higher aircraft altitude multipath interference is no longer significant. The clear air detection range is approximately 8-1/2 kilometers, and the aircraft exits the lowest antenna elevation beamwidth at approximately 1-1/2 kilometers. 4 mm/hr rainfall does not have a significant impact on detection performance at these ranges. Aircraft approaches within 600 feet of the radar location do not noticeably alter the detection performance from the straight-on cases.

To assess the possibility of achieving the desired 15 kilometer detection range, Georgia Tech recommends computation of detection performance for a modified VPS-2 system. Realistic changes in radar parameters should include at least the following:

1. Higher peak transmitter power or duty factor (increased average power)
2. Fan beam antenna elevation pattern
3. Staggered pulse repetition rate
4. Specific detection and signal processing algorithms
5. Slower azimuthal antenna scan rate
6. Improved front end noise figure

A staggered pulse repetition rate will be required to extend the detection range to 15 kilometers. The maximum unambigious range of the production VPS-2 is 7.5 kilometers, and the first aircraft blind speed is approximately 300 m/sec. Straightforward halving of the pulse repetition rate to double the maximum unambiguious range would have the undesirable effect of also halving the first blind speed. Staggering the pulse repetition rate will extend both the detection range and blind speeds to acceptable values.

Georgia Tech recommends that General Electric authorize work on Task 2 of our Proposal RI-RAD-1213, dated 29 January 1982. Task 2 will extend the aircraft detection performance analysis to include potential optimization of radar parameters for the General Electric application.

Respectfully submitted,

Robert N. Trebits
Project Director

RNT/ss

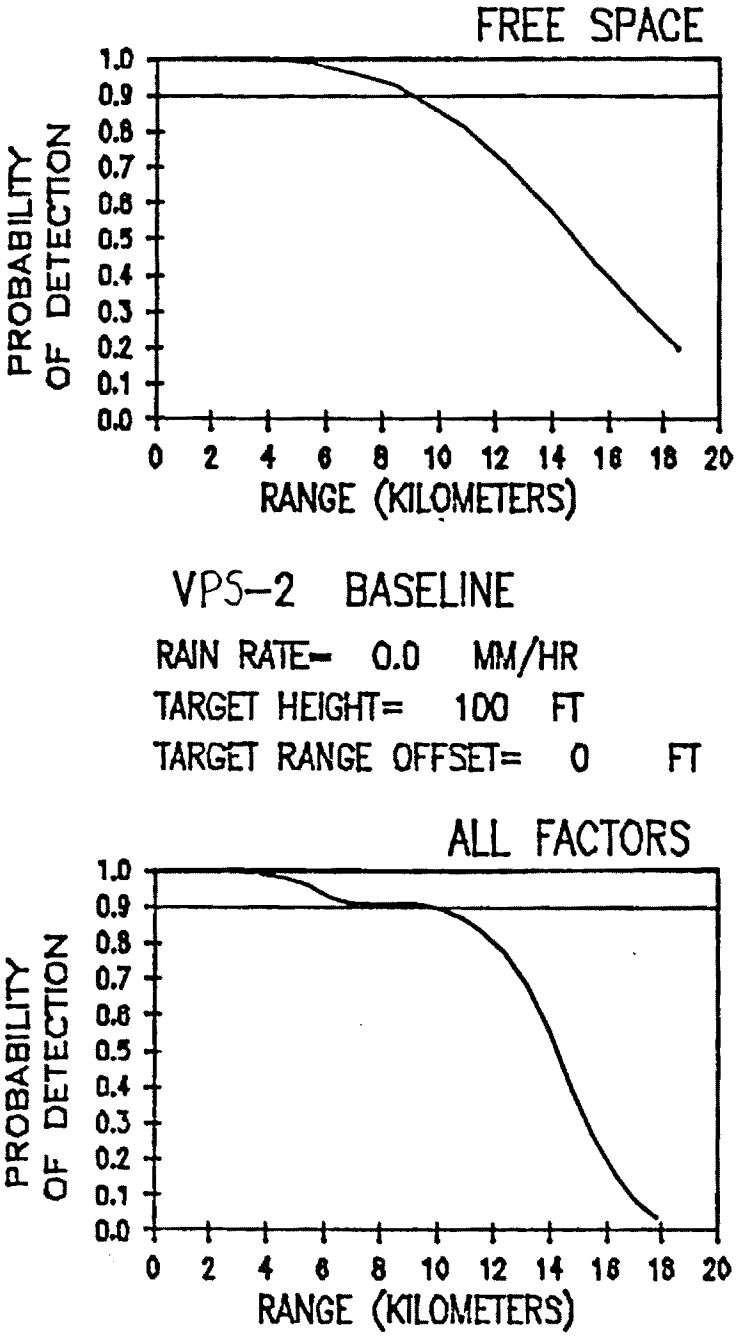

Figure 1. VPS-2 Baseline Detection Probability for 100 ft Aircraft Altitude, Clear Air, No Range Offset

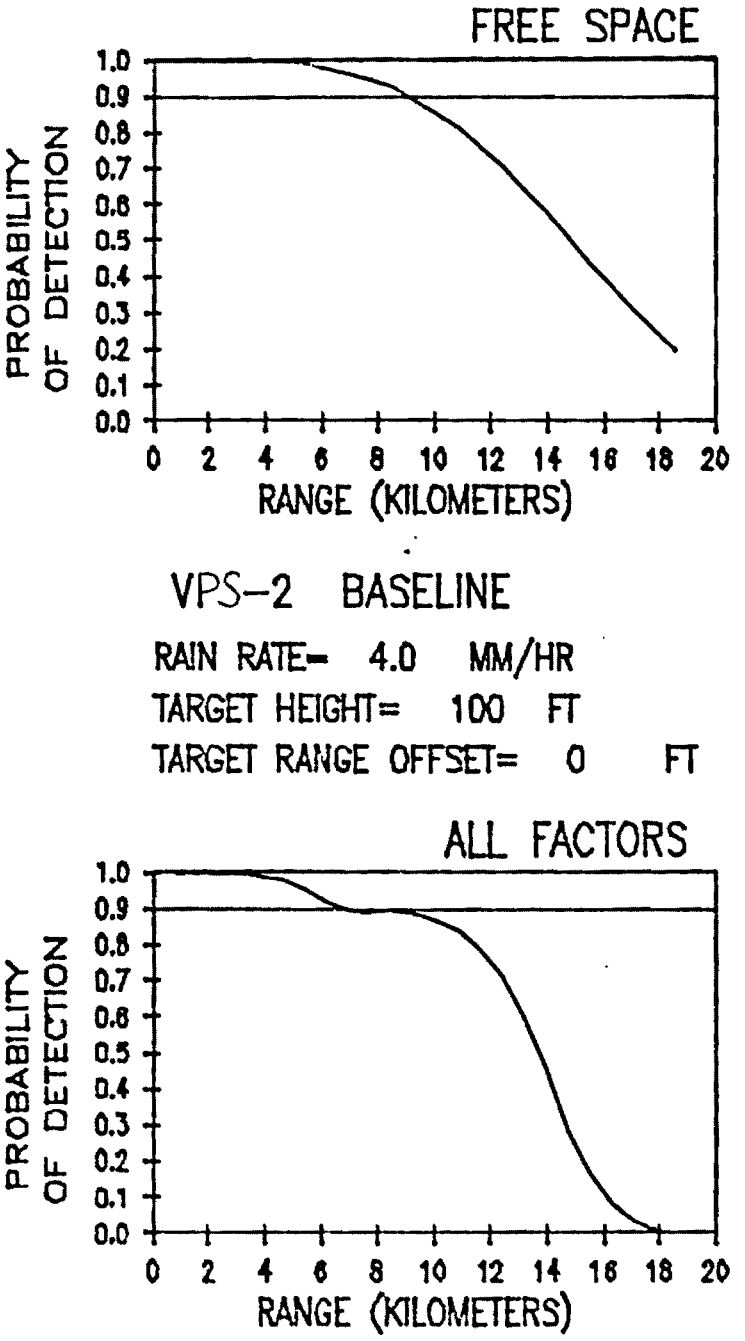

Figure 2. VPS-2 Baseline Detection Probability for 100 ft Aircraft Altitude, 4 mm/hr Rain, No Range Offset.

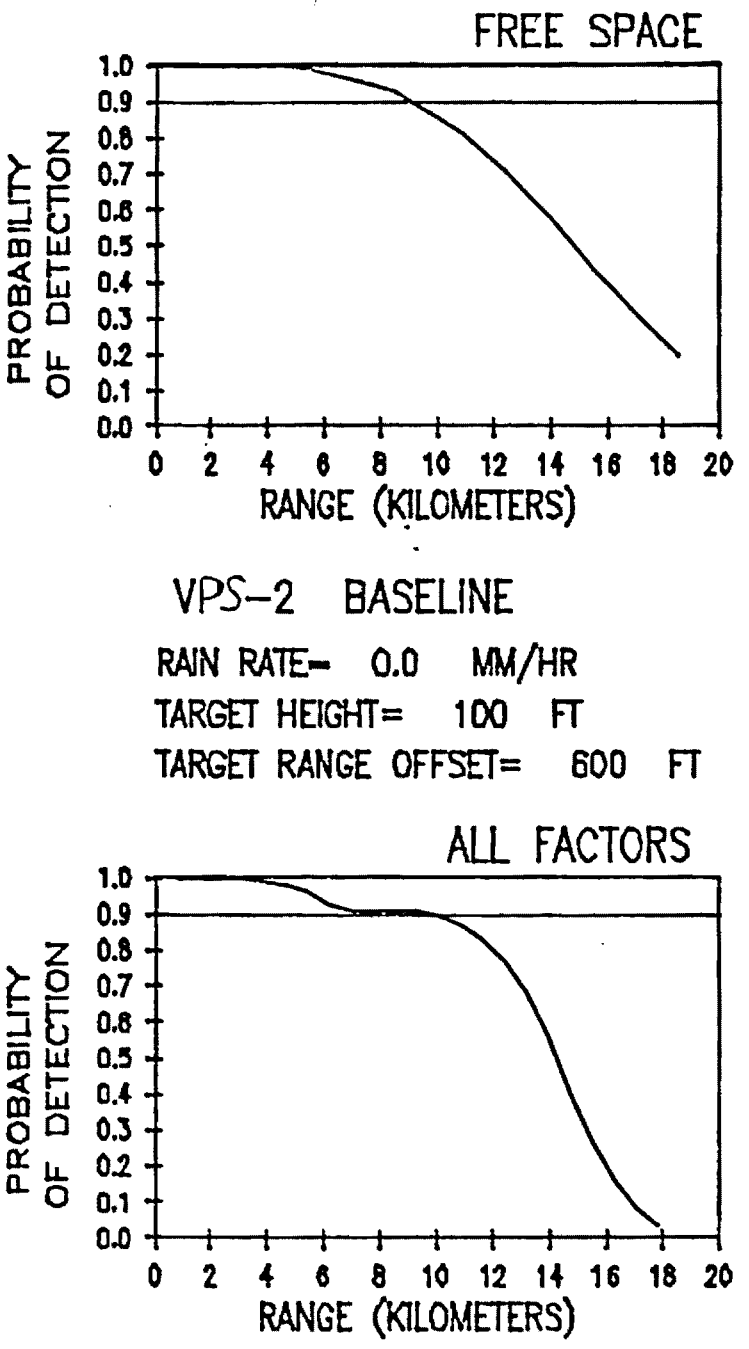

Figure 3. VPS-2 Baseline Detection Probability for 100 ft Aircraft Altitude, Clear Air, 600 ft Range Offset

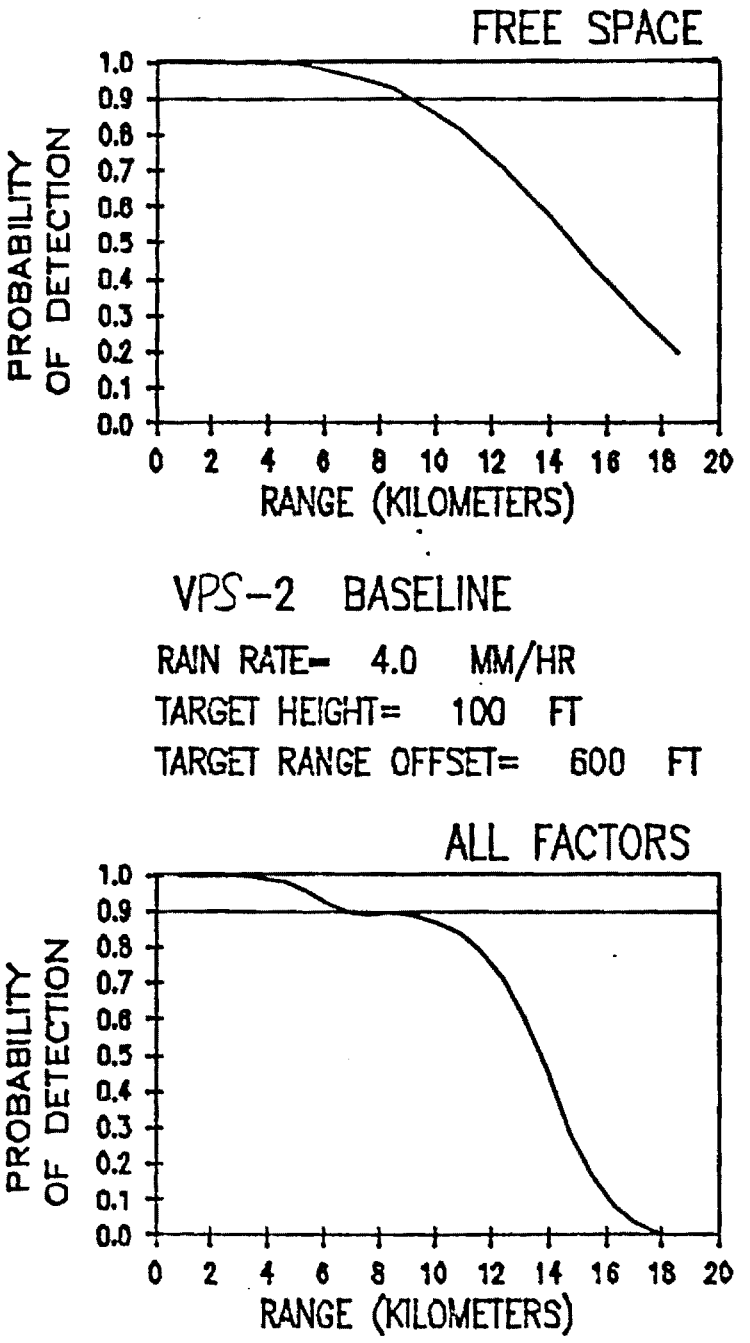

Figure 4. VPS-2 Baseline Detection Probability for 100 ft Aircraft Altitude, 4 mm/hr Rain, 600 ft Range Offset

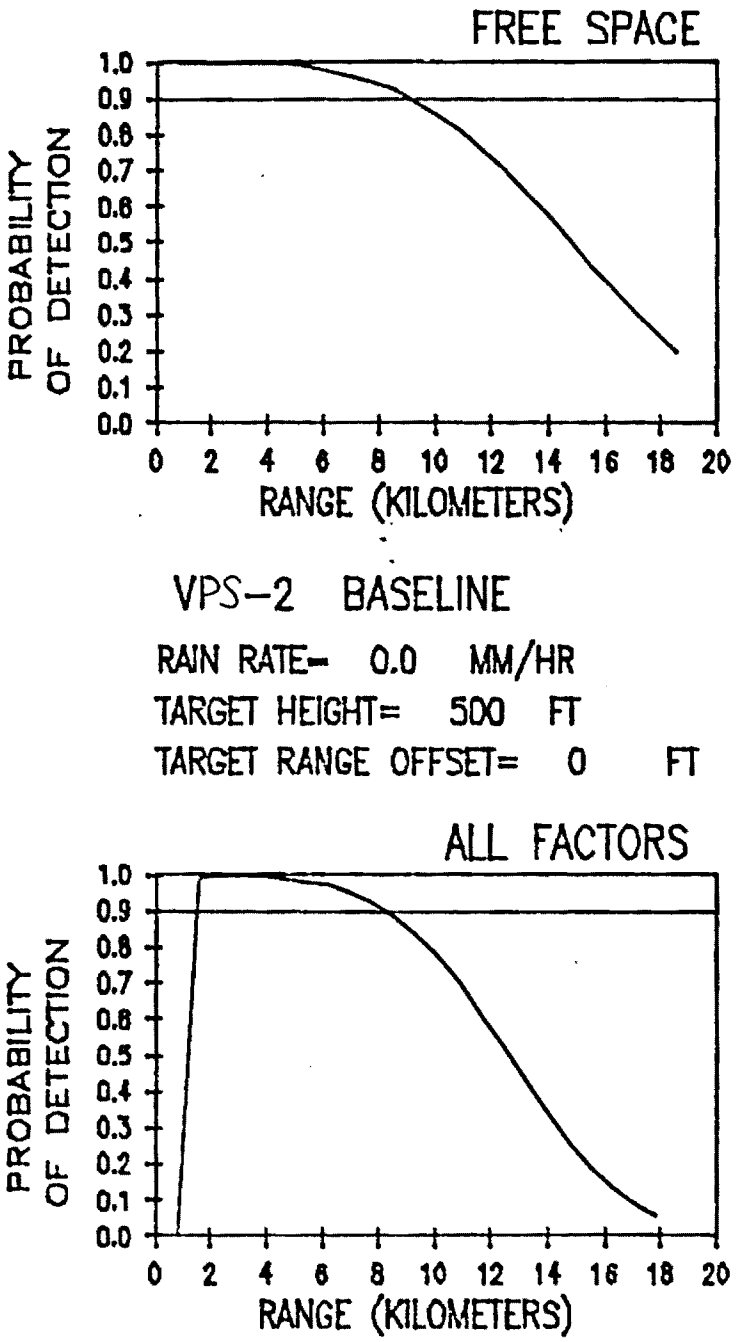

Figure 5. VPS-2 Baseline Detection Probability for 500 ft Aircraft Altitude, Clear Air, No Range Offset

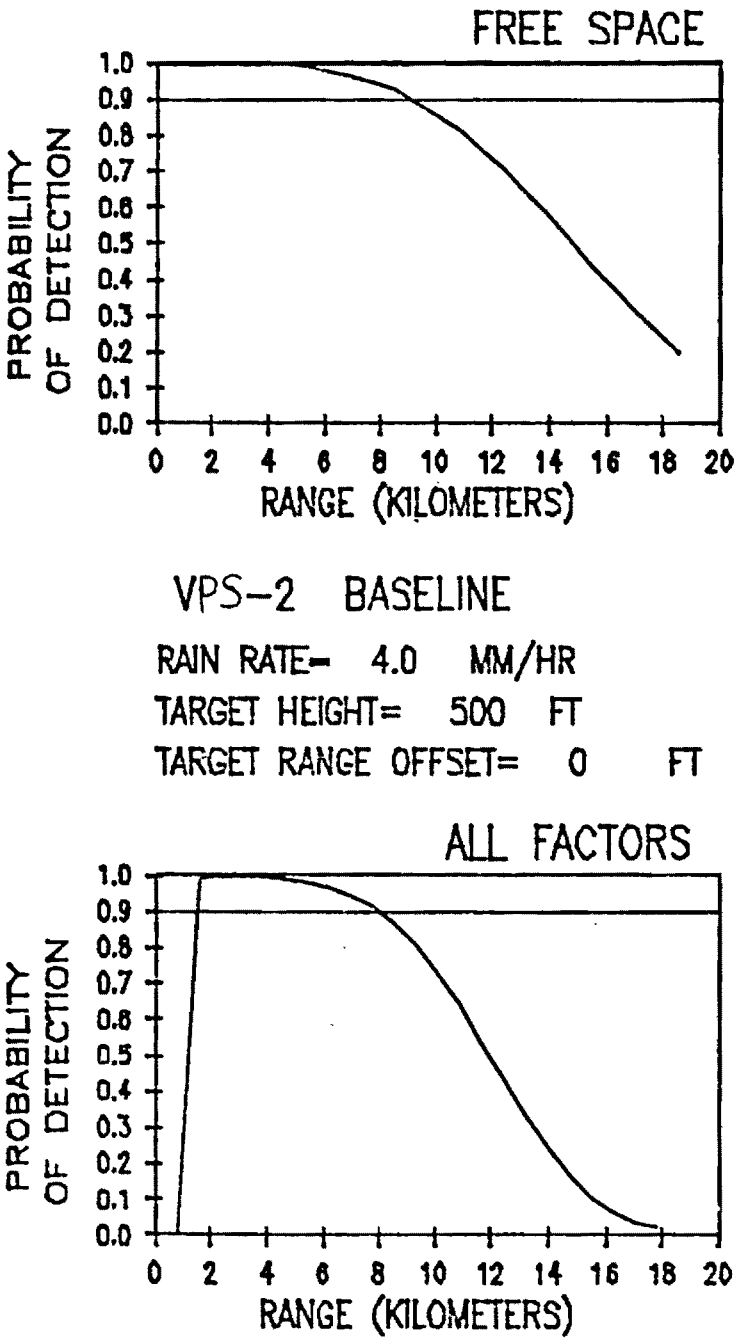

Figure 6. VPS-2 Baseline Detection Probability for 500 ft Aircraft Altitude, 4 mm/hr Rain, No Range Offset

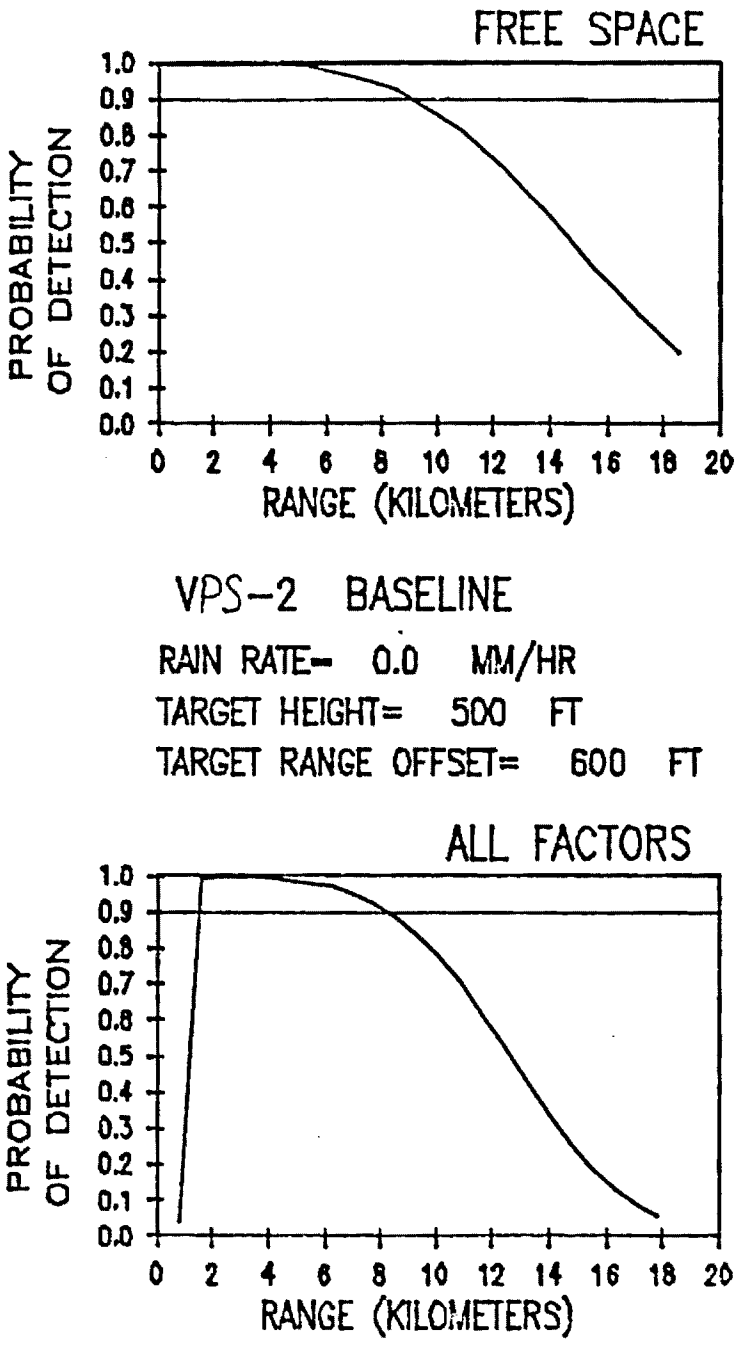

Figure 7. VPS-2 Baseline Detection Probability for 500 ft Aircraft Altitude, Clear Air, 600 ft Range Offset

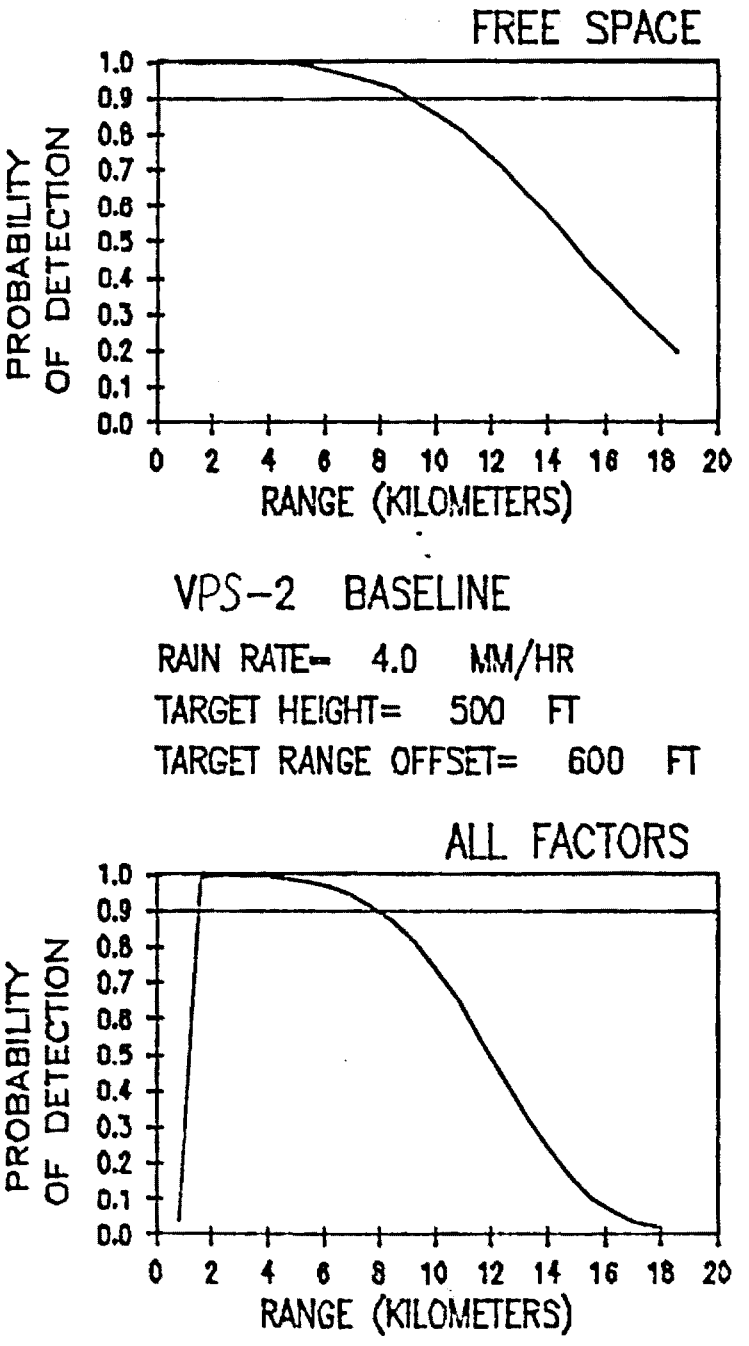

Figure 8. VPS-2 Baseline Detection Probaility for 500 ft Aircraft Altitude, 4 mm/hr Rain, 600 ft Range Offset

FINAL TECHNICAL REPORT
GEORGIA TECH PROJECT A-3157

PERFORMANCE EVALUATION OF THE AN/VPS-2 RADAR FOR LIGHT DIVADS UTILIZATION

By:

R. N. Trebits
W. A. Holm
N. T. Alexander
M. N. Cohen

Prepared for

GENERAL ELECTRIC COMPANY
ARMAMENT SYSTEMS DEPARTMENT
BURLINGTON, VERMONT 05402

Under
Purchase Order D24-SJ350K

GEORGIA INSTITUTE OF TECHNOLOGY
Engineering Experiment Station
Atlanta, Georgia 30332

July 1982

TABLE OF CONTENTS

SECTION	TITLE	PAGE
1	OVERVIEW AND SUMMARY	1
2	AN/VPS-2 SURVEILLANCE PERFORMANCE	5
3	THE MODIFIED AN/VPS-2 SYSTEM	17
4	MODIFIED AN/VPS-2 SURVEILLANCE PERFORMANCE	45
5	CONCLUSIONS AND RECOMMENDATIONS	67
APPENDIX		
A	FAST FOURIER TRANSFORM MODULES	69
REFERENCES		71

LIST OF FIGURES

FIGURE	TITLE	PAGE
1.	VPS-2 baseline detection probability for 100 ft aircraft altitude, clear air, no range offset.	7
2.	VPS-2 baseline detection probability for 100 ft aircraft altitude, 4 mm/hr rain, no range offset	8
3.	VPS-2 baseline detection probability for 100 ft aircraft, clear air, 600 ft range offset	9
4.	VPS-2 baseline detection probability for 100 ft aircraft altitude, 4 mm/hr rain, 600 ft range offset	10
5.	VPS-2 baseline detection probability for 500 ft aircraft altitude, clear air, no range offset	12
6.	VPS-2 baseline detection probability for 500 ft aircraft altitude, 4 mm/hr rain, no range offset	13
7.	VPS-2 baseline detection probability for 500 ft aircraft altitude, clear air, 600 ft range offset	14
8.	VPS-2 baseline detection probability for 500 ft aircraft altitude, 4 mm/hr rain, 600 ft range offset	15
9.	Receiver and signal processor functional modules of the modified VPS-2 radar system	18
10.	Shaped antenna pattern approximation for gain loss calculations	22
11.	Time-averaged filter response of three-pulse DDLC and four-pole Butterworth filter DDLC	33
12.	Received signal-to-clutter ratio versus range	36
13.	X-band spectral content of trees in a 6-10 mph wind	39
14.	(a) Filter response of target frequency bin with Dolph-Chebyshev weighting applied. (b) Mathematical model of filter response of target frequency bin.	41
15.	Improvement factor limitation due to internal clutter motion (trees: 6-10 mph wind) and system instabilities (SCV = 40 dB)	43

LIST OF FIGURES

(continued)

FIGURE	TITLE	PAGE
16.	Recommended VPS-2 configuration detection probability for 100 ft. aircraft altitude, clear air, 3 degree antenna tilt	46
17.	Recommended VPS-2 configuration detection probability for 100 ft. aircraft altitude, clear air, 5 degree antenna tilt	47
18.	Recommended VPS-2 configuration detection probability for 100 ft. aircraft altitude, 4 mm/hr rain, 3 degree antenna tilt	48
19.	Recommended VPS-2 configuration detection probability for 100 ft. aircraft altitude, 4 mm/hr rain, 5 degree antenna tilt	49
20.	Recommended VPS-2 configuration detection probability for 100 ft. aircraft altitude, clear air, 3 degree antenna tilt, multipath interference removed	50
21.	Modified VPS-2 configuration (1.5 kW) detection probability for 100 ft. aircraft altitude, clear air, 3 degree antenna tilt	52
22.	Modified VPS-2 configuration (1.5 kW) detection probability for 100 ft. aircraft altitude, clear air, 5 degree antenna tilt	53
23.	Modified VPS-2 configuration (1.5 kW) detection probability for 100 ft. aircraft altitude, 4 mm/hr rain, 3 degree antenna tilt	54
24.	Modified VPS-2 configuration (1.5 kW) detection probability for 100 ft. aircraft altitude, 4 mm/hr rain, 5 degree antenna tilte	55
25.	Modified VPS-2 configuration (1.5 kW) detection probability for 100 ft. aircraft, altitude, clear air, 3 degree antenna tilt, multipath interference removed	56
26.	Recommended VPS-2 configuration detection probability for 2000 ft. aircraft altitude, clear air, 3 degree antenna tilt	58
27.	Recommended VPS-2 configuration detection probability for 2000 ft. aircraft altitude, clear air, 5 degree antenna tilt	59

LIST OF FIGURES

(continued)

FIGURE	TITLE	PAGE
28.	Recommended VPS-2 configuration detection probability for 2000 ft. aircraft altitude, 4 mm/hr rain, 3 degree antenna tilt	60
29.	Recommended VPS-2 configuration detection probability for 2000 ft. aircraft altitude, 4 mm/hr rain, 5 degree antenna tilt	61
30.	Modified VPS-2 configuration (1.5 kW) detection probability for 2000 ft. aircraft altitude, clear air, 3 degree antenna tilt	62
31.	Modified VPS-2 configuration (1.5 kW) detection probability for 2000 ft. aircraft altitude, clear air, 5 degree antenna tilt	63
32.	Modified VPS-2 configuration (1.5 kW) detection probability for 2000 ft. aircraft altitude, 4 mm/hr rain, 3 degree antenna tilt	64
33.	Modified VPS-2 configuration (1.5 kW) detection probability for 2000 ft. aircraft altitude, 4 mm/hr rain, 5 degree antenna tilt	65

LIST OF TABLES

TABLE	TITLE	PAGE
1.	LAV-AD PERFORMANCE REQUIREMENTS	3
2.	DETECTION PARAMETERS FOR AN/VPS-2	6
3.	DETECTION PARAMETERS FOR MODIFIED AN/VPS-2	19
4.	GAIN LOSS DUE TO ELEVATION PATTERN SHAPING	24
5.	GAIN OF OPTIMIZED AN/VPS-2 ANTENNA	24
6.	MINIMUM LOWER PRF'S FOR VARIOUS SIZE DDLC'S FOLLOWED BY A 128-POINT FFT	32
A1	FFT REQUIREMENTS	69
A2	128-POINT COMPLEX FFT MODULES	70

PREFACE

This study was funded by the Armament Systems Department of the General Electric Company in Burlington, Vermont under Purchase Order D24-SJ350K. Mr. Ernie Carlson was the General Electric Project Engineer, providing technical guidance and direction to this program. Dr. Robert Trebits served as the Georgia Tech Project Director for this research program, which was designated Georgia Tech Project A-3157.

In addition to the authors, technical contributions to this final report were made by Mr. Ray Efurd and Mr. Rick Folea. The technical assistance and cooperation of Mr. Ben Gol of AEL/Emtech was also greatly appreciated.

SECTION I
OVERVIEW AND SUMMARY

The General Electric Company has responded to an Army-Marine Corps solicitation for a light-weight, low-cost variant of the Division Air Defense System (DIVADS) concept. General Electric submitted a fully compliant proposal to the Government, defining a system consisting of the General Electric GAU-12, 25 mm armament system, a modified Westinghouse AN/APG-66 radar, and an M113 vehicle. The production cost estimated for this proposed light DIVADS, however, may preclude Government funding of this system concept.

In response to this realization, General Electric is investigating still lower cost light DIVADS concepts that would not be totally compliant with the performance requirements contained in the Army-Marine Corps solicitation. Since the major cost component of the fully compliant light DIVADS concept is a Westinghouse AN/APG-66 radar variant, a lower cost system design has been sought that utilizes a less expensive, but off-the-shelf surveillance radar. General Electric designates this lower cost concept the light armored vehicle, air defense variant (LAV-AD).

A candidate radar for this role was identified by General Electric to be the AN/VPS-2 radar, currently manufactured by Emtech, a division of AEL, Inc. The AN/VPS-2 is a range-tracking-only radar currently used to provide aircraft ranging information to a fire control system for the 20 mm antiaircraft artillery gun, XM-163 (self-propelled) and XM-167 (towed), associated with the Forward Area Air Defense System (FAADS). General Electric desired to assess the aircraft target detection performance of the AN/VPS-2 radar system in an additional surveillance mode.

General Electric tasked the Engineering Experiment Station of Georgia Tech to determine the 360-degree continuous-sweep surveillance capability of the AN/VPS-2 radar system. The first phase of this program consisted of determining the range detection performance of the AN/VPS-2 radar "as is," except for the continuous azimuthal rotation of its pencil beam antenna. The second phase of this program included (1) the range detection performance evaluation of AN/VPS-2 radar variants, (2) a brief investigation of the utilization of sensitivity time control (STC) or automatic gain control (AGC) for receiver dynamic range control, (3) a brief investigation of homodyne versus heterodyne receiver operation for the General Electric application, and

(4) an assessment of moving target indication (MTI) and Fast Fourier transform (FFT) signal processor hardware availability.

Specifications for the LAV-AD radar surveillance performance are listed in Table 1. These parameters represent a composite of General Electric and Georgia Tech interpretation of sensor requirements in response to the LAV-AD mission definition. Detection of fixed wing aircraft only are addressed in Table 1, although General Electric has formulated similar performance requirements for detection of rotary wing aircraft.[1] Note that detection performance is specified for multiple scans and that position/speed ambiguities within the search volume must be resolved.

Georgia Tech evaluated the baseline AN/VPS-2 aircraft detection performance using the MERGE computer program (see Section 2) and a set of radar and environmental data supplied by General Electric and Emtech. The free space detection range was calculated to be approximately 7 kilometers, based on a 90 percent probability of detection and a 10^{-6} false alarm rate. With weather and terrain factors considered, the detection range is 7 to 10 kilometers for 30 meter (100 foot) target altitudes and approximately 8 kilometers for 152 meter (500 foot) target altitudes, for benevolent multipath conditions. Moderate rainfall does not seriously degrade the detection performance of the X-band AN/VPS-2 radar at these target ranges.

The detection range of this radar is limited by: (1) its antenna beamshape and scan pattern, (2) its high receiver noise figure, and (3) its moving target indication signal processing. A set of modifications to the AN/VPS-2 radar was proposed collaboratively by Emtech, Georgia Tech, and General Electric personnel:

1. A shaped antenna pattern for wider elevation coverage than that provided by a pencil beam,
2. A GaAsFET preamplifier for an improved receiver noise figure, and
3. A combination of digital MTI and FFT processing for clutter rejection.

The preferred system configuration should include a heterodyne receiver that employs STC to limit the received signal dynamic range. Digital signal processing of in-phase (I) and quadrature (Q) baseband signals to detect moving targets and reject clutter should be effected before presentation of detected targets to the radar display.

The detection range for the modified AN/VPS-2 was computed to be approximately 14 kilometers for a 30 m (100 foot) aircraft altitude, with all weather and terrain factors considered. Detection of targets at higher altitude is limited by lack of

TABLE I. LAV-AD PERFORMANCE REQUIREMENTS

Target Parameters	
Radial Speed	15 m/sec (min), 320 m/sec (max)
Radar Cross Section	2 square meters
Radar Return Model	Swerling I
Environmental Parameters	
Azimuth Coverage	360 degrees, continuous
Elevation Coverage	0 to 30 degrees
Detection Range	0.75 km (min), 15 km (max)
Target Altitude	Nap of earth (min), 2000 m (max)
Rainfall Rate	4 mm/hr, beam-filled
Radar Parameters	
Maximum Time (Unmask to Detection)	2 sec. (range $\leq$ 4 km) 4 sec. (4 km $<$ range $\leq$ 6 km) 8 sec. (6 km $<$ range)
Probability of Detection	90 percent, multiple scans
False Alarm Rate	10^{-6}
Range and Speed Ambiguities	Must be resolved
Signal Processing	Clutter rejection

higher elevation antenna pattern coverage. The modified AN/VPS-2, therefore, appears to be a viable candidate for the General Electric light DIVADS concept.

SECTION 2
AN/VPS-2 SURVEILLANCE PERFORMANCE

Georgia Tech evaluated the aircraft detection performance of the AN/VPS-2 range-only radar modified for continuous 360 degree azimuth search over a 30 degree elevation sector. Pertinent radar system parameters and operational parameters were obtained from Emtech and General Electric, respectively, and are summarized in Table 2.

The radar parameters listed in Table 2 are those of the standard AN/VPS-2 radar system. An additional parameter specified is azimuthal antenna scanning at 6 revolutions per minute (36 degrees per second) so that seven full azimuthal scans are required to search the 30 degree elevation volume in a raster fashion. Since maximum detection range was the quantity to be computed, only the lowest elevation of the seven elevation scans was used in the detection computations. Environmental parameters were obtained from open literature sources and represent generalized averages.

The radar analysis computer program used for this detection performance evaluation was created by Georgia Tech from the radar performance prediction program RGCALC developed by L. V. Blake at NRL.[2] Blake's work has been widely used throughout the radar community in a variety of versions. The Georgia Tech version of this computer program is titled MERGE and contains both surveillance and tracking radar performance evaluation modules.[3]

MERGE accepts radar descriptions, an environment description, and a target description and uses these inputs to calculate signal-to-noise ratios, signal-to-clutter ratios, and probabilities of detection as a function of range to the target. The antenna pattern was assumed to be sin x/x, and the MTI filter response was assumed to be trapezoidal, with corner frequencies at 650 and 19,336 Hz. The signal processing was also assumed to provide perfect integration of all 283 pulses within a beam dwell time.

Figures 1 through 4 summarize the probability of detection versus range for a constant 30 m (100 feet) aircraft altitude. (In all figures that follow, the upper graph depicts the free space detection performance of the radar, i.e., the aircraft follows a constant elevation angle to the radar). The free space detection range is approximately 9 kilometers. Figure 1 depicts a detection range of approximately 7 to 10 kilometers (90 percent detection, single scan) in clear air, where the plateau of the detection curve is a

TABLE 2. DETECTION PARAMETERS FOR AN/VPS-2

Peak Transmitter Power	1.0 kW
Pulse Width	280 nsec
Peak Antenna Gain	33 dB
Frequency	9.225 GHz
Pulse Repetition Frequency	19,986 pps
Two-way Transmission Line Loss	2.2 dB
Scanning Antenna Pattern Loss	1.6 dB
Miscellaneous Losses	1.4 dB
Receiver Noise Figure	13 dB
Number of Pulses Integrated	283
False Alarm Rate	10^{-6}
Antenna Tilt Angle	2 degrees
Rain Rate	4 mm/hr
Rainfall Extent	0 to 18 kilometers
Antenna Height	3 meters
Elevation Beamwidth	4.3 degrees
Azimuth Beamwidth	4.1 degrees
Sidelobe Peak below Main Peak	24 dB
Surface Roughness Factor	3 meters
Polarization	Horizontal
Antenna Scan Rate	36 degrees/second
Clutter Improvement Factor	50 dB
Probability of Detection	.90 single scan
Aircraft Radar Cross Section	1 square meter
Target Model	Swerling I
Terrain Reflectivity	-30 dB
Rain Reflectivity	-70 dB

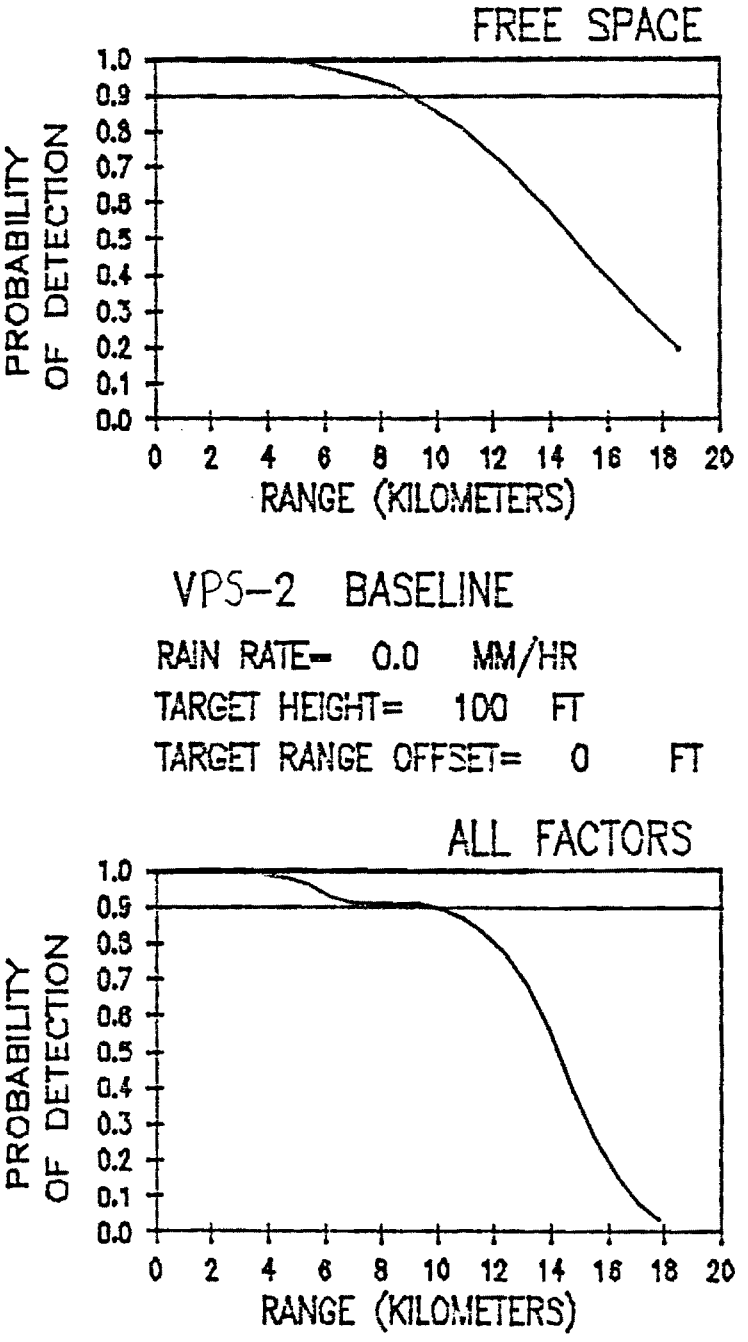

Figure 1. VPS-2 Baseline Detection Probability for 100 ft Aircraft Altitude, Clear Air, No Range Offset

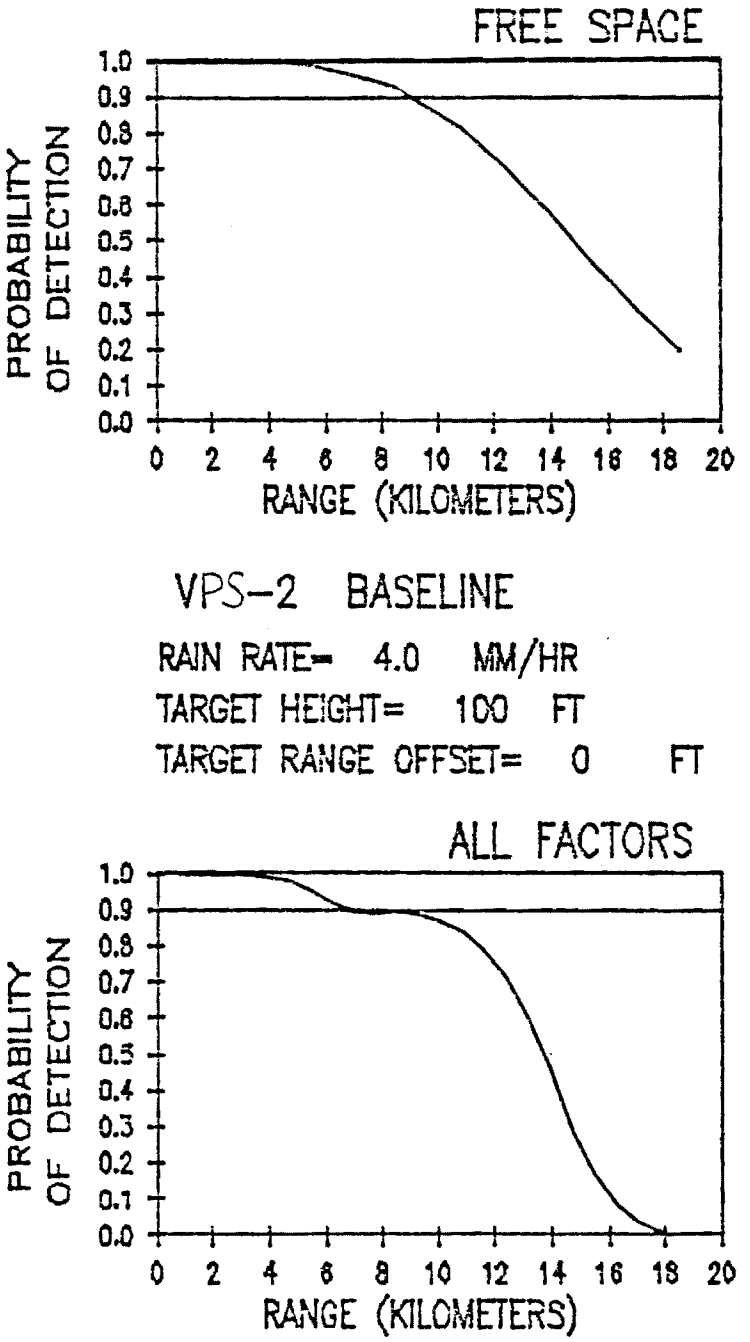

Figure 2. VPS-2 Baseline Detection Probability for 100 ft Aircraft Altitude, 4 mm/hr Rain, No Range Offset.

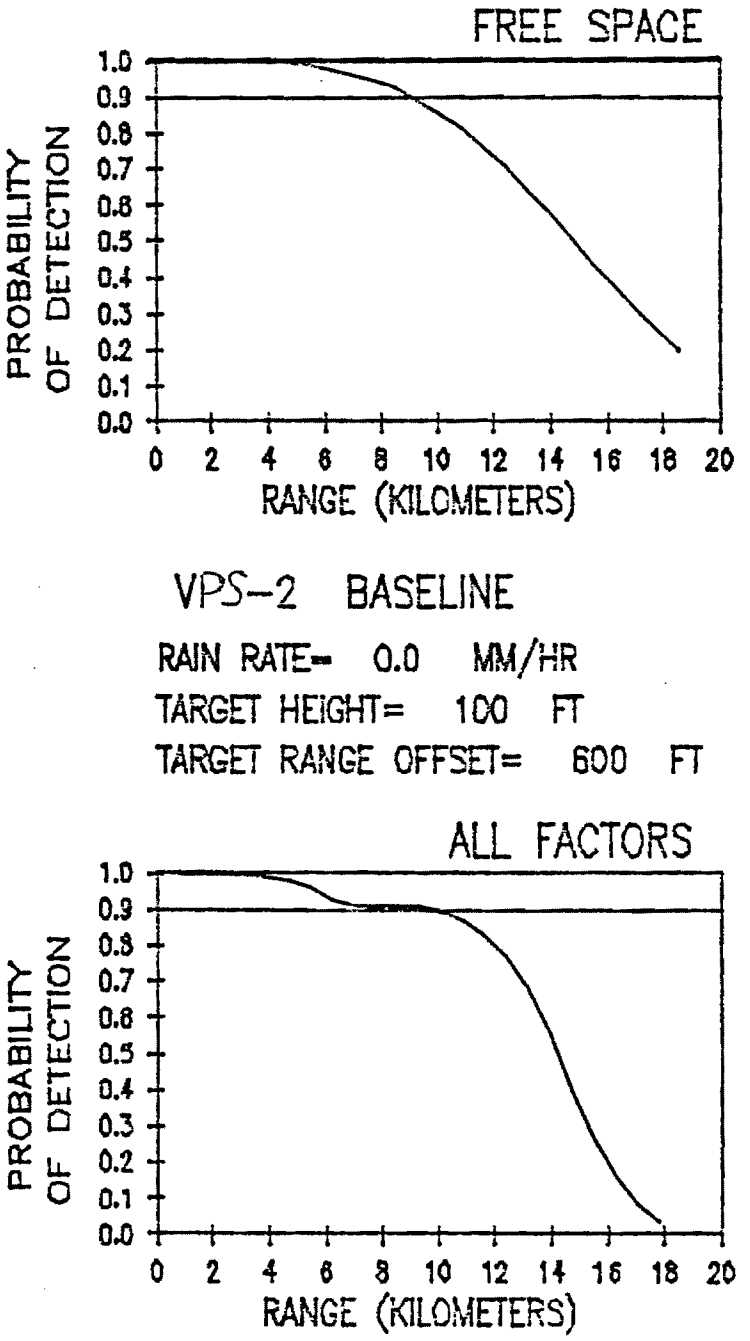

Figure 3. VPS-2 Baseline Detection Probability for 100 ft Aircraft Altitude, Clear Air, 600 ft Range Offset

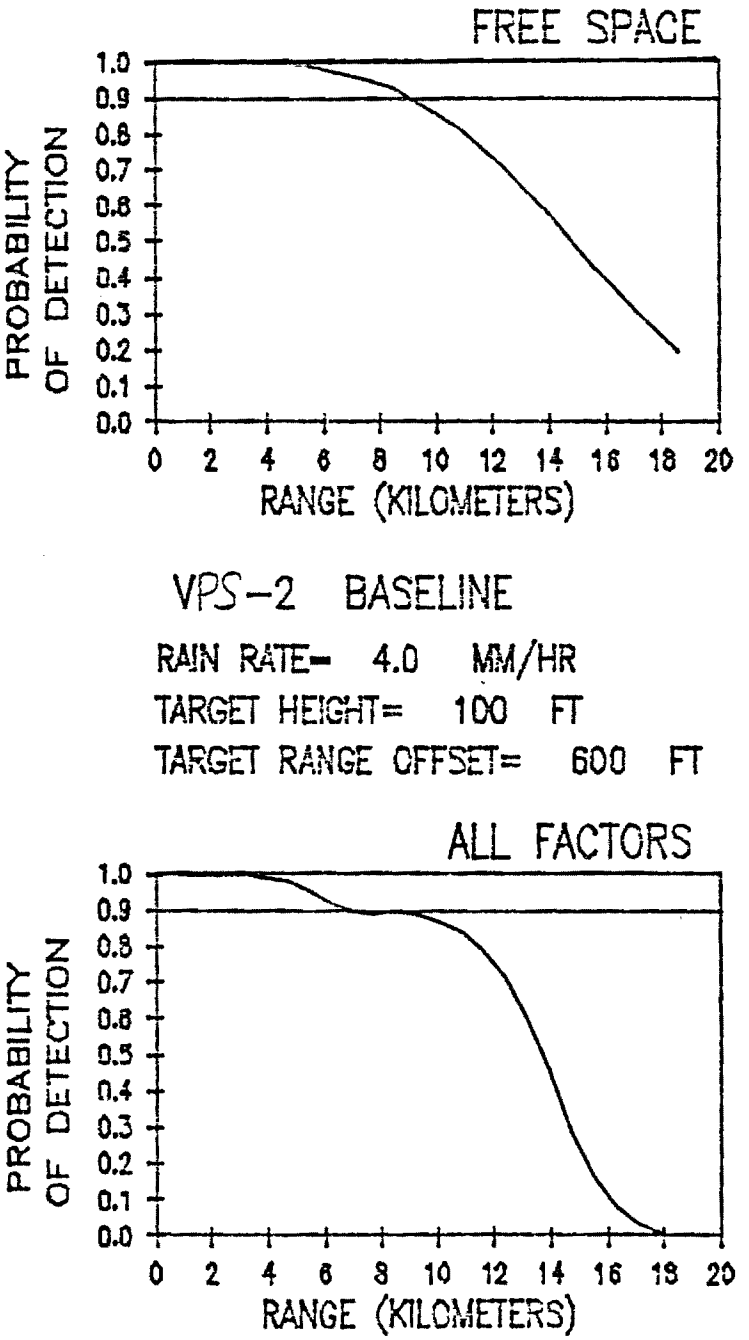

Figure 4. VPS-2 Baseline Detection Probability for 100 ft Aircraft Altitude, 4 mm/hr Rain, 600 ft Range Offset

manifestation of multipath interference. Detection performance is only minimally degraded in 4 mm/hr rain, as shown in Figure 2. Figures 3 and 4 depict nearly the same detection performance, where the aircraft's straight line approach to the radar is offset by approximately 183 m (600 ft).

Figures 5 through 8 depict aircraft detection probability versus range for a constant 152 m (500 ft) aircraft altitude. Comparison of these detection curves with the previous set of four figures demonstrates that multipath interference is not significant at the higher aircraft altitude, since no detection plateaus are present in the curves. In all cases aircraft detection occurs at approximately 8 kilometers. Note that the detection probability falls to zero where the aircraft exits the antenna elevation beamwidth at approximately 1-1/2 kilometers. 4 mm/hr rainfall does not have an appreciable effect on detection performance at these ranges. 183 m flight path offsets do not change the essential features of these detection curves, as shown in Figures 7 and 8.

Five specific areas have been identified where radar detection performance, in a continuous search mode, can be enhanced toward meeting a 15 kilometer design goal. Realistic changes to the AN/VPS-2 should be considered in at least the following areas:

1. Increased average power transmitted,
2. Fan beam or shaped beam antenna elevation pattern,
3. Staggered pulse repetition rate,
4. Specific detection and signal processing algorithms, and
5. Improved front end noise figure.

Increasing the average power will obviously improve the signal-to-noise ratio. Stretching the pulse and/or increasing the transmitter peak power are mechanisms for increasing the average power. However, while a longer pulse results in higher target return power and a smaller matched receiver bandwidth (and less noise into the receiver), the clutter return also increases. There are also practical limits to increasing the transmitter peak power or pulse repetition rate, which ultimately are klystron limited.

A shaped antenna elevation pattern, such as cosecant-squared, will provide full 30 degree elevation coverage without the necessity of multiple scans to search the entire volume, as required by a pencil beam pattern. However, no target elevation angle information would be available, and for equivalent size apertures, the shaped-beam antenna peak gain will be several dB less than that of a pencil beam.

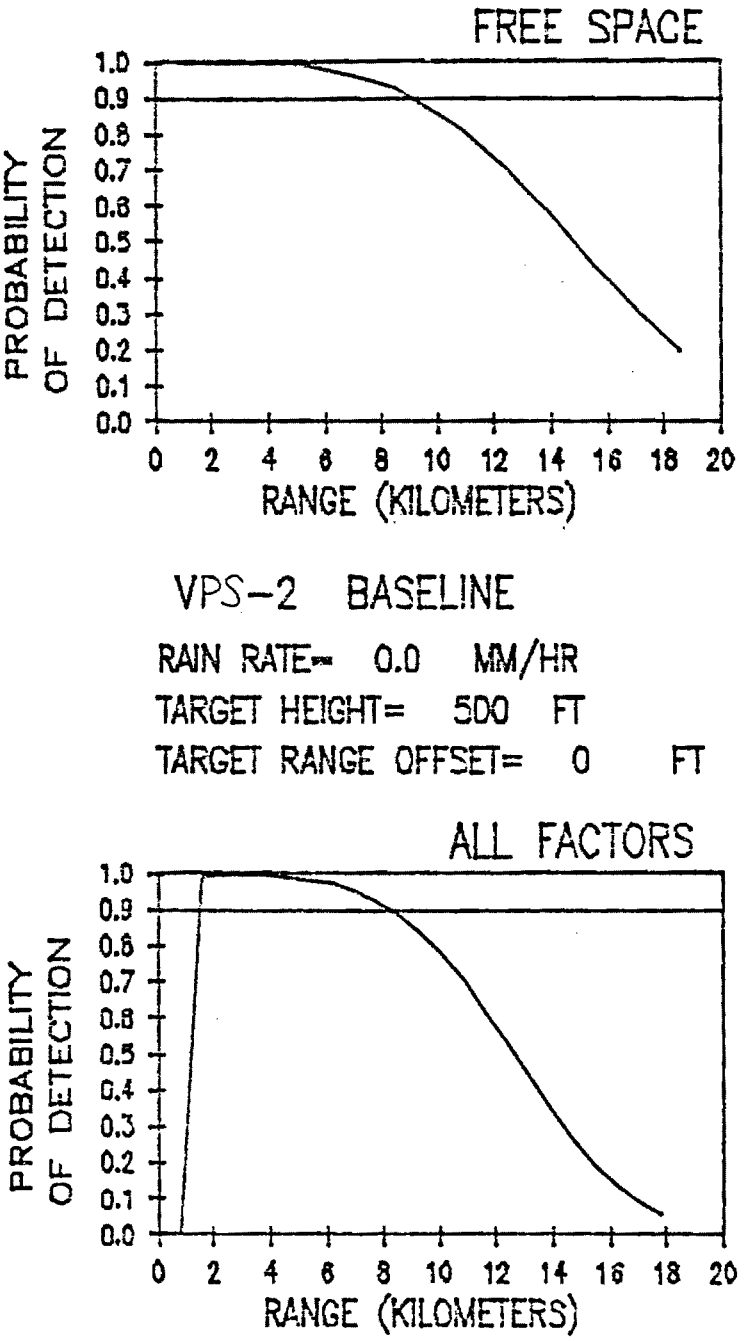

Figure 5. VPS-2 Baseline Detection Probability for 500 ft Aircraft Altitude, Clear Air, No Range Offset

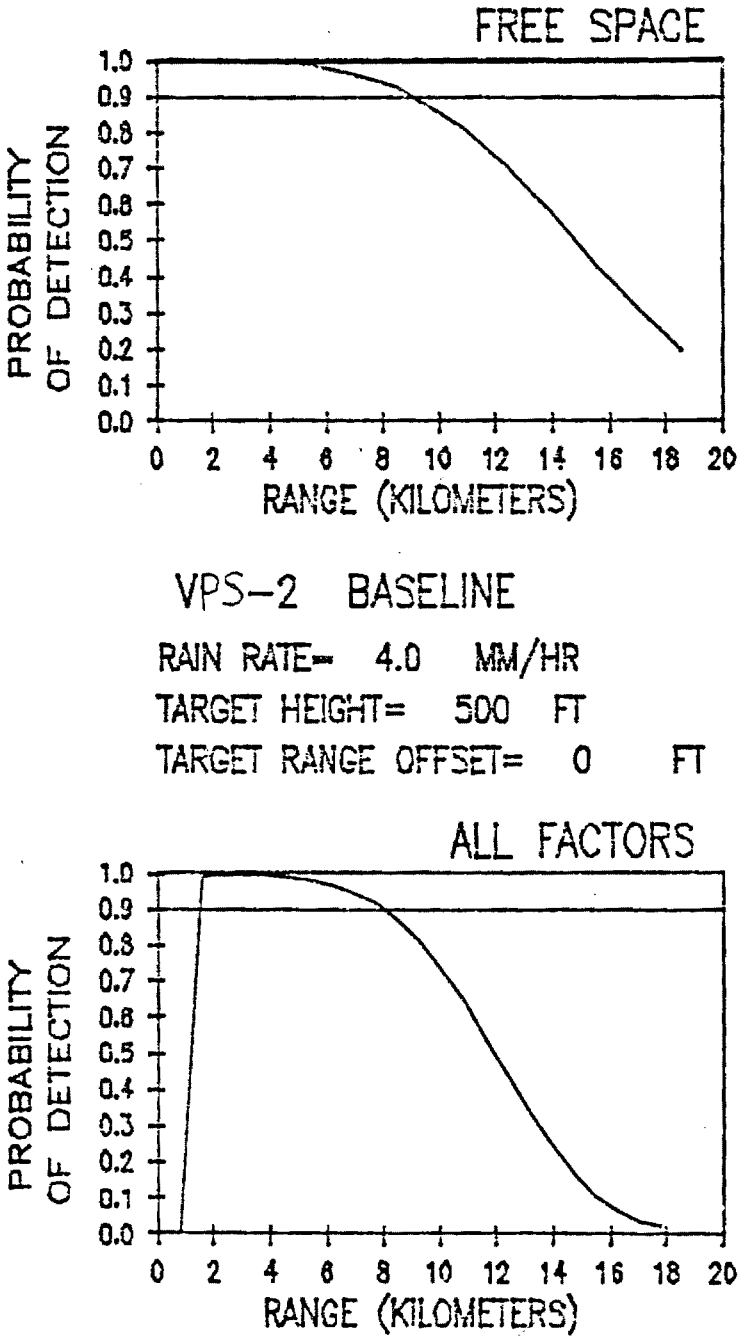

Figure 6. VPS-2 Baseline Detection Probability for 500 ft Aircraft Altitude, 4 mm/hr Rain, No Range Offset

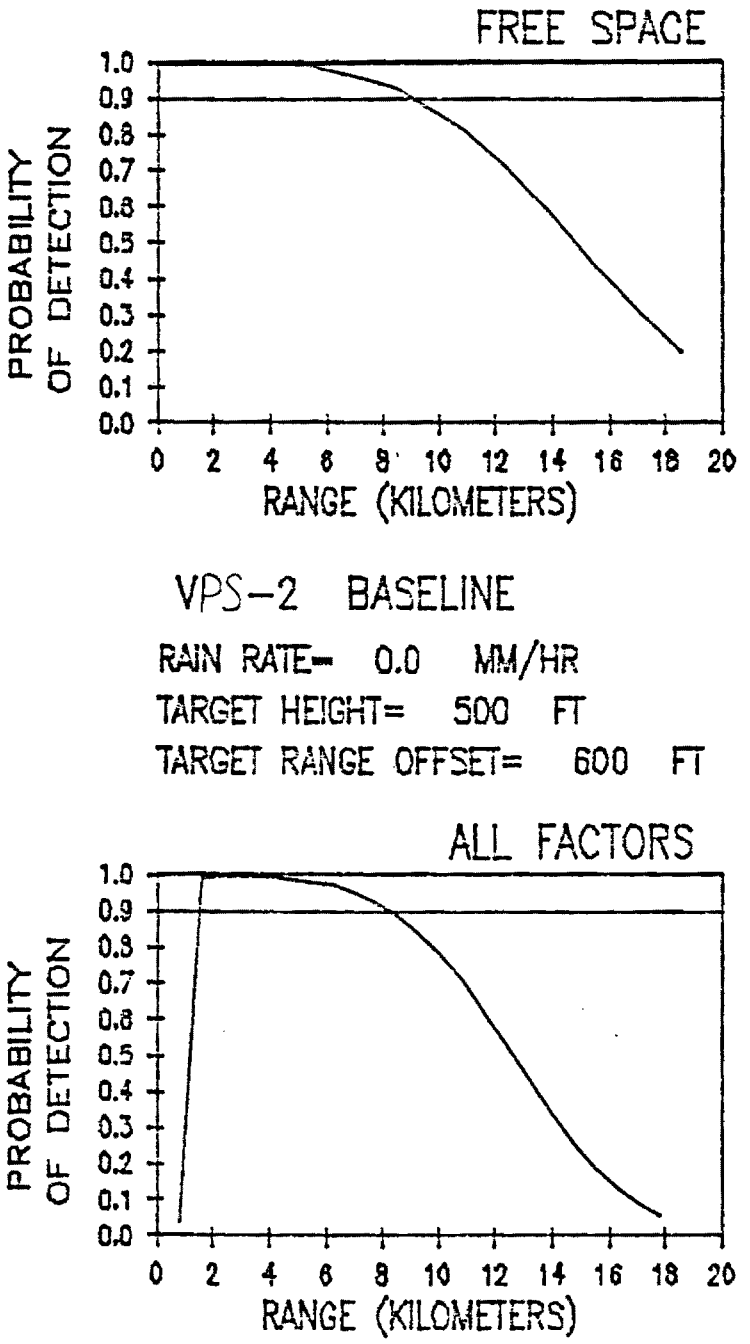

Figure 7. VPS-2 Baseline Detection Probability for 500 ft Aircraft Altitude, Clear Air, 600 ft Range Offset

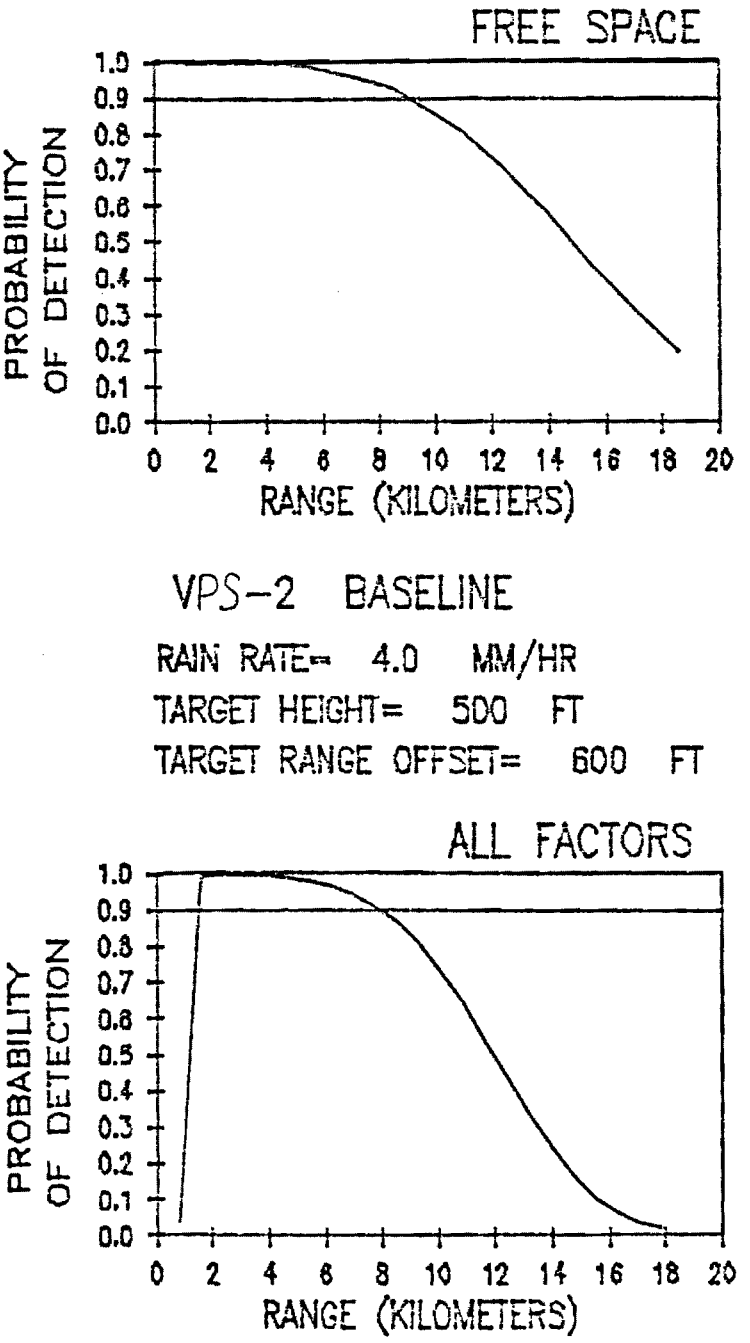

Figure 8. VPS-2 Baseline Detection Probaility for 500 ft Aircraft Altitude, 4 mm/hr Rain, 600 ft Range Offset

A staggered pulse repetition rate will be required to extend the unambiguous detection range to 15 kilometers and resolve velocity ambiguities. The maximum unambiguous range of the AN/VPS-2 is 7.5 kilometers, and the first aircraft blind speed is approximately 300 m/sec. Straightforward halving of the pulse repetition rate to double the maximum unambiguous range would have the undesirable effect of halving the first blind speed. Staggering the pulse repetition rate, however, will permit extending the detection range and moving blind speeds to acceptable values.

Moving Target Indication (MTI) and Fast Fourier Transform (FFT) processing will filter out clutter returns and perform the signal integration needed to achieve a high signal-to-noise ratio. Multiple pulse, weighted MTI processing (implemented digitally) can be used along with commercially available FFT firmware. Conversion rates and FFT processing rates, however, will impact the quantity of data that can be processed by off-the-shelf processing modules. Limited processing speeds may require decreasing the number of discrete range cells to be processed, resulting in decreased range resolution, signal-to-noise ratios, and signal-to-clutter ratios.

Improving the front end noise figure by utilizing a low noise RF preamplifier can only improve radar performance. While some front-end passive component losses cannot be decreased further, a GaAsFET amplifier would directly enhance the radar's signal-to-noise ratio.

SECTION 3
THE MODIFIED AN/VPS-2 SYSTEM

3.1 SYSTEM DESCRIPTION

Emtech, Georgia Tech, and General Electric personnel collaboratively defined a modification of the basic AN/VPS-2 radar system that meets the detection performance requirements of a light DIVADS. The philosophy of defining these system modifications was to retain as much of the basic AN/VPS-2 as possible to minimize cost, yet to upgrade those components whose replacement would lead to improved radar surveillance performance. The existing tracking modules are retained without change, so all radar operating parameters will revert to those of the existing AN/VPS-2 radar during track mode. In the discussions that follow, it must be understood that unless otherwise noted specified radar parameters are relevent only for the radar surveillance function.

The significant areas of radar system modifications are the (1) transmitter, (2) antenna, (3) receiver, and (4) signal processor modules. The transmitter modifications consist of a longer pulse length (2 μsec) with two alternating pulse repetition frequencies. The antenna pattern modifications consist of a slightly wider (5 degree) azimuthal beamwidth and a cosecant-squared elevation beamwidth. The significant receiver modification is the addition of a GaAsFET RF preamplifier before the mixer. The signal processor modifications include digital range cell averaging, MTI filtering, FFT processing, and constant false alarm rate (CFAR) processing.

The receiver and signal processing functional modules of the modified AN/VPS-2 radar system are shown in Figure 9. Note that the existing analog tracking module is retained. All modules coming after coherent detection represent new digital circuitry dedicated to surveillance. The parameters of the modified AN/VPS-2 radar system are summarized in Table 3.

3.2 TRANSMITTER

The klystron power amplifier is retained in the modified AN/VPS-2 radar system with two significant operational changes. The basic 0.28 sec pulselength has been stretched to 2 sec and has been reshaped with a rectangular pulse profile. The basic fixed pulse repetition frequency of 19,986 pps has been changed to an alternating set of 9360 pps and 10,000 pps.

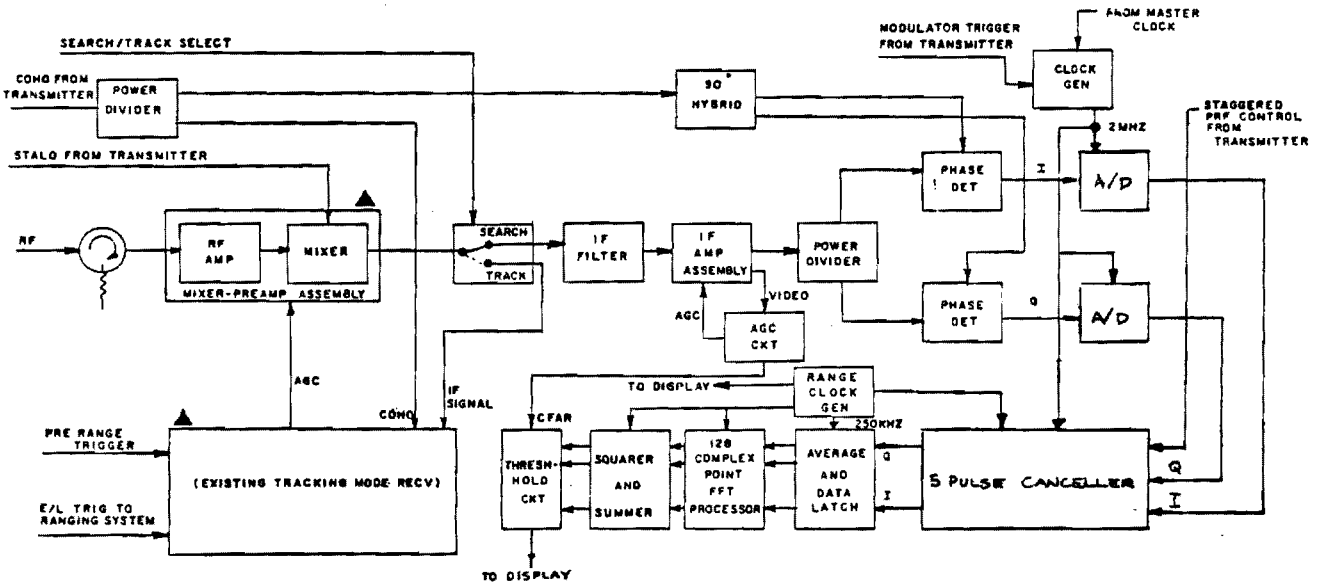

Figure 9. Receiver and Signal Processor Functional Modules of the Modified AN/VPS-2 Radar System.

TABLE 3. DETECTION PARAMETERS FOR MODIFIED AN/VPS-2

Peak Transmitter Power	1.0 kW
Pulse Width	2 μ sec
Peak Antenna Gain	24 dB
Frequency	9.225 GHz
Pulse Repetition Frequency	9,360 and 10,000 pps
Two-way Transmission Line Loss	2.2 dB
Scanning Antenna Pattern Loss	1.6 dB
Miscellaneous Losses	4.5 dB Total
Signal Processing Loss	3 dB
Non-Coherent Integration Loss	.5 dB
Field Degradation Loss	1 dB
Receiver Noise Figure	4.2 dB
Collapsing Loss	3.0 dB
Number of Pulses Integrated	264
False Alarm Rate	10^{-6}
Rain Rate	4 mm/hr
Rainfall Extent	0 to 18 kilometers
Antenna Height	3 meters
Elevation Beamwidth	5 degrees
Azimuth Beamwidth	shaped
Sidelobe Peak below Main Peak	27 dB
Surface Roughness Factor	3 meters
Polarization	horizontal
Antenna Scan Rate	180 degrees/second
Probability of Detection	.90, multiple single scans
	1 scan (range $\leq$ 4 km)
	2 scans (4 km $<$ range $\leq$ 6 km)
	4 scans 6 (km $<$ range)
Aircraft Radar Cross Section	2 square meters
Target Model	Swerling 1
Terrain Reflectivity	-20 dB
Rain Reflectivity	-70 dB
Data Averaging	2 resolution cells

The longer pulse length is achievable within the duty cycle limits of the klystron and power supplies. For the same peak transmitted power of 1 kW, the basic 0.006 duty cycle is increased to 0.02, which represents an increase in average power of approximately 5 dB. A second result of the longer pulse length is that the receiver matched bandwidth can be decreased from the original 3.5 MHz to approximately 0.5 MHz, a change which decreases the receiver noise level by over 8 dB.

On the negative side, the longer pulse length changes the achievable range resolution from approximately 42 m (138 feet) to approximately 300 m (984 ft) and increases the received clutter power by the same ratio. The poorer range resolution is tolerable, and the increased clutter power should not be a problem for most scenarios. Refer to Section 4 of this report for the results of the aircraft detection performance evaluation for the modified AN/VPS-2 radar system.

3.3 ANTENNA CONSIDERATIONS

The desired coverage of the radar extends in elevation from the horizon to plus 30°, and encompasses 360° in azimuth. The achievement of such a large volume coverage in the specified detection time essentially precludes the use of a pencil beam antenna. Fortunately, target elevation information is not required, so that elevation coverage by means of a fan-shaped beam encompassing the entire elevation sector during a single azimuth scan is acceptable. The antenna analysis presented here, therefore, considered the use of a fan beam or shaped elevation beam design based on the dimensional parameters of the current AN/VPS-2 pencil beam reflector antenna.

3.3.1 AN/VPS-2 ANTENNA PARAMETERS

General Electric data indicate that the current AN/VPS-2 antenna provides a pencil beam with an azimuth beamwidth of 4.1° and an elevation beamwidth of 4.3°. The reflector dimensions are approximately 24 inches horizontally and 24 inches vertically, and the net antenna gain (measured) is 33 dB. The antenna peak sidelobes are at least 24 dB below the main lobe in both principal planes. One design contraint imposed by General Electric was that the new antenna be approximately the same size as the current AN/VPS-2 antenna because of vehicle space limitations.

3.3.2 MODIFIED AN/VPS-2 ANTENNA PARAMETERS

A fan beam that has a 3 dB beamwidth to effectively cover the entire 30^{o} elevation sector will not have sufficient gain to enable the AN/VPS-2 to detect aircraft at 15 kilometers range. Since targets of interest will most certainly be at relatively low altitudes such that their range is very small at high elevation, it is acceptable to use a shaped elevation beam which has reduced gain at higher elevation; such an antenna pattern was assumed for the modified AN/VPS-2 radar.

A cosecant-squared antenna pattern yields a power pattern (gain) response which, above the upper 3 dB point of the elevation main beam, is proportional to the square of the cosecant of the elevation angle. If the radar is to be used in an environment where there is little clutter and no unwanted targets at close ranges, such an elevation pattern is ideal since a constant altitude aircraft (presuming it is above the elevation angle of the peak of the beam) produces a constant signal return regardless of range.

For a pencil beam, the return from rain clutter, for example, varies with range R as $1/R^2$ (since the return is related to the volume of the clutter cell). For a pencil beam antenna pattern the aircraft return will vary as $1/R^4$ because of the range term in the denominator of the radar equation and, therefore, the aircraft return will increase faster than the rain clutter return as the range is decreased. For the cosecant-squared gain pattern, however, the target return remains constant, so the rain clutter return will overwhelm the aircraft return at close ranges. A cosecant gain pattern will produce an aircraft return which varies in the same way that the rain return varies, so that the aircraft-to-rain-clutter power ratio will remain constant, and detection can be maintained.

Georgia Tech's antenna analysis, therefore, considered both cosecant-squared and cosecant elevation gain variations and the resulting effect on the overall peak gain of the antenna. The analysis assumed a Gaussian main beam elevation pattern with the shaped portion of the pattern beginning at the upper 3 dB point (θ_0) and continuing to a maximum elevation angle of θ_m as shown in Figure 10. The main beam normalized gain pattern is described by the equation

$$G(\theta) = e^{-0.693\ (\theta/\theta_3)^2}, \qquad (1)$$

where θ_3 = one-half of the 3 dB beamwidth $(BW_3/2)$. The normalized gain pattern of the shaped portion $(\theta_0 \leq \theta \leq \theta_m)$ is given by

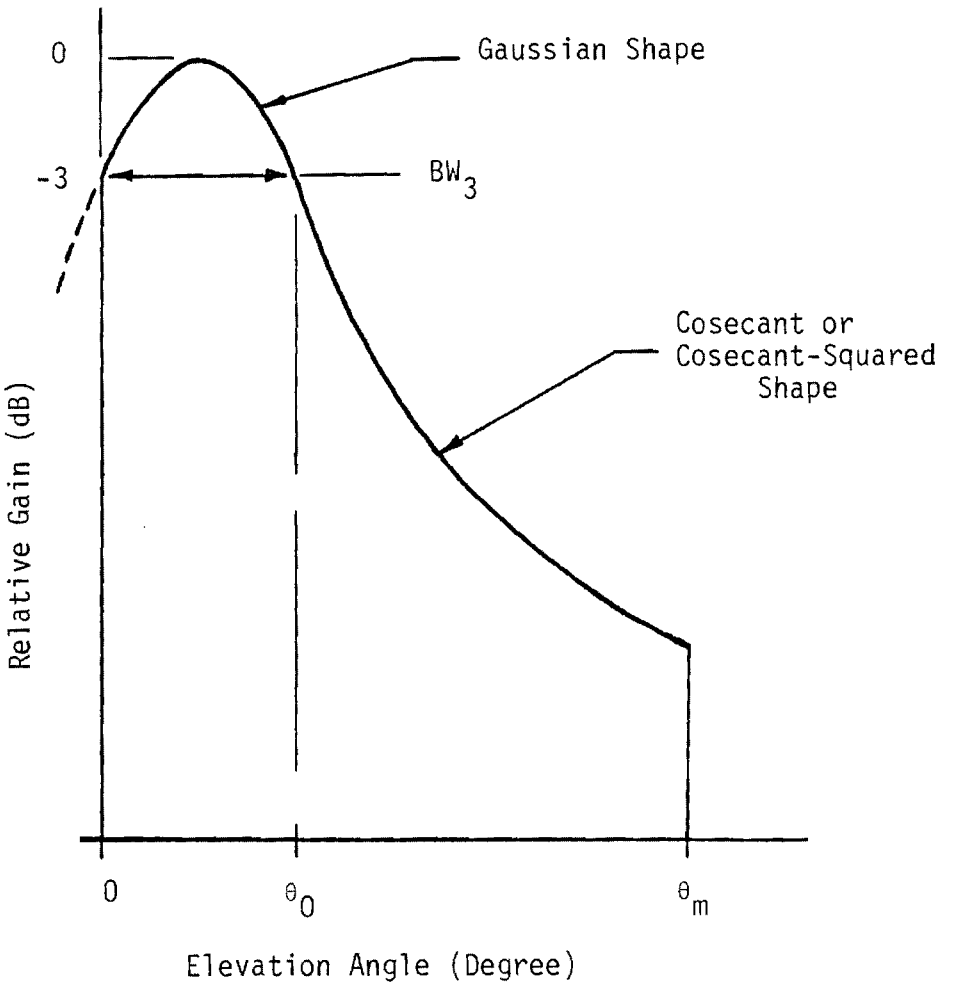

Figure 10. Shaped Antenna Pattern Approximation for Gian Loss Calculations.

$$G(\theta) = \frac{\csc \theta}{2 \csc \theta_0} \tag{2}$$

for cosecant shaping and

$$G(\theta) = \frac{\csc^2 \theta}{2 \csc^2 \theta_0} \tag{3}$$

for cosecant-squared shaping. The factor of two in the denominator accounts for normalizing the shaped pattern to the -3 dB level of the main beam pattern.

The peak gain of the shaped pattern relative to that of the unshaped pattern is given approximately by the ratio of the integrals of the two patterns over the angles of interest, since the energy placed in the shaped portion must have come at the expense of the energy in the main beam. The result for the cosecant pattern is

$$G_R = \frac{0.807\theta_0 + 0.5 \sin\theta_0 (\ell n \tan \theta_m/2 - \ell n \tan \theta_0/2)}{0.807\theta_0} \tag{4}$$

and for the cosecant-squared pattern is

$$G_R = \frac{0.807\theta_0 + 0.5 \sin^2\theta_0 (\cot \theta_0 - \cot \theta_m)}{0.807\theta_0}. \tag{5}$$

Assume that a reflector with approximately the same dimensions as that of the current AN/VPS-2 antenna is employed and that the reflector is shaped to provide the diversion of energy necessary to produce a shaped elevation beam. The main beam of the modified antenna will have essentially the same 3 dB beamwidths as that of the present antenna, but a relative gain loss will exist which is proportional to the chosen elevation beam shaping parameters. The AN/VPS-2 elevation beamwidth is 4.3°. Assume a slight increase in the elevation aperture (to about 26 inches) to give an elevation beamwith of 4.0°. The peak gain relative to AN/VPS-2 will increase by 0.3 dB. However, it is desirable from system considerations to have a 5° azimuth beamwidth in order to collect sufficient pulses for processing. Reducing the AN/VPS-2 antenna's horizontal aperture to about 20 inches to accomplish this results in a gain loss of 0.9 dB. The net gain change due to modifying the aperture dimensions is thus -0.6 dB. By placing the lower 3 dB point

of the elevation beam on the horizon, θ_0 becomes 4°. The resulting gain loss due to shaping alone for two representative values of θ_m (the maximum elevation coverage angle) is given in Table 4 below:

TABLE 4. GAIN LOSS DUE TO ELEVATION PATTERN SHAPING

θ_m	Cosecant Shaping	Cosecant-Squared Shaping
20°	3.0 dB	1.8 dB
30°	3.5 dB	1.9 dB

The maximum possible net gain of the modified antenna, based on the 33 dB gain value for the present antenna and the 0.6 dB decrease due to the new aperture dimensions is given in Table 5.

TABLE 5. GAIN OF OPTIMIZED AN/VPS-2 ANTENNA

θ_m	Cosecant Shaping	Cosecant-Squared Shaping
20°	29.4 dB	30.6 dB
30°	28.9 dB	30.5 dB

3.4 RECEIVER

3.4.1 FRONT-END COMPONENTS

The receiver design of the modified AN/VPS-2 incorporates two significant changes to the original configuration. A low noise RF preamplifier improves the receiver noise performance of the modified receiver, and a decreased bandwidth IF amplifier, matched to the lengthened transmitted pulse, further decreases the noise level of the receiver output signal.

The front end of the AN/VPS-2 receiver has a noise figure of 13 dB. The contributors are the preselector filter (0.7 dB), the TR limiter (0.4 dB), the diode switch (0.7 dB), and the mixer-preamplifier (11.2 dB). The preselector subassembly has a 3 dB bandpass between 9.135 and 9.265 GHz and eliminates RF signals outside the frequency

range of the radar. The TR limiter subassembly protects the mixer-preamplifier from high level RF signals that might be present due to reflections from nearby metal buildings or vehicles. The diode switch subassembly protects the mixer-preamplifier during the transmission of the radar pulse. These three subassemblies will be retained in the modified AN/VPS-2 radar configuration.

The new RF preamplifier precedes the modified downconversion process and essentially establishes the noise figure for the radar receiver, since the GFET amplifier has a power gain of 29 dB. The actual unit selected by Emtech is a Narda model N6244S-713, an X-band, gallium arsenide amplifier advertized by the manufacturer as an off-the-shelf item. Narda has promised a noise figure of 2.4 dB for this model, which, when combined with the three other sub-assemblies, results in a net 4.2 dB noise figure for the modified AN/VPS-2 radar receiver.

The IF amplifier need only have a bandwidth of approximately 0.5 MHz when matched to the longer 2 μsec pulse length. Thus, the noise content of the radar signal passing through the receiver will be significantly decreased, since the AN/VPS-2 amplifier is matched to the 0.28 μsec pulse length currently employed.

3.4.2 RECEIVER DESIGN

A limited scope evaluation of basic receiver design was made to assess the relative advantages and disadvantages of a homodyne receiver as opposed to the heterodyne receiver of the AN/VPS-2. The conclusion was reached that a heterodyne receiver is technically superior to a homodyne receiver for this radar application.

Homodyne receivers are characterized by a local oscillator (LO) set at the frequency of the transmitted signal. The LO signal and the received radar return signal are electrically combined in a mixer assembly that yields a set of sum and difference intermediate frequencies (IF) of these signals and their harmonics. The lowest difference frequency returns the modulation to baseband. For this pulsed radar, this baseband signal will be composed of the transmitted pulse envelope modulated by target and clutter reflectivity effects.

Heterodyne receivers are characterized by a local oscillator set at a fixed offset from the transmitted signal frequency. The LO and received radar signals are mixed, producing an intermediate frequency signal centered at the offset frequency, plus all the usual sum and difference frequencies of the harmonics. The IF signal is then usually amplified prior to second detection (demodulation) to baseband.

The homodyne receiver usually employ amplification at RF, while heterodyne receiver amplification is performed at IF. An IF amplifier operating at a fixed center frequency can be straightforwardly designed for optimal performance with a bandwidth matched to the transmitted pulse length (e.g., BW = 1 MHz for a 1 μsec pulse length). The RF amplifier, however, must cover all possible transmission frequencies, (e.g., 9.135 to 9.265 GHz for the AN/VPS-2), resulting in significantly more noise into the receiver than the heterodyne case.

If the homodyne receiver employs no RF amplification at all (to avoid this high noise input), then the received signal into the mixer assembly will be small. The mixer's response to low level received signals will be in the non-linear region of the mixer transfer function, resulting in less than maximum output signals. The resulting low signal-to-noise ratio cannot be adequately compensated for by video amplification. Furthermore, video amplification would add another noise increment because noise power increases as the inverse of frequency for amplification performed at these low baseband frequencies.

The conclusion is that the heterodyne receiver is technically superior to the homodyne receiver for this coherent, surveillance radar application. The higher output signal-to-noise power ratio of the heterodyne makes it the preferred receiver configuration.

3.4.3 STC AND AGC

Sensitivity time control (STC) is a desired radar feature for the modified AN/VPS-2 system configuration. This function compensates for the range dependency of the reflected power from an airplane as the plane closes in on the radar position. Thus, for a pencil beam antenna, the STC function compensates for a $1/R^4$ range dependency, where R is the slant range to the aircraft. For the shaped beam desired for the modified AN/VPS-2 radar, the STC range dependency will be less severe than the inverse fourth power of range, since the airplane target return will not change as rapidly as $1/R^4$.

The STC function, in effect, keeps aircraft returns within the receiver dynamic range, i.e., above the noise floor and below receiver saturation. A gated automatic gain control (GAGC) performs the same function by sampling the aircraft return level and setting the amplifier gain accordingly. However, such an operation is clearly not possible in search mode, since the aircraft position is not known a priori. The GAGC is more properly a track mode function.

Therefore, STC is the preferred function for maintaining target returns within the receiver dynamic range for the modified AN/VPS-2 system. Gated AGC is not appropriate for a surveillance radar function.

3.5 MODIFIED AN/VPS-2 SIGNAL PROCESSOR

3.5.1 INTRODUCTION

The main function of the modified AN/VPS-2 signal processor is to detect aircraft at the speeds and ranges of interest (see Table I). This requirement implies that the processor should: (1) reject radar returns from stationary targets and clutter, and (2) maximize the moving-target probability of detection. Two generic classes of radar signal processors satisfy the first requirement, moving-target-indication (MTI) signal processors and pulse-Doppler (PD) signal processors. Both classes of processors separate moving targets from fixed clutter background through exploitation of the Doppler effect, which, applied to the radar problem, states that the echo signal received from a moving target is shifted in frequency relative to the transmitted signal by an amount proportional to the radial speed of the target. Thus, moving target discrimination is accomplished by simply ignoring (filtering out) all zero-frequency-shifted received signals, presumably reflected from stationary targets and clutter.

The second requirement, i.e., maximizing moving-target probability of detection, implies narrow-band filtering of the received moving target signal to maximize the signal-to-noise ratio (SNR). Narrow-band filtering is the only way to realize the full coherent integrated SNR gain obtainable with the AN/VPS-2 system. Of the two generic classes of processors discussed, only the PD processor achieves narrow-band filtering of the received moving target signal. This processing is accomplished by employing either a bank of contiguous (in frequency) Doppler filters or a discrete or fast-Fourier-transform (FFT) algorithm. Therefore, the modified AN/VPS-2 signal processor should be a PD processor.

Since a radar operating at a single pulse repetition frequency (PRF) would be unable to unambiguously detect targets at all specified aircraft speeds and ranges of interest, a multiple PRF radar system is required. The recommended modified AN/VPS-2 signal processor will use two PRF's, alternated every one-half beam dwell. Therefore, within one beam dwell, an aircraft is illuminated by the radar in both PRF modes. This technique eliminates all range ambiguities and blind speeds within the specified aircraft ranges and speeds.

The recommended modified AN/VPS-2 signal processor is a PD processor consisting of a synchronous (I and Q) detector, analog-to-digital(A/D)converters, digital-delay-line cancellers (to reduce signal dynamic range), FFT processors, and magnitude detectors. A block diagram of this processor is shown in Figure 9. This processor is a variant of the moving target detection (MTD) processor conceived by Muehe.[4] A detailed description and predicted performance of the modified AN/VPS-2 processor are discussed in the following sections.

3.5.2 THEORY OF OPERATION

In a coherent radar, both amplitude and phase information are retained in the intermediate frequency (IF) signal. This information is extracted by splitting the IF signal into two phase-quadrature channels. In the in-phase (I) channel, the IF signal is applied directly to a linear (phase) detector which converts the IF signal to a video signal. In the quadrature (Q) channel, the IF signal is phase shifted by 90^{o} with respect to the I channel before it is applied to the linear detector. This two (phase-quadrature) channel detection is called synchronous detection. The signals in these two channels represent the rectangular coordinate system components of the complex video signal. The video outputs of both channels are sent through a sample-and-hold circuit and an A/D converter, and then are introduced into the digital-delay-line canceller (DDLC).

The DDLC is essentially a comb-filter which filters out all signals with frequencies equal to zero, to the PRF, and to multiples of the PRF by comparing returns from contiguous pulse repetition intervals. Returns that have a Doppler frequency shift equal to zero, to the PRF, or to multiples of the PRF (as will be the case with stationary clutter) will have the same unmodulated amplitude from pulse to pulse. Thus, by simply subtracting the returns from two contiguous pulse repetition intervals, as is done in a simple single-stage DDLC, these particular signals are cancelled, i.e., filtered out. Returns from radially moving targets will be modulated by their Doppler frequency and thus will not cancel out (unless that Doppler frequency is equal to the PRF or a multiple of the PRF). The number of stages and the configurations and weightings of the feedback (comparison) loops among the stages will determine the actual frequency response of the DDLC. The filtered output signal from the DDLC is then introduced into an N-point FFT processor. The use of a DDLC before the FFT processor eliminates stationary clutter and reduces the dynamic range required of the FFT processor.

The sample-and-hold circuit samples the return video at a rate commensurate with obtaining one sample within each of the M range resolution cells contained within one pulse repetition interval (PRI). After these samples are digitized by the A/D converter and filtered by the DDLC, they are stored in the buffer memory of the N-point FFT processor. This process is repeated N times (for N PRIs) so that N x M digital words, i.e., numbers, are stored in the buffer memory. The FFT processor then begins computing an N-point FFT for each of the M range bins while the next set of N x M digital words are being stored.

The N-point FFT processor will take N samples of the complex video signal (2N numbers) sampled at rate R_s (in this case the PRF) for a time $T=N/R_s$, perform a discrete Fourier transform on these samples, and arrange the results at N discrete frequencies of magnitude k/T (where k is an integer) extending in frequency from $-R_s/2$ to $+ R_s/2$. These results, or outputs, of the N-point FFT processor are N, complex-valued (2N real-valued) numbers, i.e., an I and Q channel for each of the N discrete frequencies. The frequency-domain magnitude and phase diagrams of the video signal can then be constructed from these N complex-valued numbers. Of interest here is only the frequency-domain magnitude diagram, i.e., frequency magnitude spectrum, which is determined in the magnitude detector by taking the square root of $I^2 + Q^2$ for each discrete frequency.

The frequency resolution of the FFT processor is 1/T, i.e., a signal whose frequency f is in the frequency range of bin n, i.e.,

$$\frac{n - 1/2}{T} < f < \frac{n + 1/2}{T} \tag{6}$$

will appear in the output of the FFT processor at frequency n/T. This signal will also appear in other bins due to the finite sampling time, T, which causes the filter response of any given bin to have frequency sidelobes; however, this effect can be minimized with appropriate window weighting (e.g., Hamming) to reduce the sidelobe levels. The maximum unambiguous frequency determinable by the FFT processor is $\frac{R_s}{2}$, and higher signal frequencies present will be "folded over" into the FFT processor's frequency interval $[-R_s/2, R_s/2]$, i.e., an arbitrary frequency, $f = kR_s + f'$, where k is an integer and $-R_s/2 \leq f' \leq R_s/2$, will appear in the frequency bin containing f'.

The output from each of the N magnitude detectors is then sent to a constant false alarm rate (CFAR) and thresholding circuit. The output of this circuit can be sent through a digital-to-analog (D/A) converter, then displayed.

The recommended modified AN/VPS-2 signal processor will operate in a dual PRF mode such that a target is illuminated by one PRF for the first half of a beam dwell and by the other PRF for the second half. As discussed below, this dual PRF mode eliminates "blind speeds" in the range of specified target speeds.

3.5.3 PRF SELECTION

The modified AN/VPS-2 radar system must detect targets moving with radial speeds up to 320 m/s at ranges of up to 15 km. As discussed above, targets moving with a speed V such that its Doppler frequency shift $f_d = 2V/\lambda$ is an integer multiple of the radar's PRF, where λ is the transmitter wavelength, will be "blind" to the radar. The radar's PRF must, therefore, be greater than 19.7 kHz for the first blind speed to be greater than 320 m/s.

A radar's maximum unambiguious detection range is also determined by its PRF. To determine range unambiguously, the echo from a target illuminated by a given transmitted pulse must be received by the radar before the next pulse is transmitted. The radar's PRF must be equal to or less than 10 kHz for a maximum unambiguous range of 15 km. Therefore, no single PRF will satisfy <u>both</u> the target speed and range requirements of the modified AN/VPS-2.

The detection strategy employed in the recommended modified AN/VPS-2 signal processor is to implement a dual PRF capability. One PRF is chosen to be 10 kHz and the other PRF is chosen to be less than 10 kHz so that range ambiguities are eliminated. Blind speeds are eliminated by the two PRF's, i.e., a target speed that is a blind speed to the radar at one PRF is not a blind speed at the other PRF.

The <u>minimum</u> value of the lower PRF is determined by the dwell time on the target. The 2-second target unmasking requirement dictates an 180 degrees/second antenna scan rate, which, when coupled with the 5 degree azimuth antenna beamwidth results in a 27.8 ms dwell time. At a PRF of 10 kHz, 139 pulses are received in one-half of the beam dwell time. These are enough pulses for a 128-pt. FFT processor preceded by up to an 11-pulse DDLC. The minimum value of the lower PRF will now depend on the size of the DDLC chosen. For example, a 3-pulse canceller followed by the 128-pt. FFT requires 130 pulses, which takes 13 ms at the 10 kHz PRF. This leaves 14.8 ms at

the lower PRF to obtain the 130 pulses, or a minimum lower PRF of 8.79 kHz. The minimum lower PRFs associated with various size cancellers are shown in Table 6.

The maximum value of the lower PRF will depend on the frequency response curve of the digital-delay-line canceller, in that the PRF's should be chosen so that there is little or no overlap between the minimum response portions (notches) of the response curves at the two PRF's.

An example of a DDLC that is acceptable for use with the modified AN/VPS-2 processor is one built by General Dynamics for the I^2 SOTAS radar system.[5] This is a five-pulse DDLC with a 4-pole Butterworth frequency response H(f),

$$\left|H(f)\right|^2 = \frac{1}{1+\left(\frac{f_o}{f}\right)^8}, \qquad -\frac{PRF}{2} < f < \frac{PRF}{2} . \tag{7}$$

where f_o is a specified corner frequency. The minimum cut-off frequency f_o of this DDLC is PRF/30, giving a blind speed notch width for a 10 kHz PRF of 667 Hz. The maximum lower PRF permitted without notch overlap is given by

$$10000 - PRF = \frac{10000 + PRF}{30} \tag{8}$$

or

$$PRF = 9.36 \text{ kHz}. \tag{9}$$

As shown in Table 6, the minimum lower PRF for a 5-pulse canceller is 9.05 kHz. Thus, for this DDLC, a lower PRF in the range of 9.05 to 9.36 kHz is acceptable. The time-averaged filter responses for this DDLC and for a standard 3-pulse canceller for PRFs of 9.36 and 10 kHz are shown in Figure 11. The two PRF's assumed in the analysis conducted on the modified AN/VPS-2 signal processor were 9.36 kHz and 10 kHz.

3.5.4 PROCESSING SPEED REQUIREMENTS

The number of FFT's to be performed during one-half of a beam dwell will equal the number of range cells to be processed. The range resolution of the modified

TABLE 6. MINIMUM LOWER PRF's FOR VARIOUS SIZE DDLC's FOLLOWED BY A 128-PT FFT

N-PULSE CANCELLER (number of pulses)	NUMBER OF PULSES REQUIRED	MINIMUM LOWER PRF (kHz)
2	129	8.66
3	130	8.79
4	131	8.92
5	132	9.05
6	133	9.18
7	134	9.31
8	135	9.45
9	136	9.58
10	137	9.72
11	138	9.86
12	139	10.00

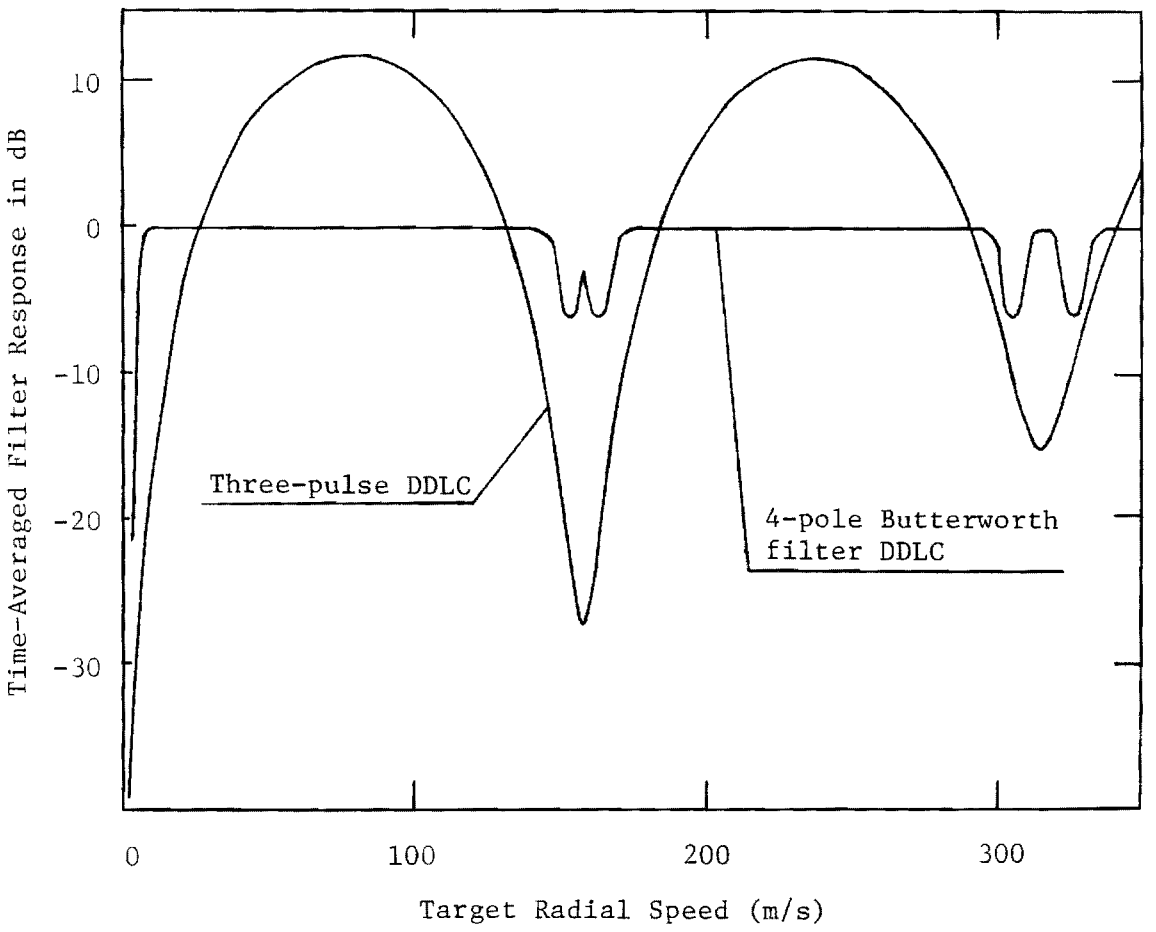

Figure 11. Time-averaged filter response of three-pulse DDLC and 4-pole Butterworth filter DDLC.

AN/VPS-2 with its $2\mu s$ pulse length is 300 m, resulting in 50 range cells over the 15 km range interval. The radar's 27.8 ms dwell time and the fact that 50 128-pt FFT's must be performed during one-half of a beam dwell result in a 0.28 ms FFT processing time. Discussions with various FFT vendors (see Appendix A) indicate that 128-pt. FFT processors with approximately 0.5 ms processing times are readily available. Faster speeds are obtainable but at a higher cost penalty.

To reduce the processing speed further, returns from two contiguous range cells will be summed before FFT processing. This summing gives 25 range cells and a resulting FFT processing time of 0.56 ms. However, range resolution is now decreased to 600 m and an additional 3 dB collapsing loss is incurred. A $1\ \mu s$ pulse length operating mode for the modified AN/VPS-2 radar was also considered. In this mode, returns from four contiguous range cells will have to be summed, resulting in a 6 dB collapsing loss.

3.5.5 IMPROVEMENT FACTOR ANALYSIS

A quantitative measure of the MTI or PD processor's ability to separate moving targets from stationary clutter is the improvement factor I. The MTI improvement factor is conventionally defined as the signal-to-clutter ratio (SCR) at the output of the MTI processor divided by the SCR at the input, averaged uniformly over all target radial velocities, i.e., Doppler frequencies of the target. Thus, the MTI improvement factor is an average measure of the performance of the MTI radar and does not indicate improvement performance for a specific target moving with a given radial speed. The Doppler return may occur for example, at a minimum response frequency of the MTI processor.

The PD improvement factor is defined as the SCR at the output of the processor divided by the SCR at the input. Since a PD processor provides target radial speed information, the magnitude of the improvement factor as a function of speed is of interest. Therefore, Doppler frequency averaging is not performed in the evaluation of the PD improvement factor.

The quantity that determines radar performance is the signal-to-interference ratio (SIR) where interference is noise power plus clutter power. The SIR at the output of the signal processor is

$$(SIR)_o = \left(\frac{S}{N+C}\right)_o = \left[\left(\frac{S}{N}\right)_o^{-1} + \left(\frac{S}{C}\right)_o^{-1}\right]^{-1} = \left[\left(I_N\left(\frac{S}{N}\right)_i\right)^{-1} + \left(I\left(\frac{S}{C}\right)_i\right)^{-1}\right]^{-1}, \quad (10)$$

where I_N is the gain in SNR due to the integration of N pulses, $(\frac{S}{N})_i$ is the SNR at the processor input, and $(\frac{S}{C})_i$ is the SCR at the processor input. Optimum detection performance is obtained when $I(\frac{S}{C})_i \gg I_N(\frac{S}{N})_i$, in which case $(SIR)_o \simeq (S/N)_o$. That this condition is satisfied is particularly important at maximum ranges where the SNR is a minimum and additional clutter interference effects cannot be tolerated. Shown in Figure 12 is the input SCR as a function of range for various values of clutter reflectivity σ^o. Here, a 2.15° antenna elevation pointing angle, a 4.3° antenna elevation beamwidth, an effective 600 m range resolution, and a standard refraction (4/3 earth radius) model are assumed. For the expected ranges of σ^o (-30 to -20 dB), the SCR varies from -32 to -42 dB. The integrated SNR, i.e., $I_N(\frac{S}{N})_i$, for the modified AN/VPS-2 at a range of 15 km is approximately 7 dB. Therefore, an improvement factor in the range of 50 to 60 dB would be desirable to eliminate clutter interference effects at maximum ranges.

Perfect PD processing performance requires a total elimination of the clutter signal. Any clutter residue present at the output of the processor results in a degradation of moving target detection performance. Clutter residue originates from two sources: (1) clutter spectral broadening and (2) imperfections (instabilities) in the radar system itself.

Radar system instabilities such as variations in transmitted power, pulse width, or frequency, and pulse-to-pulse timing errors will cause a degradation in moving target discrimination capability by spreading the received clutter energy throughout the PRF spectrum. Since this frequency-spread clutter power is noiselike, very little is cancelled by the DDLC. However, since this clutter signal does possess the statistics of noise, the effects of this clutter residue are reduced by the integration process in the FFT processor, which gives the integrated SNR upon which probability of moving target detection is ultimately based.

The ratio of this noiselike clutter C_N (due to transmitter instabilities) to the stationary clutter (i.e., clutter center around zero-Doppler frequency) in the received signal of the AN/VPS-2 is approximately -40 dB. That is, the ratio of received target signal to thermal noise plus this noiselike clutter can be written:

$$\frac{S}{N + C_N} = \frac{S/N}{1 + \frac{C_N}{N}} = \frac{S/N}{1 + \alpha \frac{C}{N}}, \qquad (11)$$

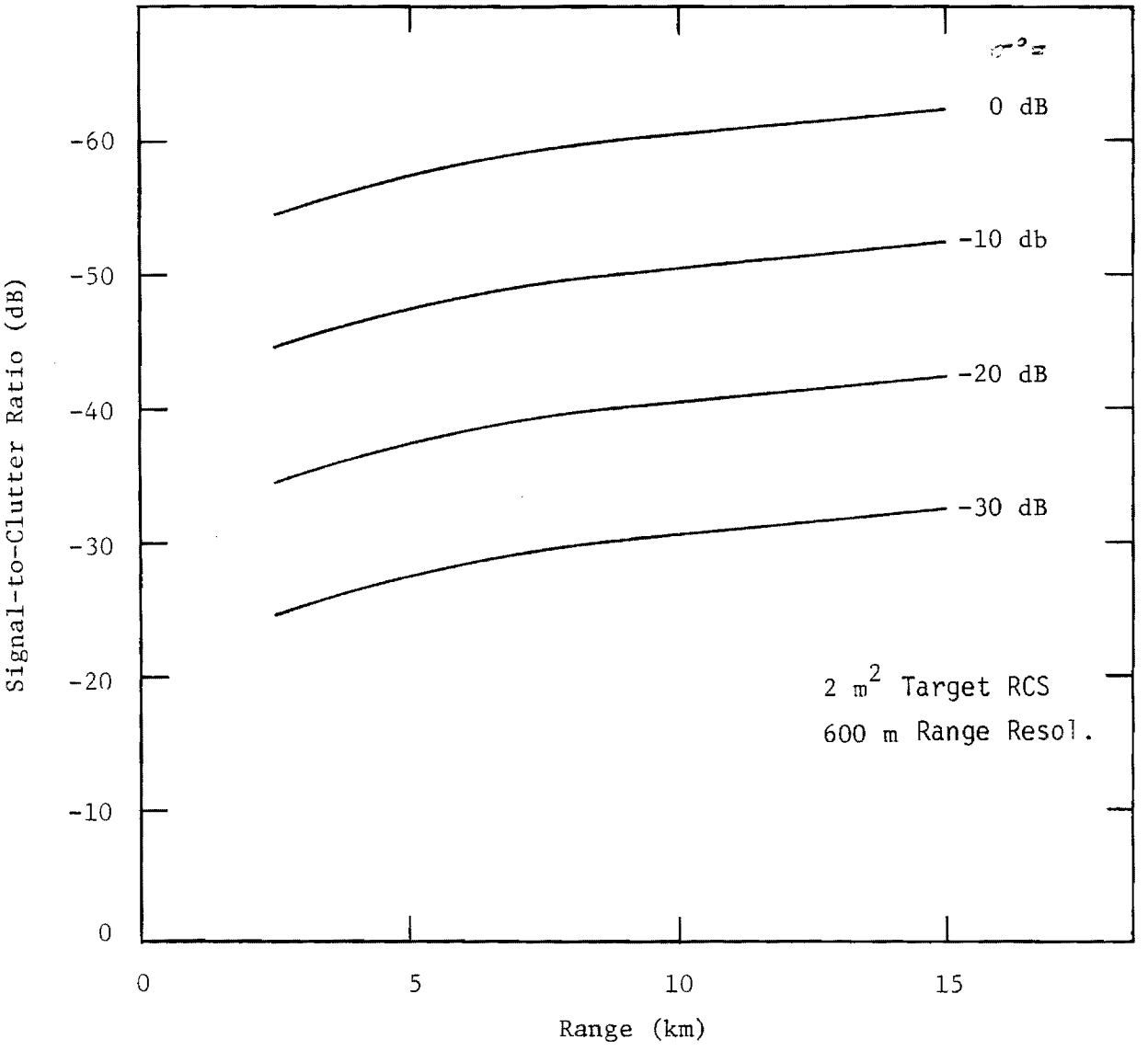

Figure 12. Received signal-to-clutter ratio versus range.

where C/N is the clutter-to-noise ratio and α = -40 dB for the AN/VPS-2 system. The quantity $1/\alpha$ is often referred to as the sub-clutter visibility (SCV) of the radar system.

The main contributions to clutter spectral broadening come from (1) scanning antenna motion, (2) radar platform motion, and (3) internal clutter motion. The modified AN/VPS-2 is assumed to be on a stationary platform; therefore, clutter spectral broadening due to platform motion is nonexistent.

The IF spectrum of the power return from extended stationary clutter is spread around the IF frequency due to the scanning antenna motion. The spectral power density function of this return can be assumed to be Gaussian, i.e.,

$$P(f) = P_o \exp -(f-f_{IF})^2/2\sigma^2 . \tag{12}$$

The standard deviation in frequency σ due to antenna motion is given by

$$\sigma = 0.265\ \dot{\theta}/\theta_1 , \tag{13}$$

where $\dot{\theta}$ is the antenna scan rate and θ_1 is the one-way, 3 dB, antenna beamwidth. For $\dot{\theta}$ = 180 deg/sec and $\theta_1 = 5^o$, σ = 9.5 Hz which can be neglected for this evaluation.

The predominant contribution to clutter spectral broadening for the modified AN/VPS-2 radar will be from the internal motion of wind-blown tree foliage. Fishbein[6] measured the spectral response of coherent CW radar echos from wind-blown trees as a function of wind speed and found that the power spectral density at X-band is given by

$$P(f) = \frac{1}{1 + (f/f_c)^3} , \tag{14}$$

where:

$f_c = Ke^{\beta v}$ (Hz),

$K = 1.334$,

$\beta = 0.1356$ (knots)$^{-1}$,

v = wind speed (knots).

The spectral content of returns from wind-blown trees was also determined by Georgia Tech with a noncoherent, pulsed radar in a multi-frequency-radar measurement program.[7] This program revealed that the wind-speed effects are piecewise continuous and related to those sections of the trees which are in motion. An analysis of both the frequency spectrum and the autocovariance function reveals that the return contains a slowly varying time component and a fast fluctuating time component, as shown in Figure 13. The slow fluctuations are due to slow clutter motion from the branches of a wind-blown tree and generally follow a Gaussian distribution

$$P(f) = Ae^{-f^2/2\sigma_1^2}, \qquad f \leq 3 \text{ Hz} \tag{15}$$

where $\sigma_1 \approx 1.14$ Hz at X-band and is relatively insensitive to wind speeds above 3 mph. The fast fluctuations are due to wind-blown leaves, small twigs, and other rapidly moving objects, and (for X-band) are described by the cubic equation

$$P(f) = \frac{B}{1 + (f/f_c)^3}, \qquad f \geq 3 \text{ Hz} \tag{16}$$

where f_c is a function of wind speed. The value of the ratio A/B has been observed to be on the average about 15 dB. The value for the half-power spectral width f_c of 9 Hz used in Figure 13 for a 6-10 mph wind was obtained from the Georgia Tech data referenced. This value is somewhat larger than that obtained from Fishbein's equations above, even accounting for the spectral spread due to noncoherent detection. These values, A/B = 15 dB and f_c = 9 Hz, were used in the improvement factor analysis represented below and represent a worst case scenario for the stated wind speeds.

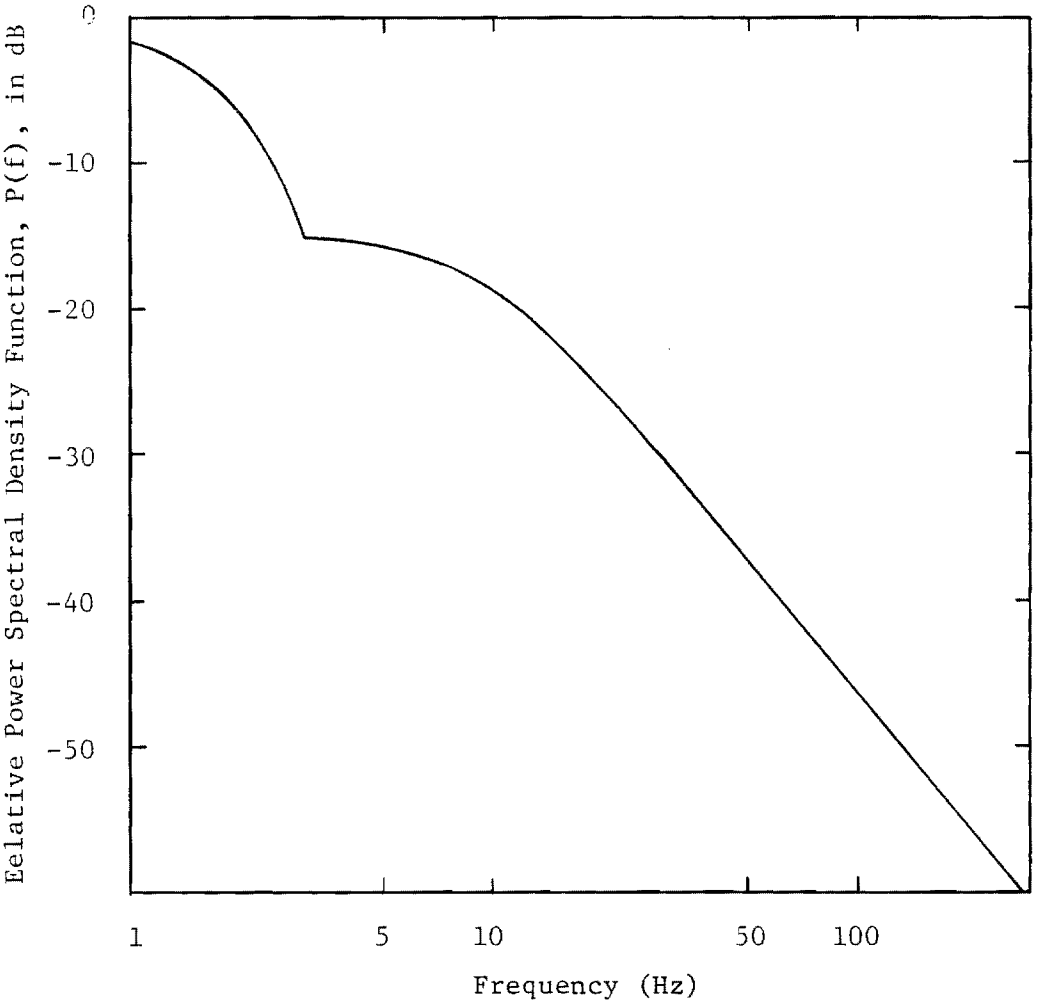

Figure 13. X-band spectral content of trees in a 6-10 mph wind.

The PD improvement factor as defined above can be written as

$$I = \frac{S_o}{S_i} \frac{C_i}{C_o} , \tag{17}$$

where S_o and S_i are the target signal powers out of and into the processor, respectively, and C_o and C_i are the clutter signal powers out of and into the processor, respectively. In this analysis, the assumption was made that the target signal resides entirely within one of the FFT frequency bins of the processor. Therefore, there is no loss in target signal out of the processor and

$$\frac{S_o}{S_i} = 1 . \tag{18}$$

The frequency response $\left| H_{FFT}(f) \right|^2$ of the target frequency bin of the FFT processor is shown in Figure 14, where a Dolph-Chebyshev weighting has been assumed. The mathematical model of this frequency response used in the improvement factor analysis is also shown in Figure 14. A modest frequency sidelobe level (FSL) of -30 dB was assumed.

The clutter power C_i into the processor is given by

$$C_i = \int_{PRF} P(f)\, df , \tag{19}$$

where the limits of integration are over one PRF interval, and P(f) is given by Equations (15) and (16). The clutter power C_o out of the processor is given by

$$C_o = \int_{PRF} \left| H_{MTI}(f) \right|^2 \left| H_{FFT}(f) \right|^2 \left(P(f) + \frac{\alpha C_i}{f_r} \right) df , \tag{20}$$

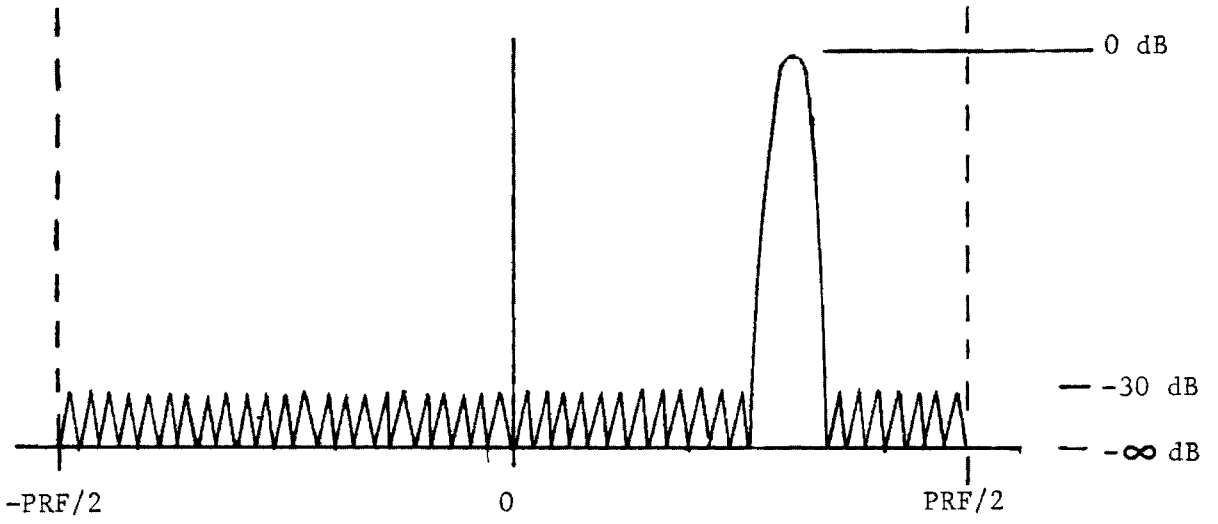

(A)

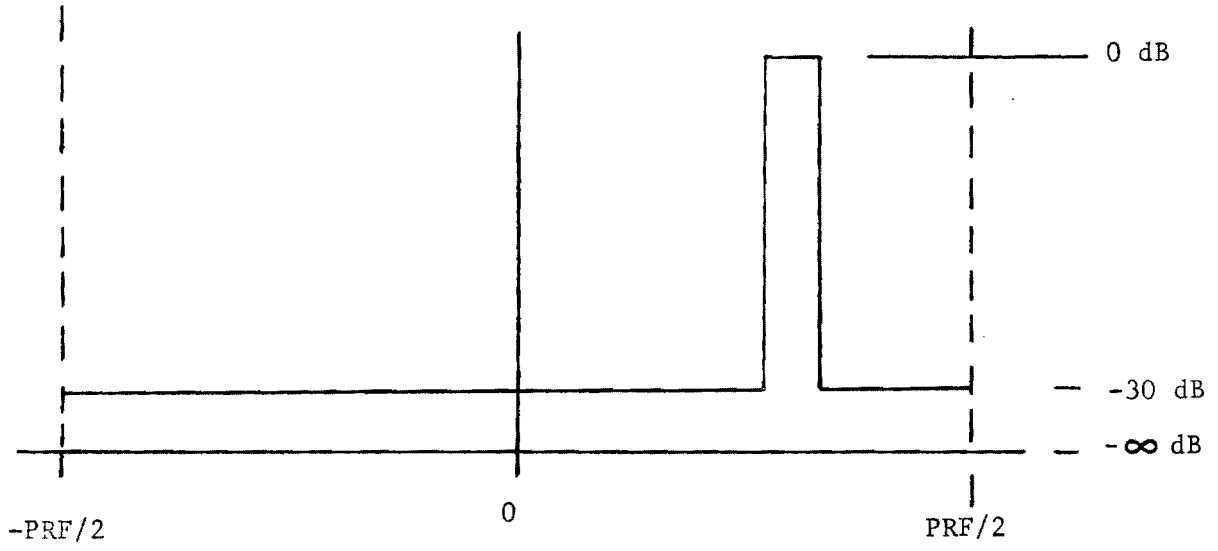

(B)

Figure 14. (A) Filter response of target frequency bin with Dolph-Chebyshev weighting applied. (B) Mathematical model of filter response of target frequency bin.

where $|H_{MTI}(f)|^2$ is the frequency response of the DDLC and f_r is the PRF. Thus, I is given by

$$I = \frac{\int_{PRF} P(f)\,df}{\int_{PRF} |H_{MTI}(f)|^2 |H_{FFT}(f)|^2 \left(P(f) + \frac{\alpha C_i}{f_r}\right) df} . \qquad (21)$$

The calculated improvement factor as a function of target radial speed is shown in Figure 15 for two DDLC/FFT configurations. The first configuration is a three-pulse canceller followed by a 128-pt. FFT. The frequency response of this canceller is given by

$$|H_{MTI}(f)|^2 = 16 \sin^4 \left(\frac{\pi f}{PRF}\right) . \qquad (22)$$

The second configuration is the five-pulse canceller mentioned above followed by a 128-pt. FFT. The frequency response of this canceller is given by Equation (7) and is modeled in this analysis as

$$H_{MTI}(f)^2 = \begin{cases} 1 & f \geq f_o \\ 10^{-6} & f \leq f_o \end{cases} , \qquad (23)$$

for $|f| \leq PRF/2$.

The improvement factor curves in Figure 15 were generated assuming $\alpha = -40$ dB and $f_r = 9.36$ kHz. Curves for both configurations asymptotically approach 61 dB, which is the limitation in improvement factor due to the remaining residue of the noise-like clutter ($1/\alpha = 40$ dB) after the 128-pt. FFT filtering (integration gain is 128 = 21 dB), i.e., $I_{max} = 40 + 21 = 61$ dB. From an improvement factor point-of-view, both configurations are adequate in that more than 50 dB of improvement factor is realized at the specified minimum radial speed of 15 m/s.

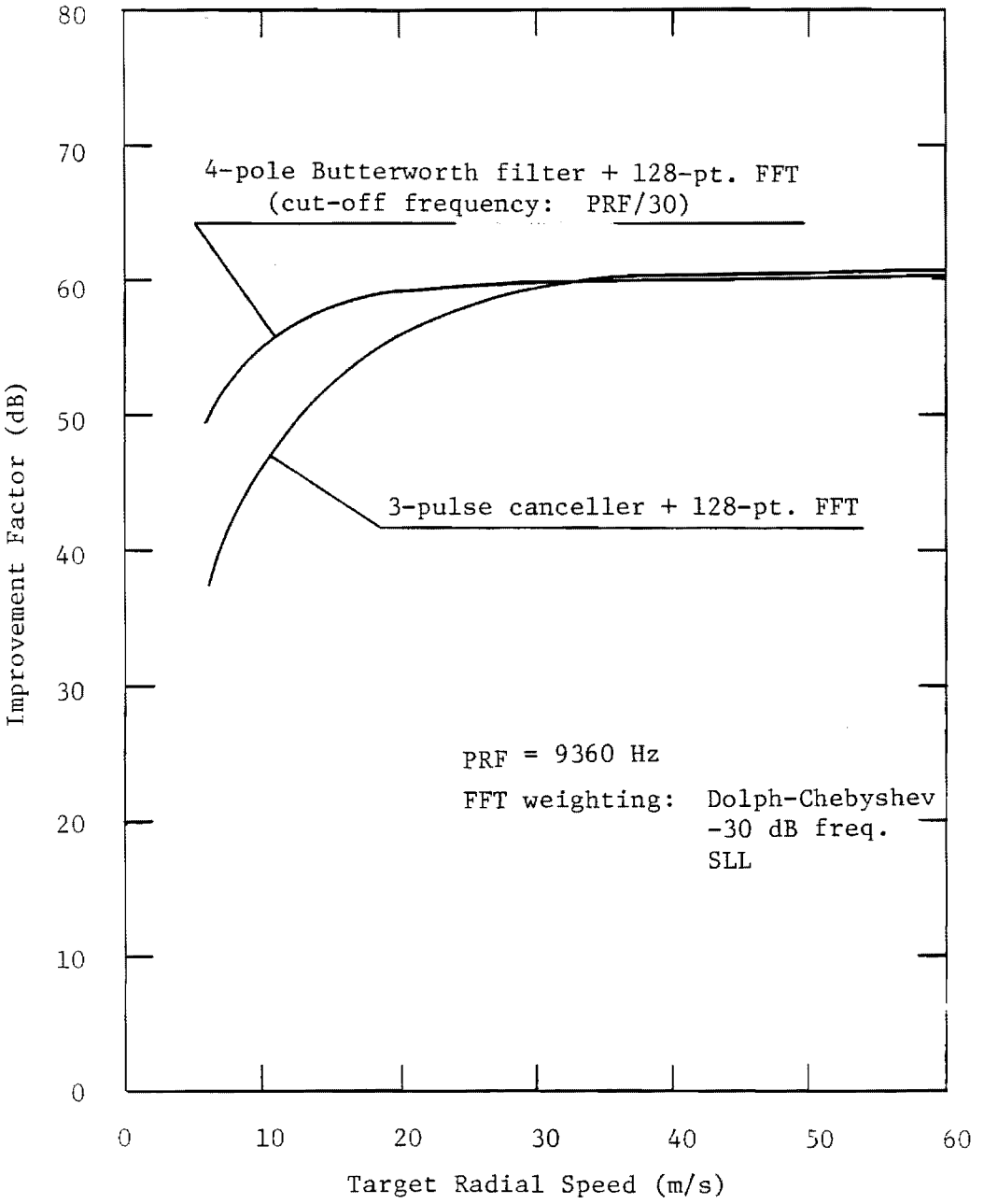

Figure 15. Improvement factor limitation due to internal clutter motion (trees: 6 - 10 mph wind) and system instabilities (SCV = 40 dB).

3.5.6 SIGNAL PROCESSING LOSSES

In addition to radar system losses mentioned in previous sections, there are additional losses associated with FFT processing, i.e., filter straddle, FFT weighting, and filter mismatch. Loss due to filter straddling occurs when the target return is not centered in one of the Doppler frequency bins. FFT weighting is necessary to reduce the level of frequency sidelobes. Otherwise, significant amounts of stationary clutter return can appear in higher frequency Doppler bins, resulting in reduced radar performance. A moderate -30 dB frequency sidelobe level, Dolph-Chebyshev weighting was assumed for this analysis. Filter mismatch occurs when the target return does not perfectly match the bandwidth of the processor Doppler bins. The amount of filter mismatch will depend on the target decorrelation time. The total FFT processing loss was assumed to be 3 dB for these three effects.

During one beam dwell, two 128-ppt. FFT's are performed. The output from these two FFT's are then summed together non-coherently. Since the SNR of the output signal from either of the FFTs will be large, the non-coherent summing of these two FFT signals will be approximately the same as coherent summing. However, a modest non-coherent summing loss of 0.5 dB was still assumed.

3.5.7 SUMMARY

The modified AN/VPS-2 signal processor is a pulse-Doppler processor consisting of a synchronous (I and Q) detector, A/D converters, digital-delay-line canceller (to reduce signal dynamic range), 128-pt. FFT processor, and magnitude detector. Both the three-pulse and five-pulse DDLC's, coupled with the 128-pt. FFT processor, yield adequate clutter suppression. However, the five-pulse DDLC is recommended due to its superior frequency response characteristics. The processor will operate in a dual PRF mode (9.36 and 10.0 kHz) such that the target is illuminated by one PRF for the first half of a beam dwell and by the other PRF for the second half. This dual PRF mode eliminates "blind speeds" in the range of specified target speeds.

A 3 dB collapsing loss, a 3 dB FFT signal processing loss, and a 0.5 dB non-coherent summing loss were assumed in the analysis of aircraft detection.

SECTION 4
MODIFIED AN/VPS-2 SURVEILLANCE PERFORMANCE

Georgia Tech evaluated the aircraft detection performance of the modified AN/VPS-2 surveillance function using the MERGE computer program detection performance capability. The radar and environment parameters used in this evaluation, listed in Table 3 in the previous section, represent a concensus of Emtech, Georgia Tech, and General Electric design concepts. The detection performance of an additional radar configuration was also evaluated, one employing a 1.5 kW peak power transmitted signal, 1 μsec pulselength, and integration of four consecutive range cells on receive. Both radar configurations were evaluated for clear air and 4 mm/hr rainfall conditions, 100 and 2000 ft aircraft altitudes, and 3 and 5 degree antenna tilt angles.

The graphs of probability of detection versus range included in this section differ somewhat in content from those shown in Section 2. The bottom graphs of each figure now represent single and multiple scan (cumulative) probability of detection. For an aircraft range exceeding 6 kilometers, the cumulative probability of detection is calculated for four consecutive antenna scans. Between four and six kilometer range, cumulative probability of detection is calculated for two consecutive scans. For ranges less than four kilometers, probability of detection is calculated on a single scan basis.

These multiple scan detection dependencies are reflected in break points of the higher value detection curve in the bottom graph. The lower value detection curve in the bottom graph represents the single scan probability of detection, for comparison. The break point in the single scan curve corresponds to the range at which the aircraft is coincident with the range to the radar horizon. The associated clutter return, which appears first at that range, degrades the detection of the aircraft, as noted by the dip in the detection curves there.

Figures 16 through 20 depict detection performance for the recommended configuration of the modified AN/VPS-2 radar against an aircraft flying at a constant 30 m (100 ft) altitude. The free space, 90 percent detection range of approximately 7 kilometers is less than the baseline AN/VPS-2 detection performance (compare Figure 1) primarily because of the new shaped pattern antenna, which has considerably decreased gain compared to the previously used pencil beam antenna gain. With all factors considered the 90 percent detection range is 14 kilometers, with a slight dip at 4

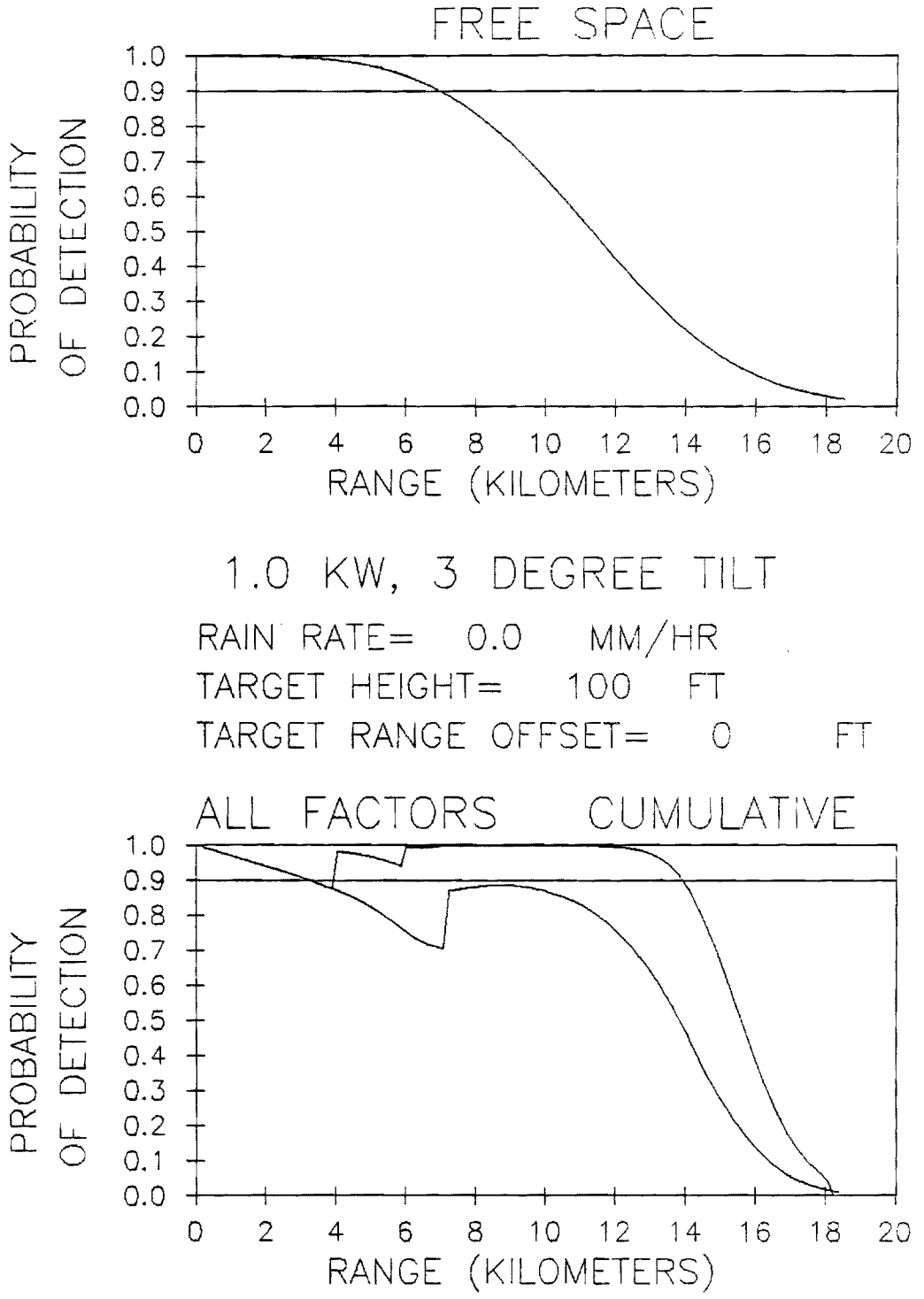

Figure 16. Recommended VPS-2 Configuration Detection Probability for 100 ft. Aircraft Altitude, Clear Air, 3 Degree Antenna Tilt.

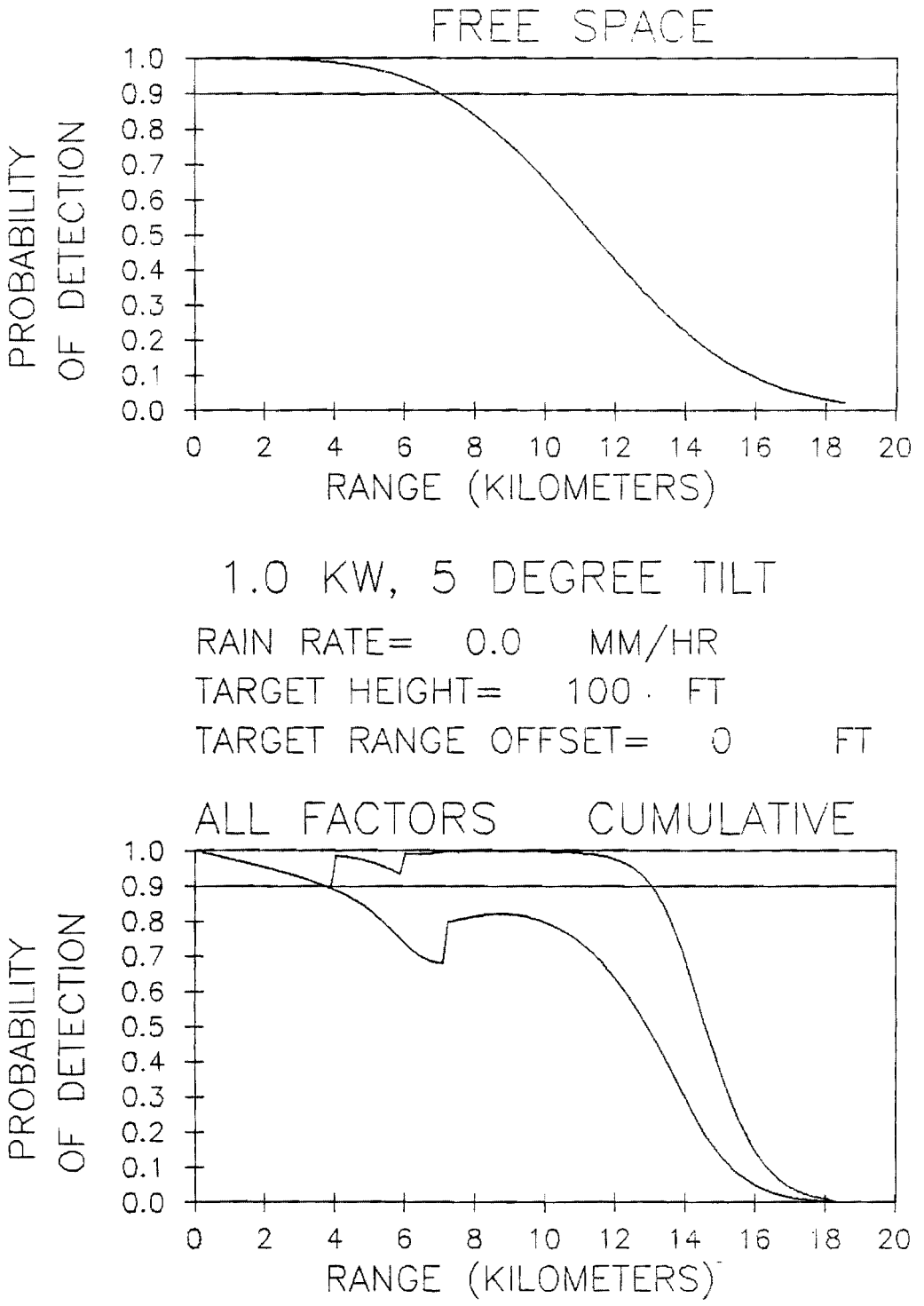

Figure 17. Recommended VPS-2 Configuration Detection Probability for 100 ft. Aircraft Altitude, Clear Air, 5 Degree Antenna Tilt.

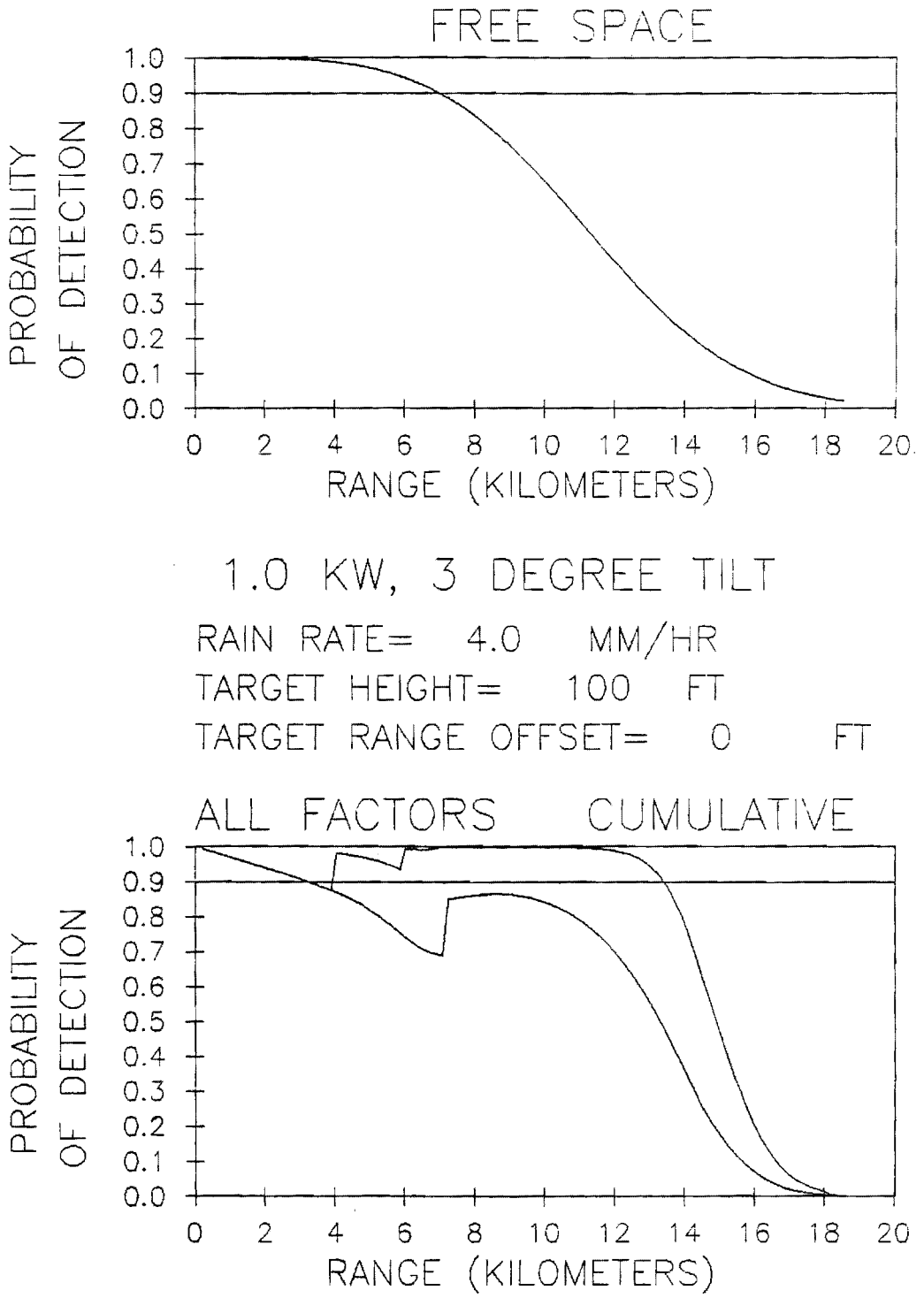

Figure 18. Recommended VPS-2 Configuration Detection Probability for 100 ft. Aircraft Altitude, 4 mm/hr Rain, 3 Degree Antenna Tilt.

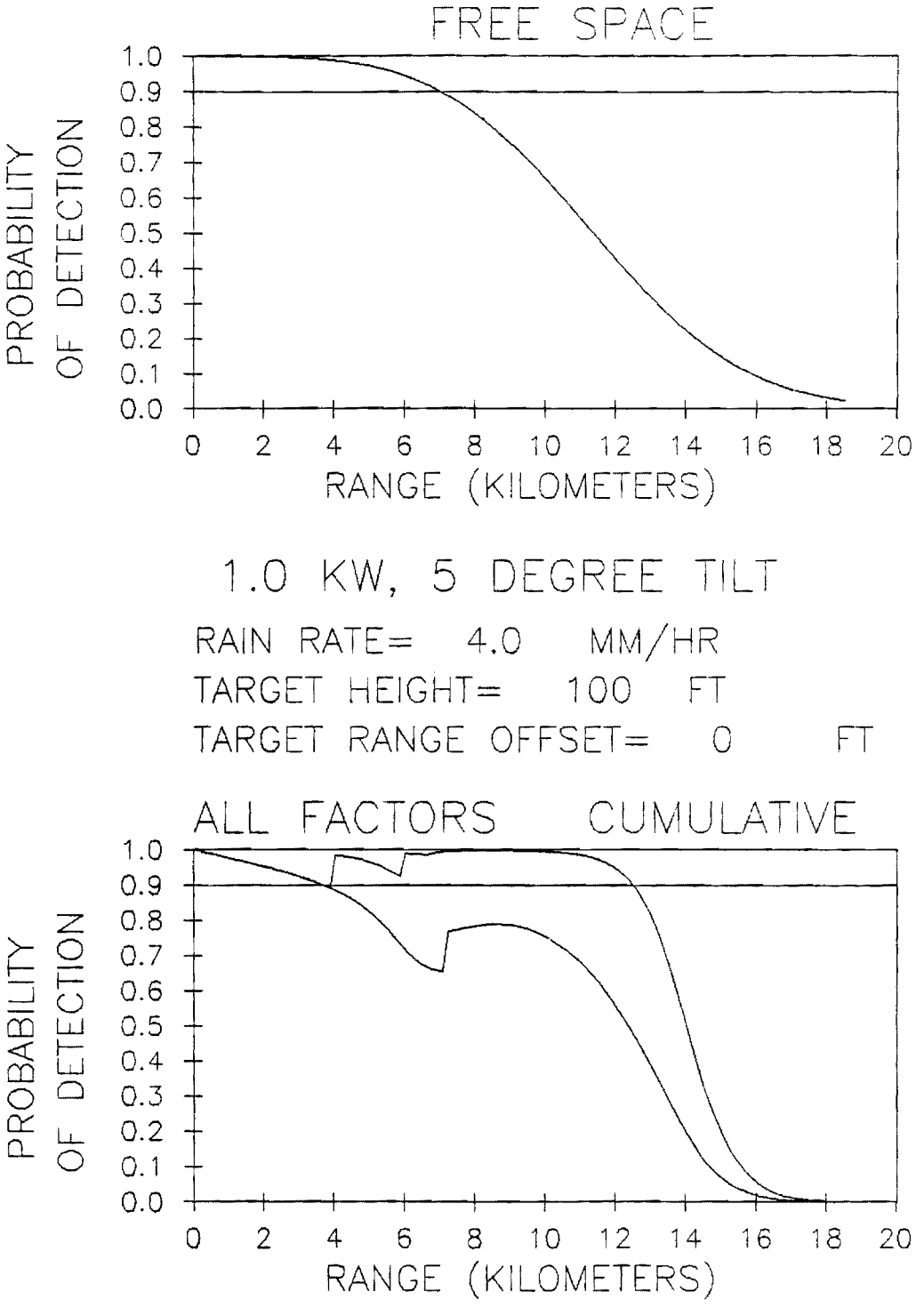

Figure 19. Recommended VPS-2 Configuration Detection Probability for 100 ft. Aircraft Altitude, 4 mm/hr Rain, 5 Degree Antenna Tilt.

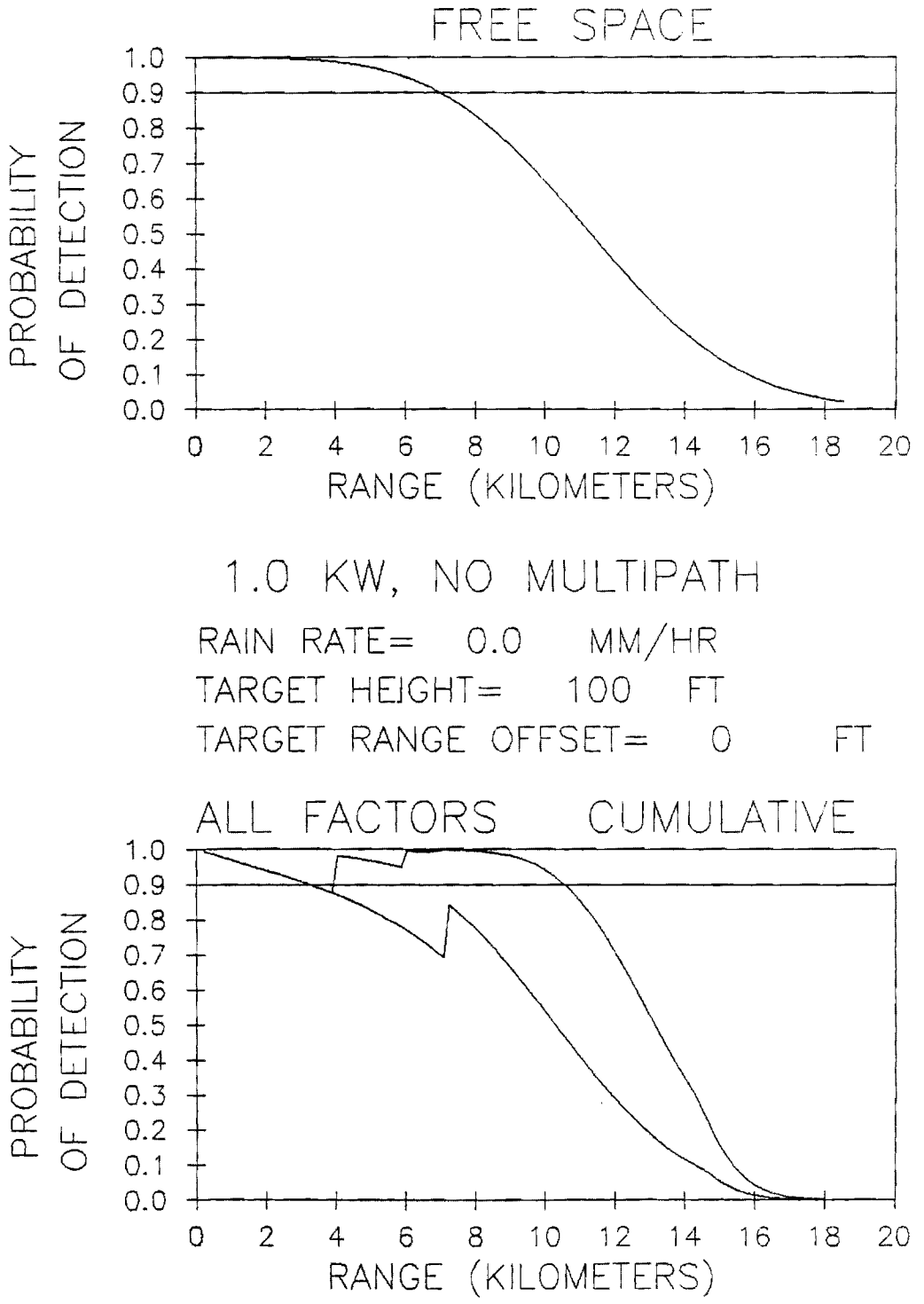

Figure 20. Recommended VPS-2 Configuration Detection Probability for 100 ft. Aircraft Altitude, Clear Air, 3 Degree Antenna Tilt, Multipath Interference Removed.

kilometers, where detection is defined on a single scan basis. Note the dip in the lower curve in the bottom graph at a range of approximately 7 kilometers, where the aircraft crosses the horizon range. With a higher, five degree antenna tilt the maximum detection range drops to 13 kilometers, but the dip in the detection curves observed in Figure 17 is not as significant.

Figures 18 and 19 depict detection performance in 4 mm/hr rainfall for a 30 m (100 ft) aircraft altitude. The nominal three degree tilt of the antenna elevation angle results in a maximum detection range of slightly less than 14 km, a slight range loss compared with clear air detection performance (see Figure 16). The slight dip in detection at four kilometers is, of course, still present. The higher antenna tilt sacrificies approximately one kilometer of detection range but improves the higher elevation angle (corresponding to nearer range) detection performance.

Figure 20 depicts detection performance with multipath interference effects removed. Since the maximum detection range is less than 11 kilometers under these conditions, multipath interference apparently enhances detection performance in low aircraft altitude, long range conditions.

Figures 21 through 25 depict detection performance for the modified AN/VPS-2 having a 1 μsec pulse length and 1.5 kW peak power. The free space detection range is less than six kilometers, compared with seven kilometers for the 1 kW, 2 μsec pulse length, recommended radar configuration. The lower range results from less average power and the higher collapsing loss in summing four rather than two consecutive range cell returns.

With all factors considered, the detection range for an aircraft flying in clear air at a constant 30 m (100 ft) altitude is 12 kilometers, as shown in Figure 21. Dips below the 90 percent detection point occur at both 4 and 6 kilometers. In 4 mm/hr rainfall, the detection performance drops slightly, as expected, as shown in Figure 22. In a five degree antenna tilt mode, the detection range is 11 kilometers with litle improvement in high elevation angle (near range) detection performance, as shown in Figure 23. Detection in 4 mm/hr rain, shown in Figure 24, is slightly poorer than in clear air.

Figure 25 depicts detection performance for the 1.5 kW radar with multipath interference effects removed. The detection range is slightly over 8 kilometers. Comparing the multiple scan detection curves with those in Figure 21, we see that the net effect of multipath interference is an enhancement in detectability outward from approximately 6 kilometers

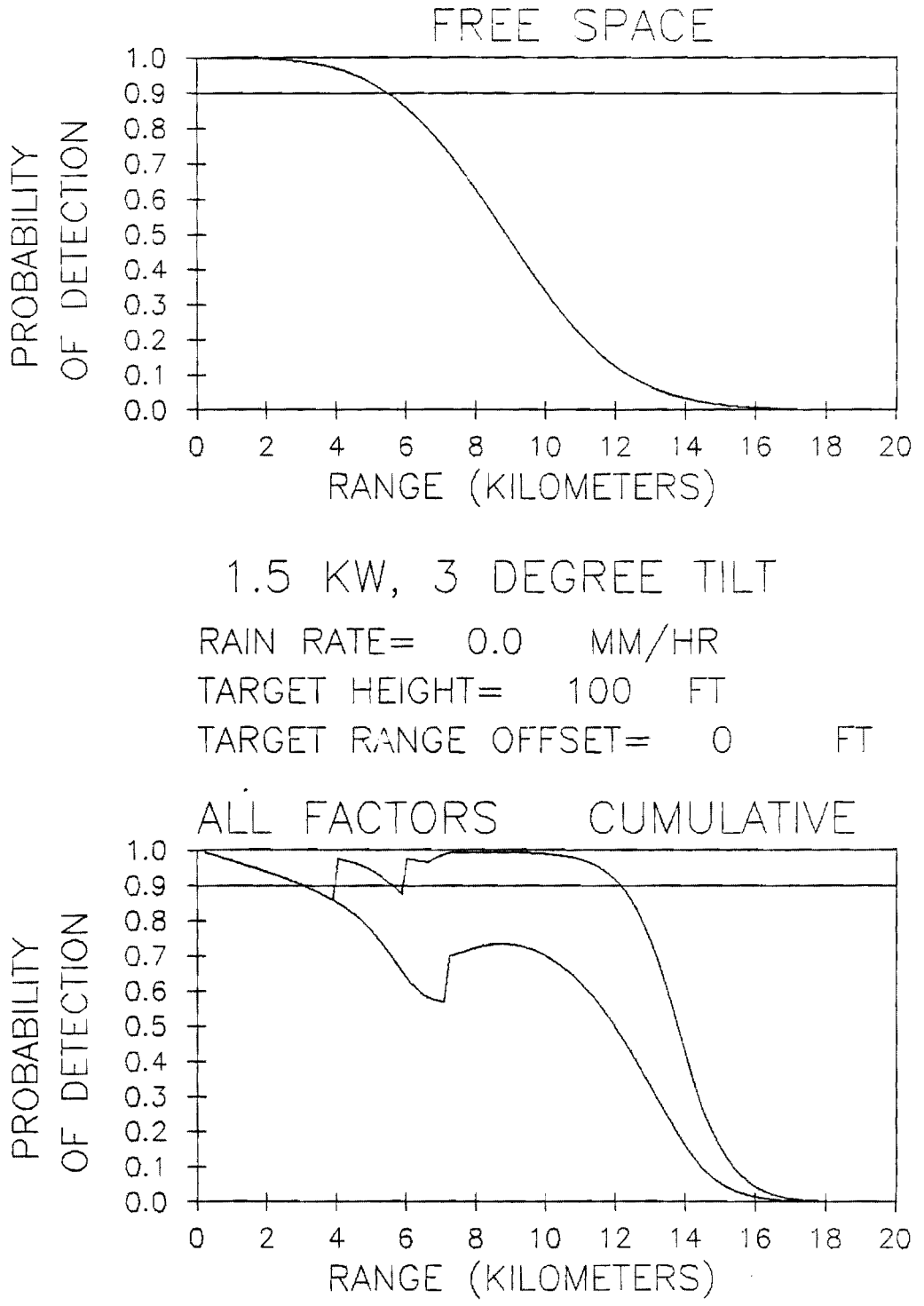

Figure 21. Modified VPS-2 Configuration (1.5 kW) Detection Probability for 100 ft. Aircraft Altitude, Clear Air, 3 Degree Antenna Tilt.

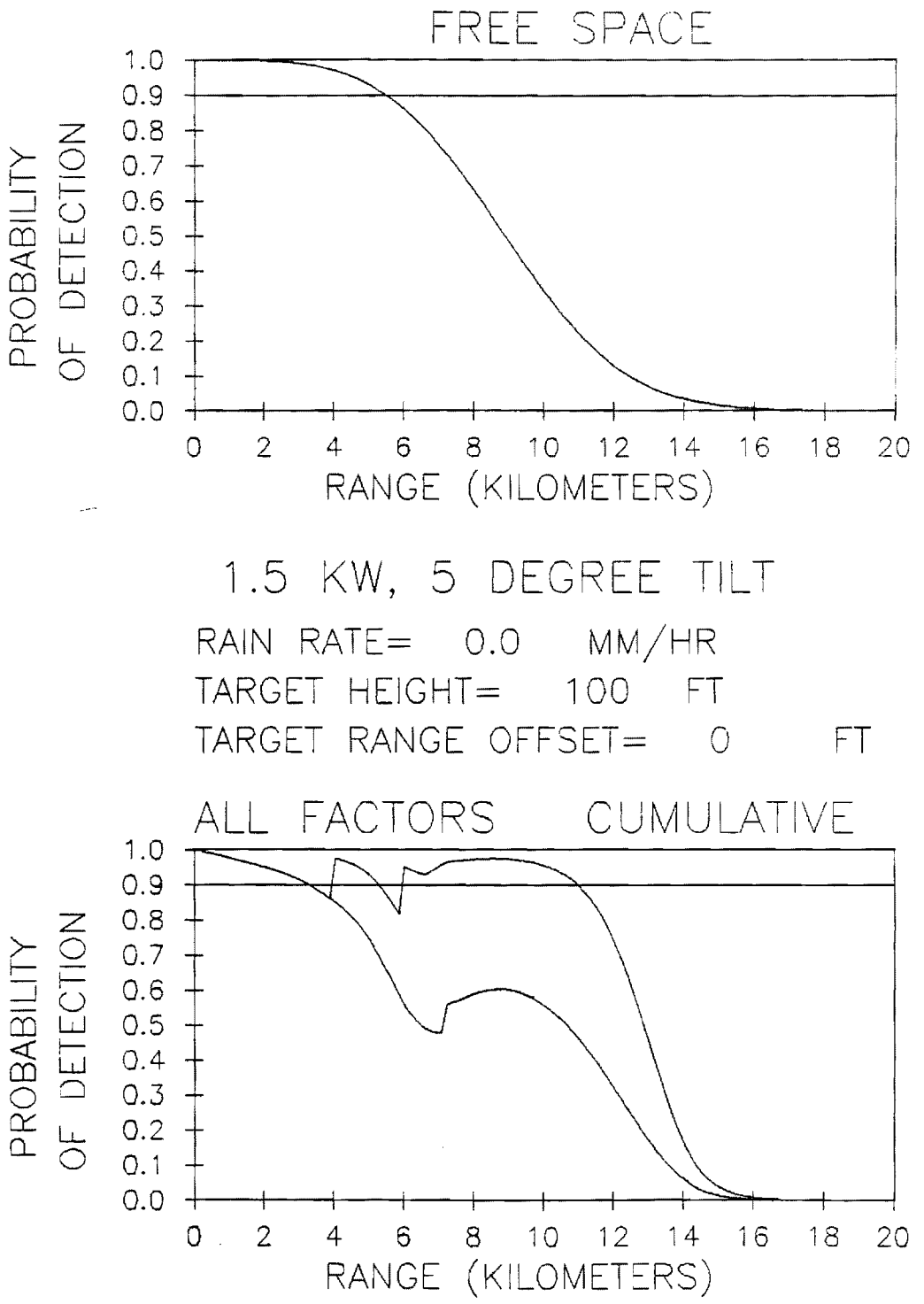

Figure 22. Modified VPS-2 Configuration (1.5 kW) Detection Probability for 100 ft. Aircraft Altitude, Clear Air, 5 Degree Antenna Tilt.

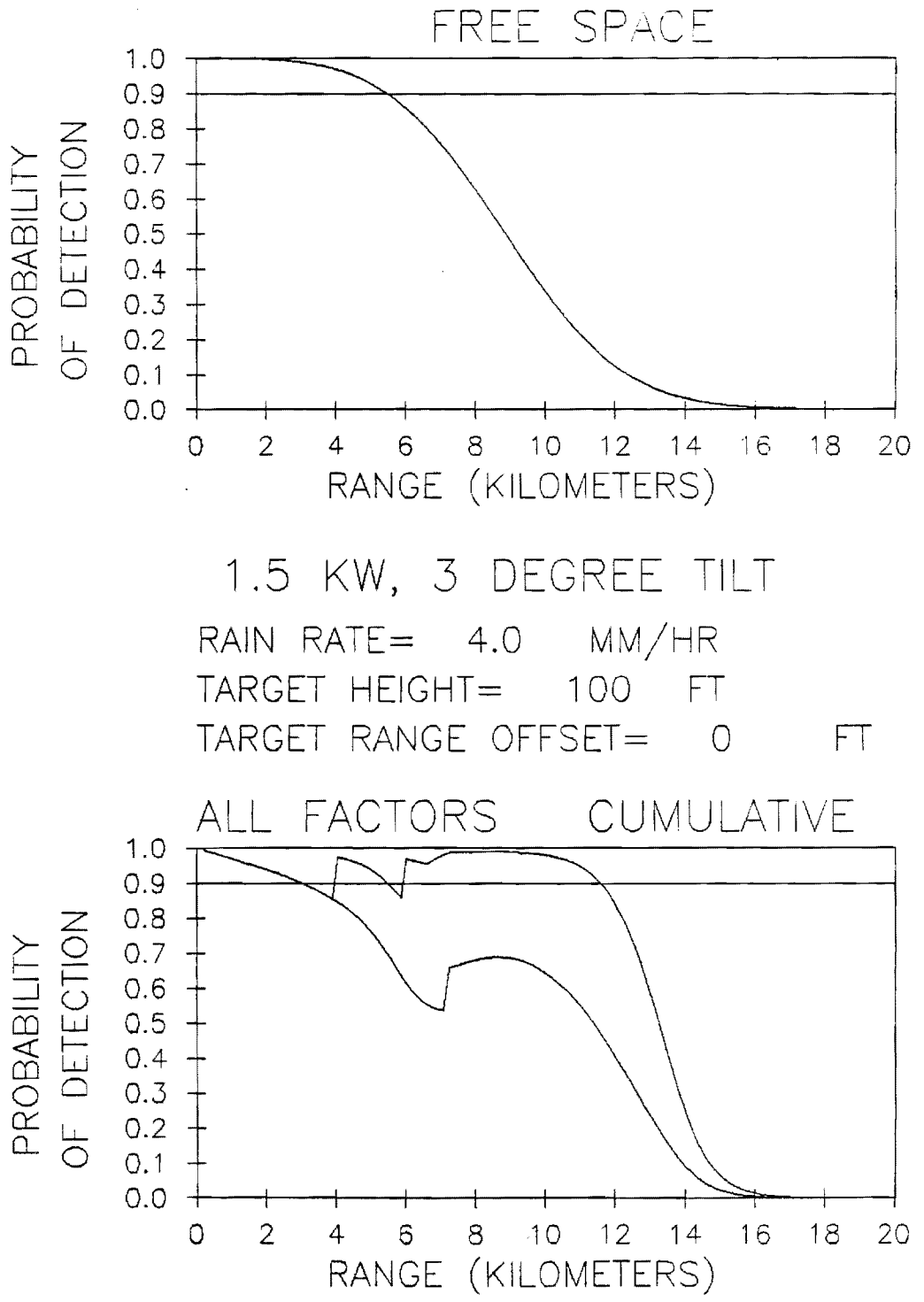

Figure 23. Modified VPS-2 Configuration (1.5 kW) Detection Probability for 100 ft. Aircraft Altitude, 4 mm/hr Rain, 3 Degree Antenna Tilt.

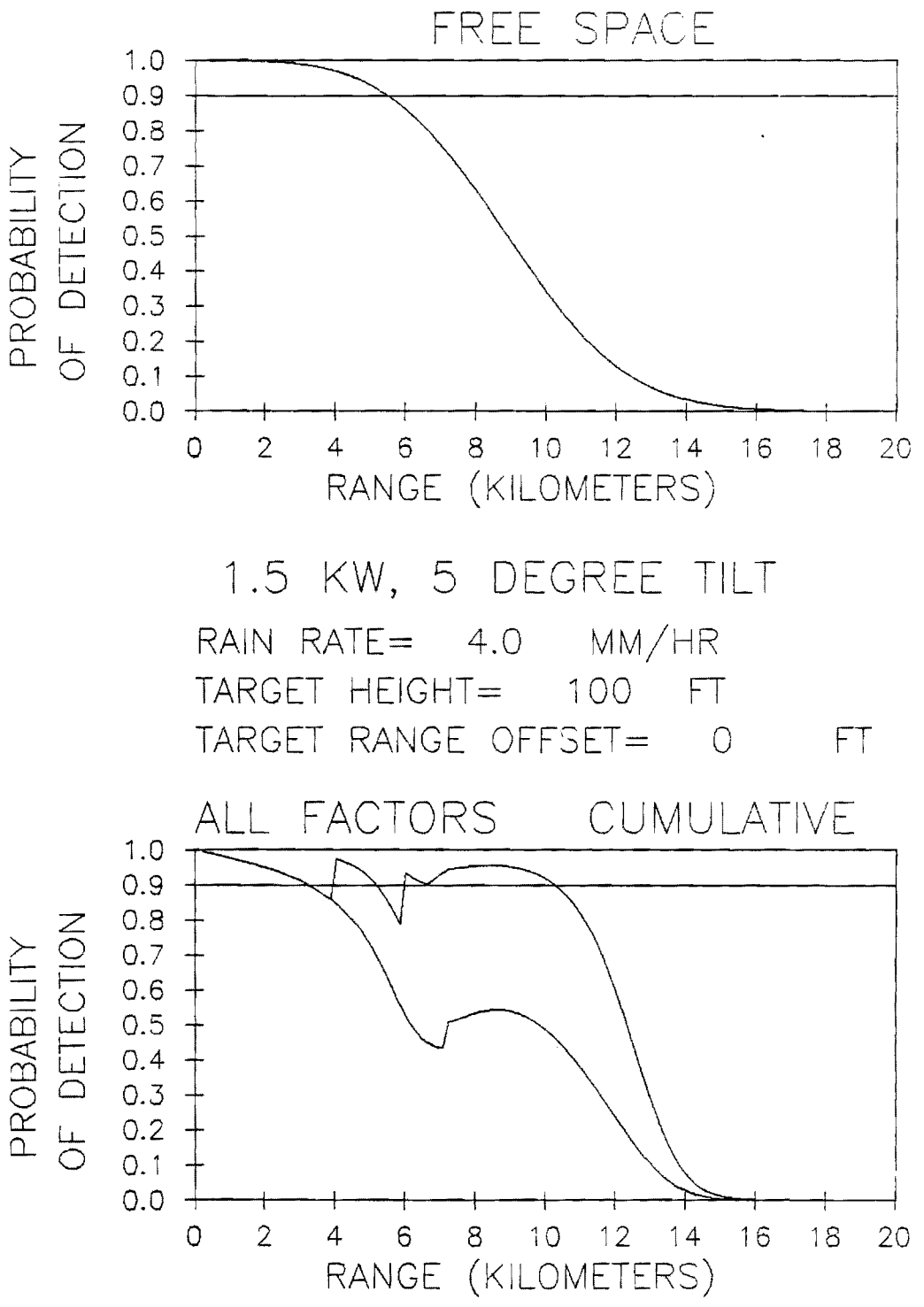

Figure 24. Modified VPS-2 Configuration (1.5 kW) Detection Probability for 100 ft. Aircraft Altitude, 4 mm/hr Rain, 5 Degree Antenna Tilt.

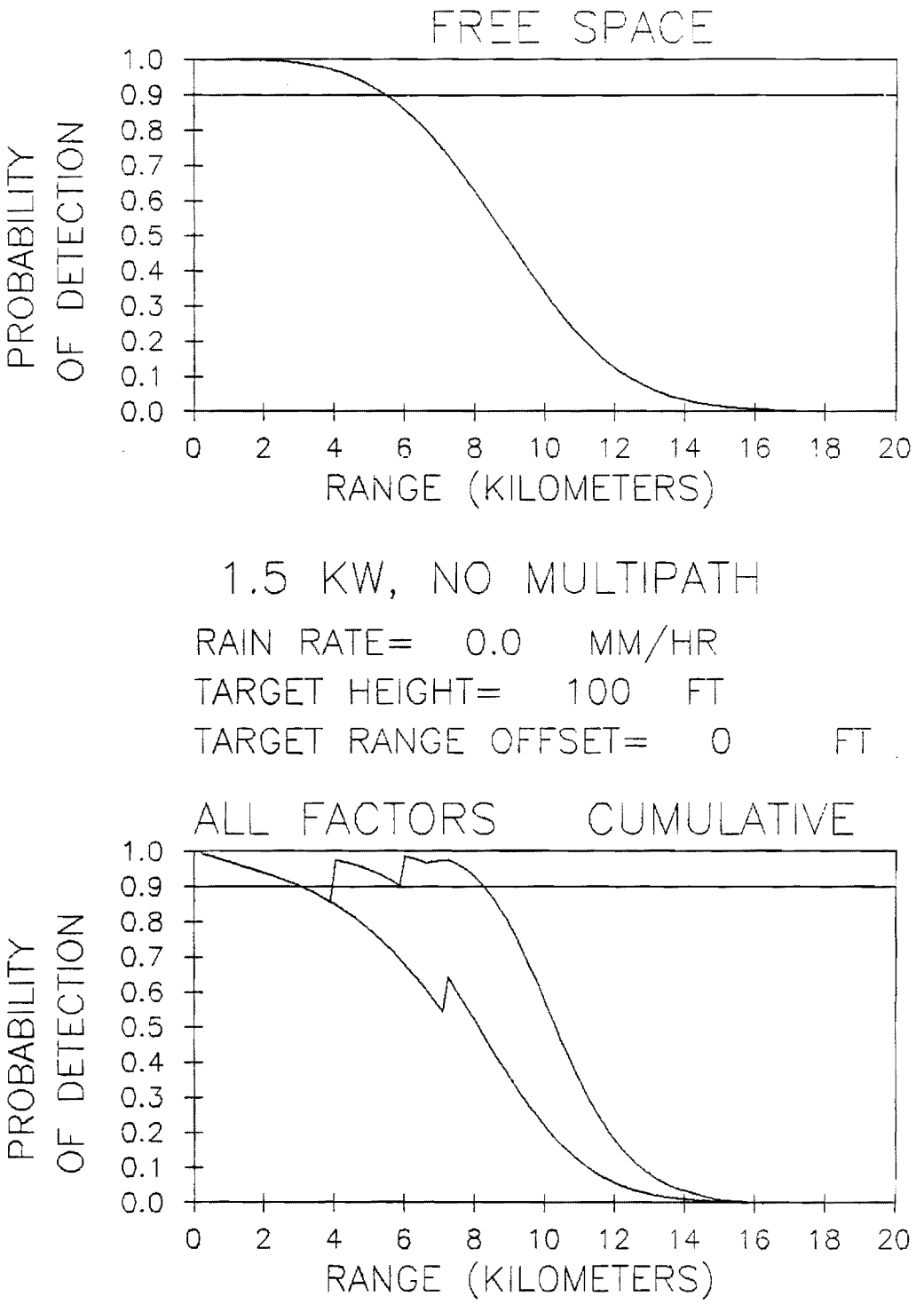

Figure 25. Modified VPS-2 Configuration (1.5 kW) Detection Probability for 100 ft. Aircraft Altitude, Clear Air, 3 Degree Antenna Tilt, Multipath Interference Removed.

Figures 26 through 29 depict detection of an aircraft at a constant 610 m (2000 ft) altitude by the recommended modified AN/VPS-2. Figure 26 shows a detection range of almost 12 kilometers. Inside four kilometers the aircraft detection drops below 90 percent because of decreased antenna gain at the higher elevation angles. The slight bump in the detection curve at 1.5 kilometers is due to an antenna elevation pattern sidelobe peak.

Figure 27 shows a similar picture for a five degree antenna elevation tilt. Detection range drops slightly to 11 kilometers, but higher elevation angle (near range) detection performance improves. 90 percent detection is not lost until a range of two kilometers.

Figures 28 and 29 depict detection performance of the recommended radar configuration in 4 mm/hr rain for three and five degree antenna tilts, respectively. Detection ranges are between 10 and 11 kilometers in both cases. Target detection falls below 90 percent at 4 kilometers for a three degree tilt, where detection is defined on a single scan basis. However, a 5 degree tilt maintains 90 percent detection until the aircraft exits the antenna elevation pattern at 2 kilometers.

Figures 30 through 33 depict detection performance of the 1.5 kW radar configuration for a 610 m (2000 ft) aircraft altitude. Figure 30 demonstrates a detection range of 9 kilometers and a loss of detection within 4 kilometers, due to decreased antenna gain. Performance at a 5 degree antenna tilt is improved over that at 3 degrees tilt, as shown in Figure 31. The detection range does not decrease significantly, but the near range performance is enhanced by the higher antenna gain. Figures 32 and 33 depict detection performance in 4 mm/hr rain for 3 and 5 degree tilt angles, respectively. Detection ranges are between 8 and 9 kilometers for both cases. Detection drops below 90 percent at 6 kilometers and from 4 kilometers inward, for the 3 degree tilt. Detection at near ranges is somewhat improved for a 5 degree tilt. In both cases the aircraft is below 90 percent detection at ranges closer than 4 kilometers.

The conclusion of this detection performance analysis is that the 1 kW peak power, 2 μsec pulse length radar configuration is the recommended configuration of an AN/VPS-2 radar modified for LAV-AD. The maximum range and high angle detection performance of this configuration is superior to that of the 1.5 kW, 1 μsec radar configurtion, as documented in the probability of detection curves shown in this section. However, further improvement in detection is required (1) to extend the maximum detection range and (2) to improve high angle (near range) performance for high altitude

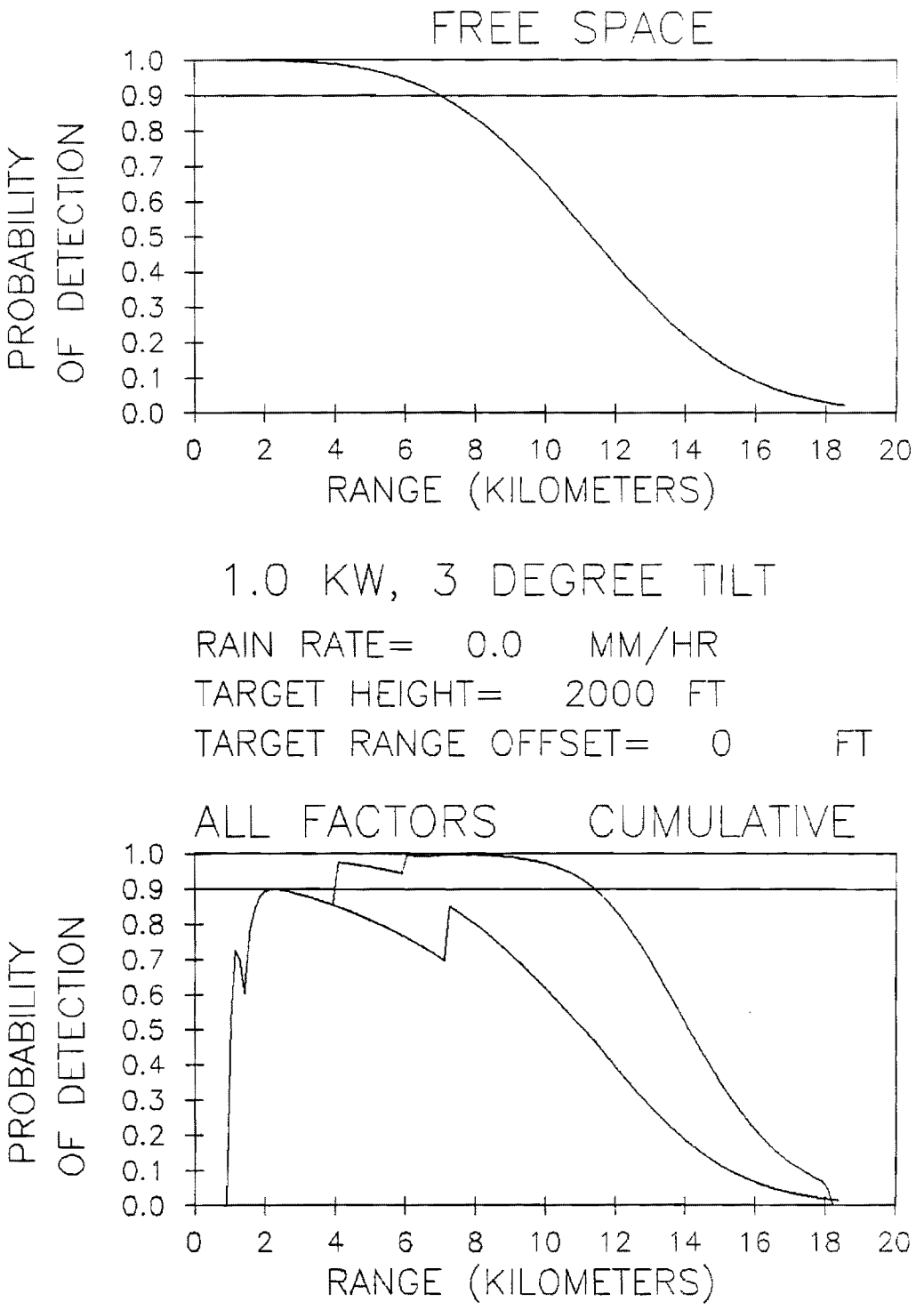

Figure 26. Recommended VPS-2 Configuration Detection Probability for 2000 ft. Aircraft Altitude, Clear Air, 3 Degree Antenna Tilt.

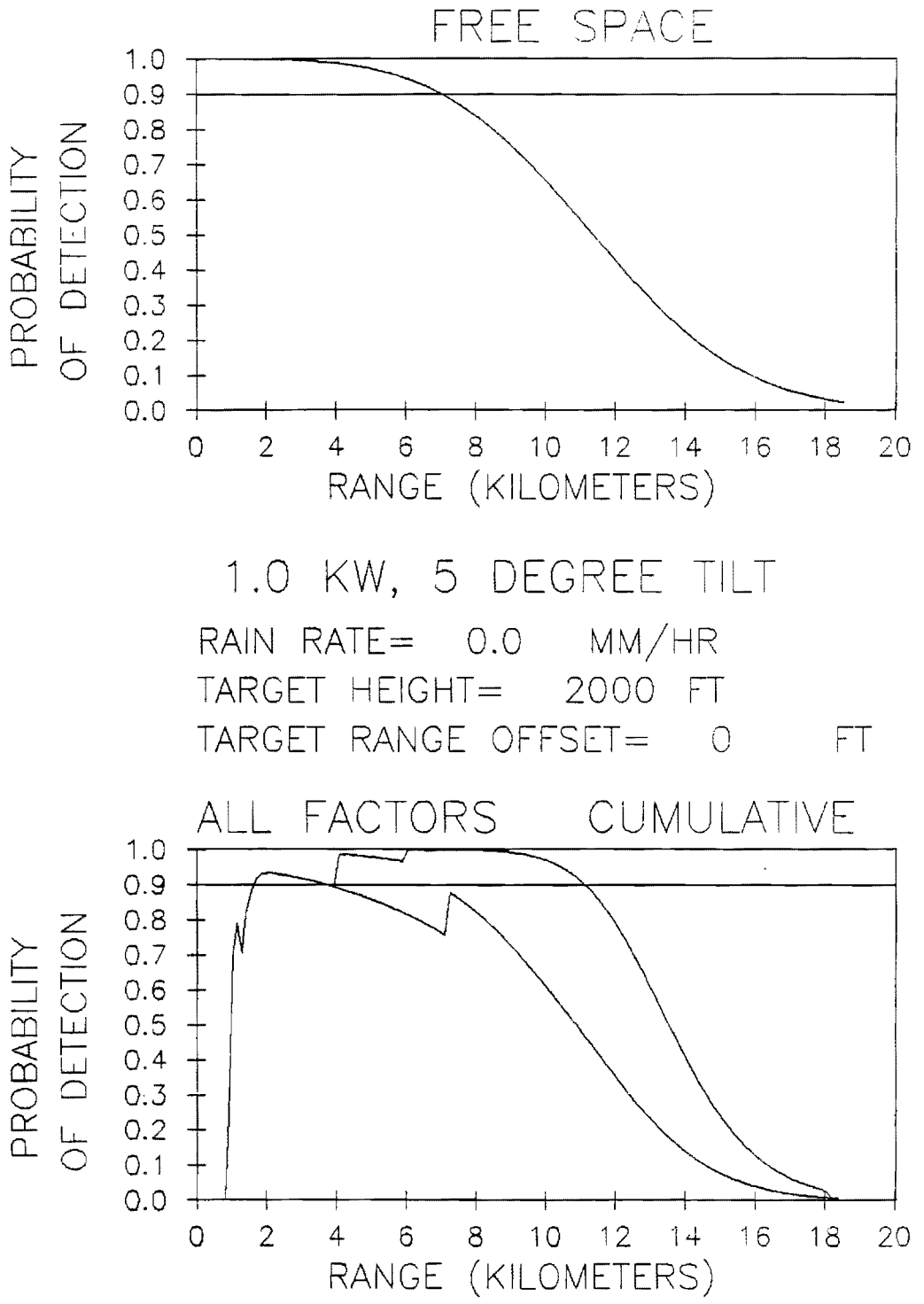

Figure 27. Recommended VPS-2 Configuration Detection Probability for 2000 ft. Aircraft Altitude, Clear Air, 5 Degree Antenna Tilt.

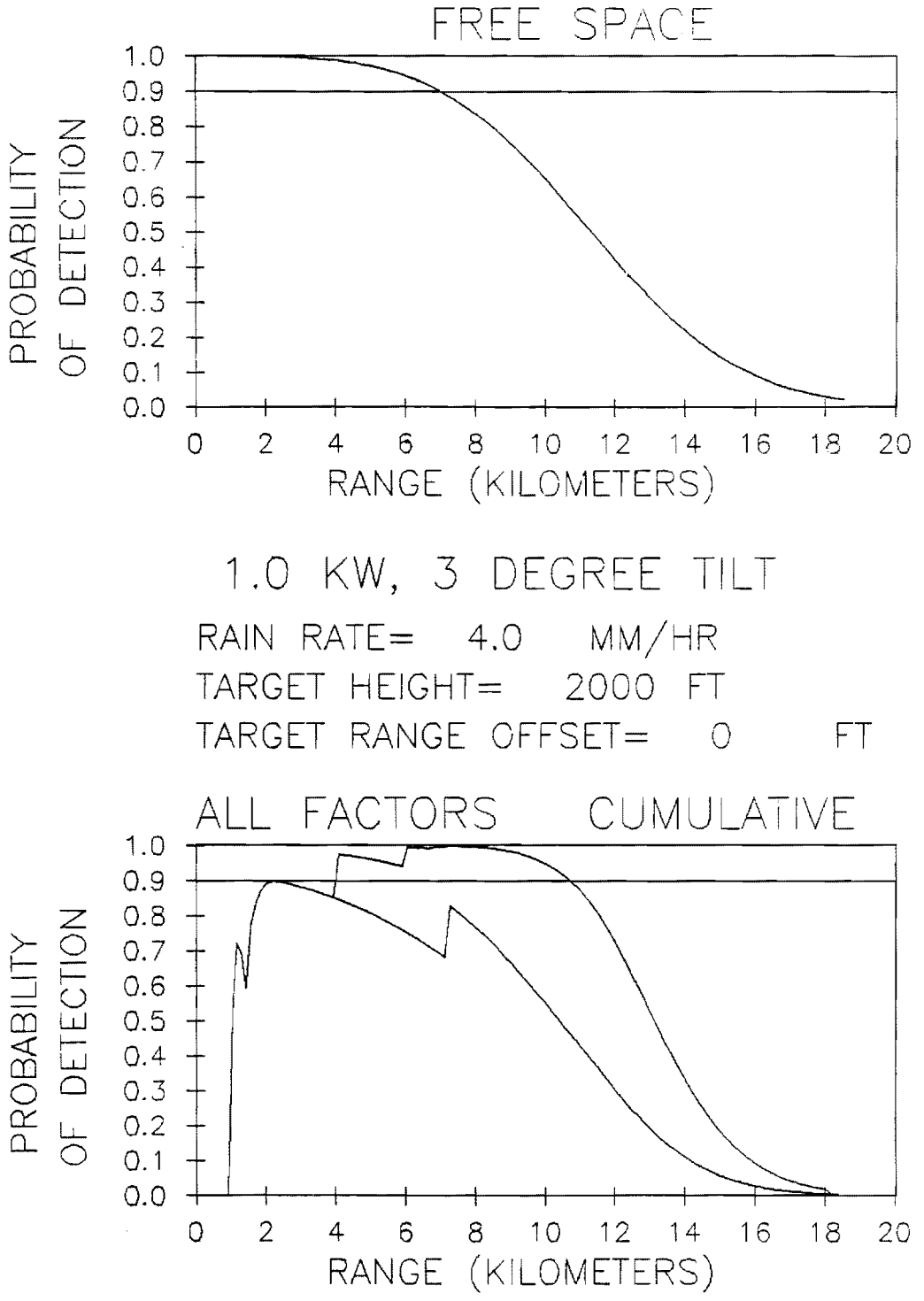

Figure 28. Recommended VPS-2 Configuration Detection Probability for 2000 ft. Aircraft Altitude, 4 mm/hr Rain, 3 Degree Antenna Tilt.

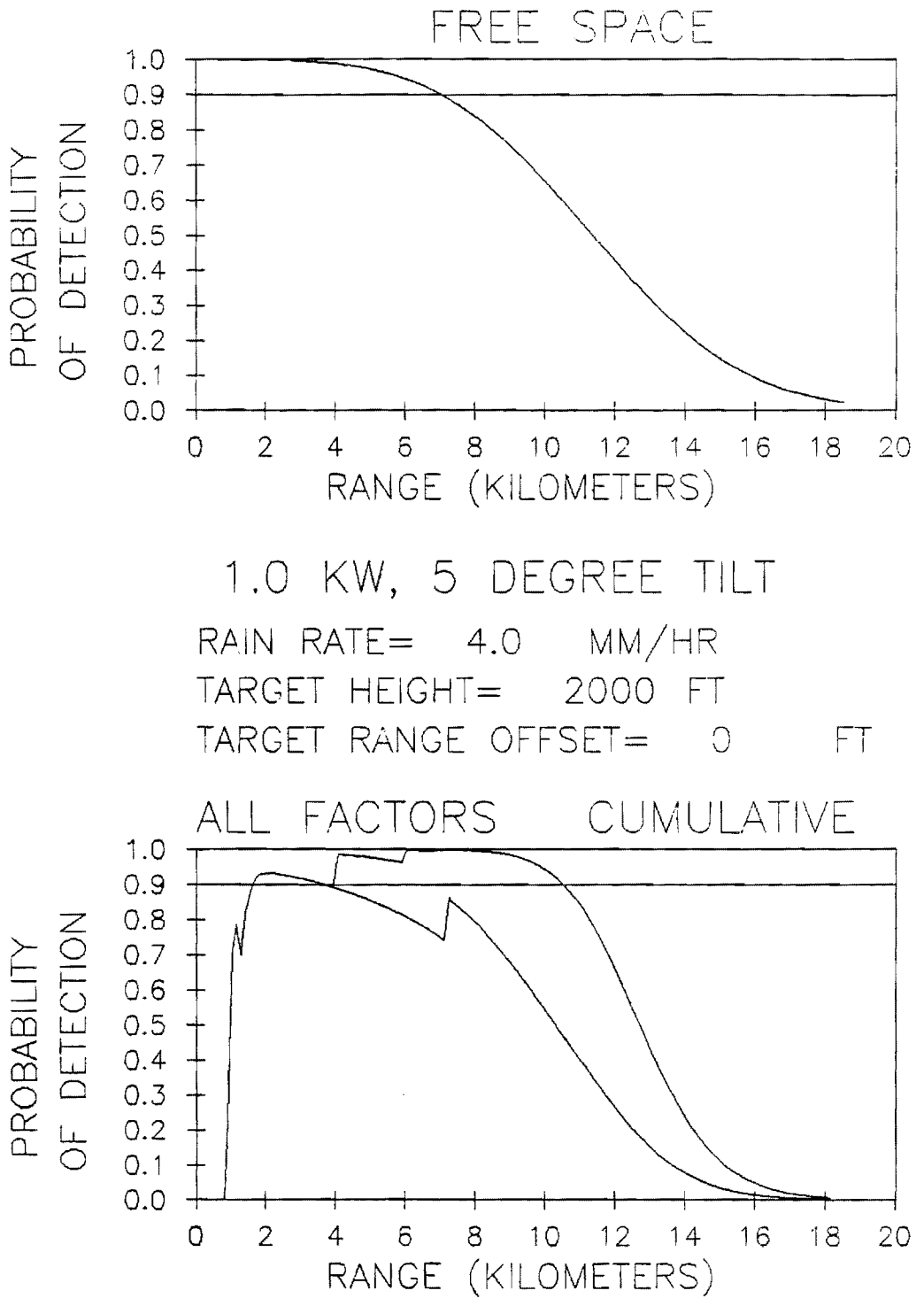

Figure 29. Recommended VPS-2 Configuration Detection Probability for 2000 ft. Aircraft Altitude, 4 mm/hr Rain, 5 Degree Antenna Tilt.

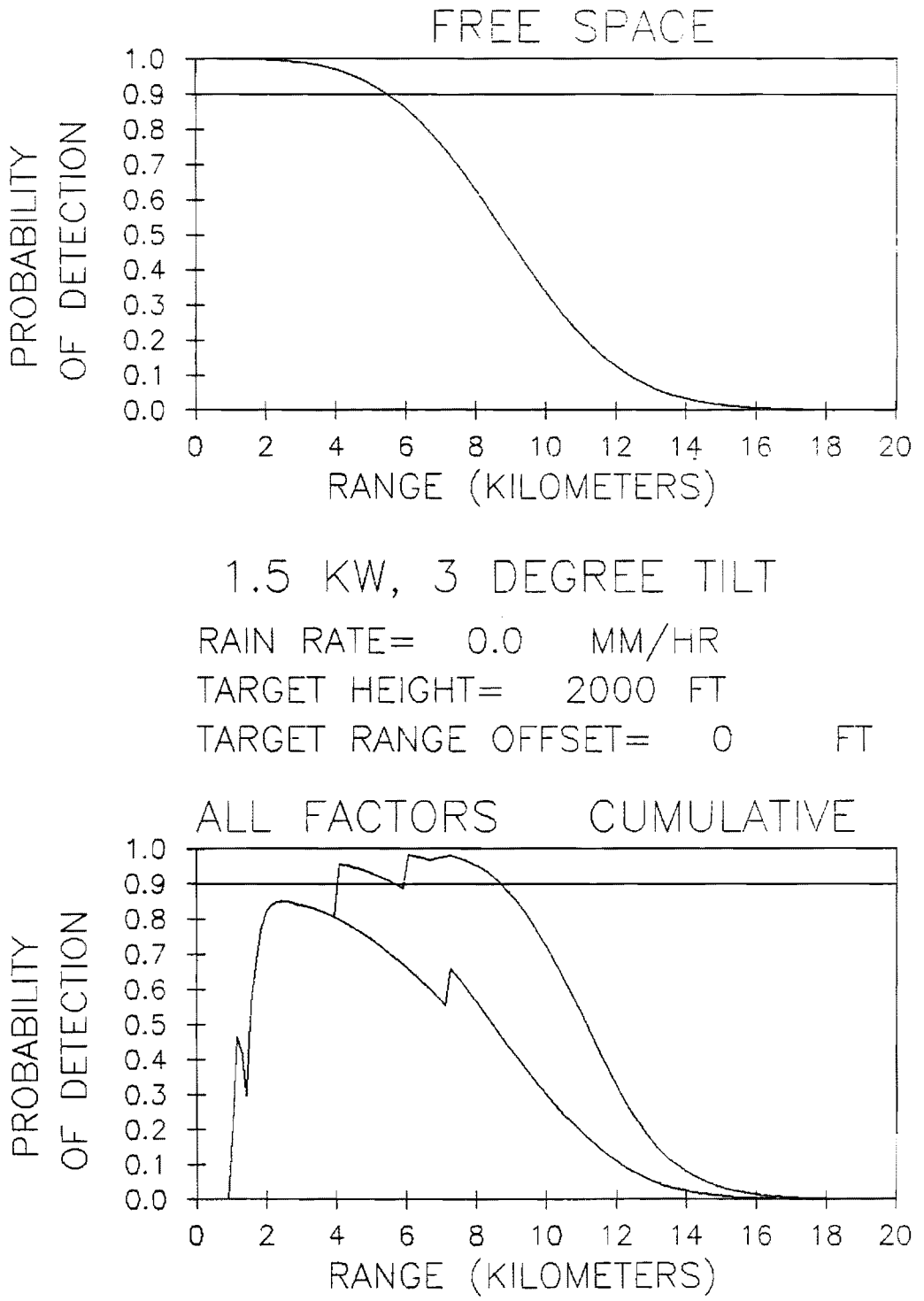

Figure 30. Modified VPS-2 Configuration (1.5 kW) Detection Probability for 2000 ft. Aircraft Altitude, Clear Air, 3 Degree Antenna Tilt.

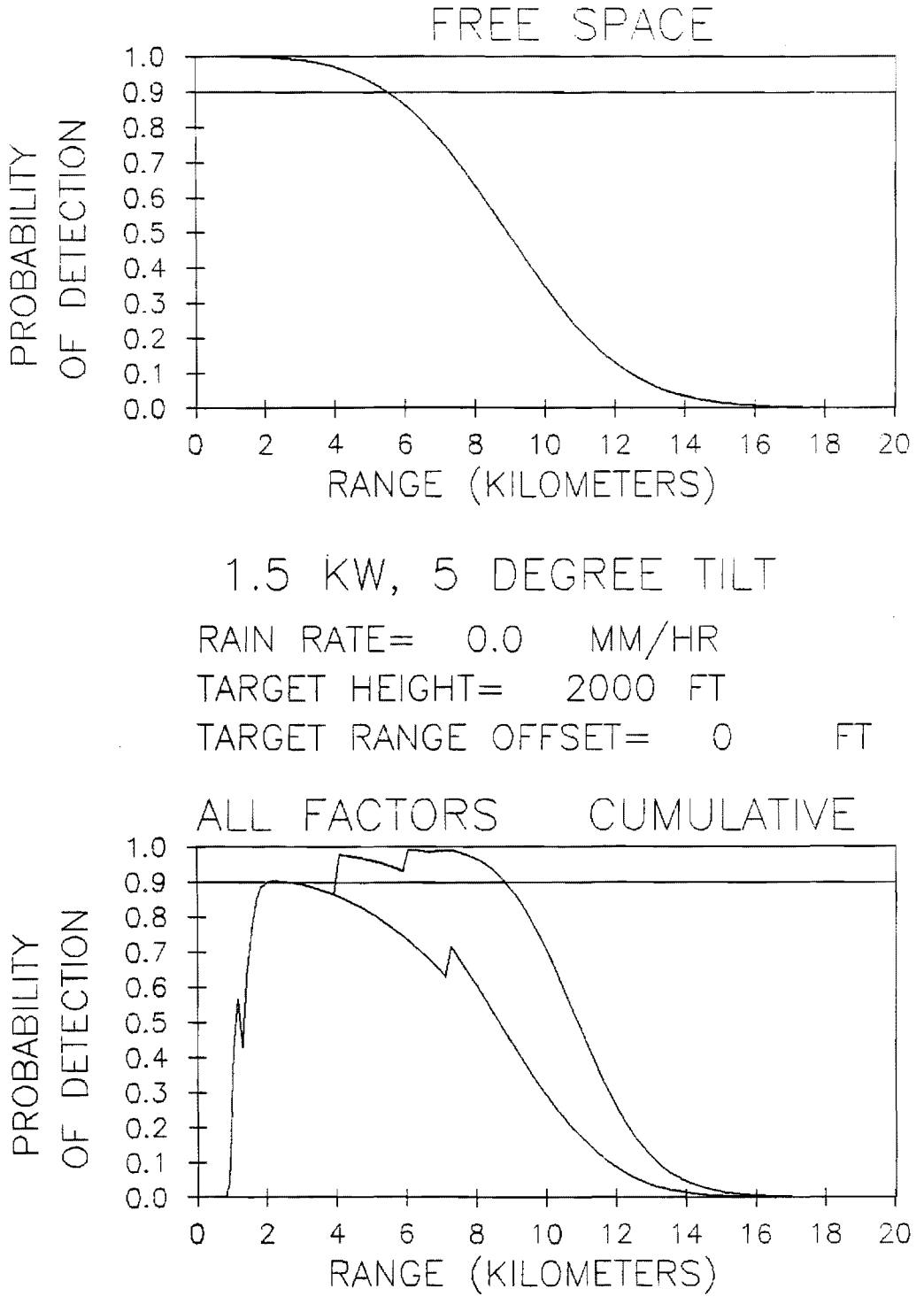

Figure 31. Modified VPS-2 Configuration (1.5 kW) Detection Probability for 2000 ft. Aircraft Altitude, Clear Air, 5 Degree Antenna Tilt.

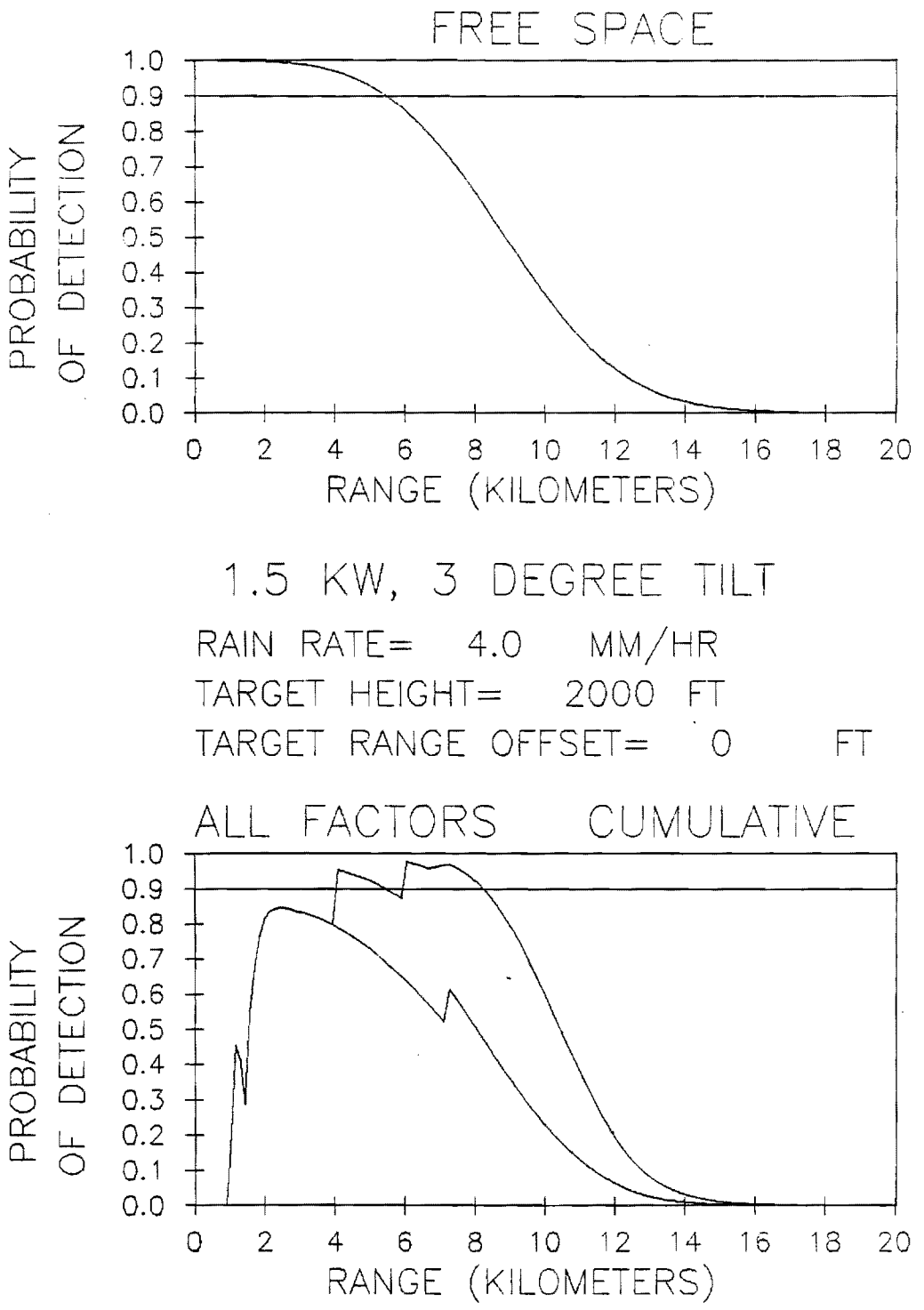

Figure 32. Modified VPS-2 Configuration (1.5 kW) Detection Probability for 2000 ft. Aircraft Altitude, 4 mm/hr Rain, 3 Degree Antenna Tilt.

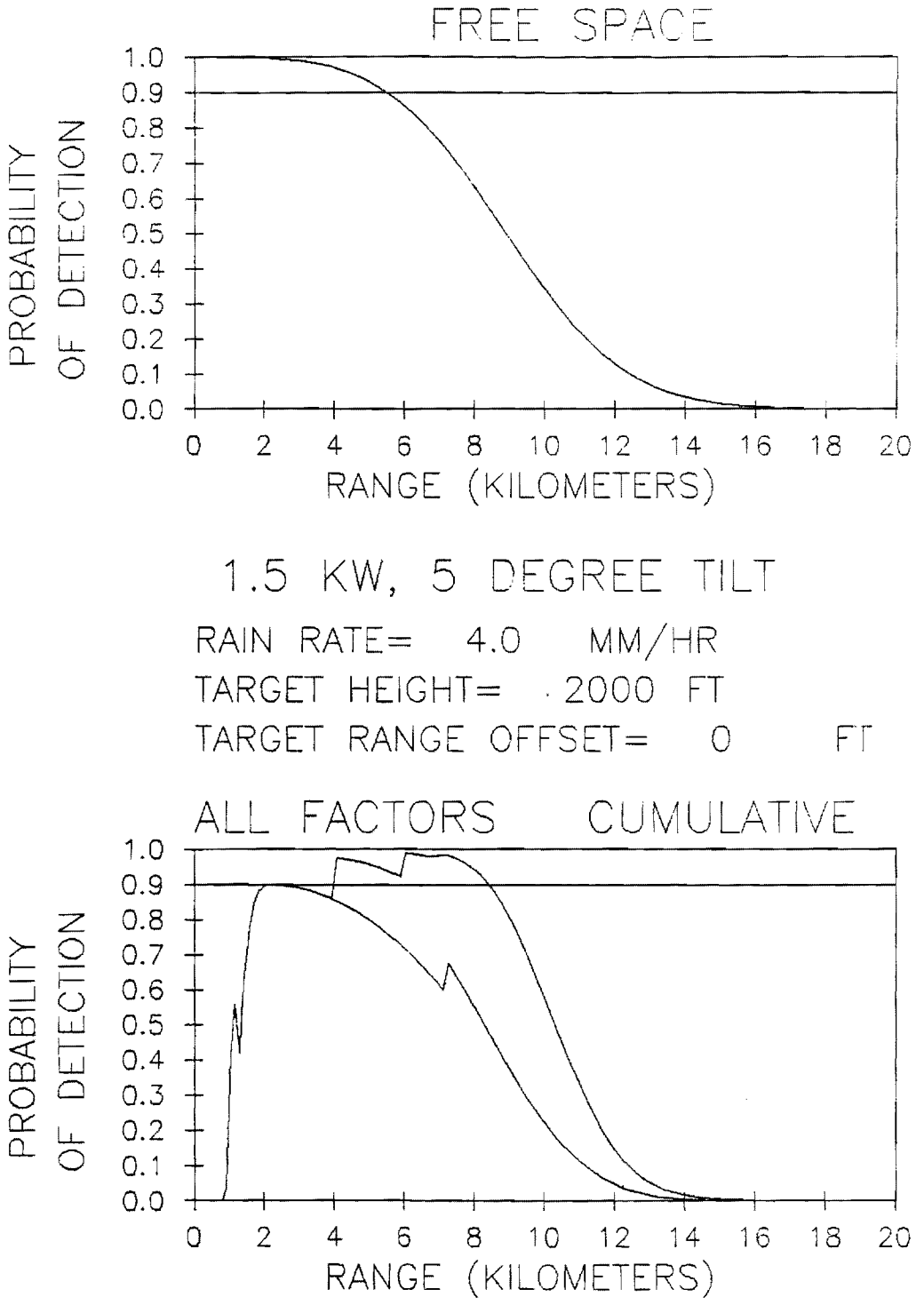

Figure 33. Modified VPS-2 Configuration (1.5 kW) Detection Probability for 20Q0 ft. Aircraft Altitude, 4 mm/he Rain, 5 Degree Antenna Tilt.

aircraft within the specified search volume. Both needs can be achieved through a refinement of antenna pattern design to increase gain.

SECTION 5
CONCLUSIONS AND RECOMMENDATIONS

Georgia Tech evaluated various AN/VPS-2 radar configurations with respect to aircraft detection performance based on a 90 percent probability of detection and a 10^{-6} false alarm rate. Radar and environmental parameter values used in this performance analysis were collaboratively selected by Georgia Tech, Emtech, and General Electric personnel. Free space and multiple scan detection performances were computed using the MERGE computer program.

The baseline AN/VPS-2 detection range was calculated to be 7 kilometers in free space. With all geometric and environmental factors included in the calculations, the maximum detection range is 7 to 10 kilometers for a 1 square meter cross section aircraft, flying at at constant 100 foot altitude, and 8 kilometers flying at a constant 500 feet altitude. Multipath interference effects are responsible for the enhanced range performance in both cases. Moderate rainfall (4 mm/hr) does not seriously degrade the detection performance of this X-band radar.

The detection performance of the baseline AN/VPS-2 radar is limited primarily in three areas: (1) antenna beam coverage, (2) receiver noise figure, and (3) signal processing. Recommendations for performance enhancement include: (1) utilizing a shaped beam antenna pattern with high angle coverage; (2) employing a low noise RF amplifier, and (3) employing digital processing techniques.

All of these recommendations were adopted in a modified AN/VPS-2 radar system, and a performance analysis was conducted. The antenna beamshape is roughly cosecant-squared in the elevation plane to provide high angle coverage and to permit aircraft detection at close range on a single scan basis. A GaAsFET RF amplifier is employed in the receiver to decrease the system noise figure by approximately 8 dB. The signal processor consists of a synchronous (I and Q) detector, A/D converters, a 4-pole Butterworth frequency response digital-delay-line canceller, a range bin summer, a 128-point FFT processor, a magnitude detector, and a CFAR processor. A three pulse canceller was considered, but was eliminated due to its poorer frequency response. The processor will operate in a dual PRF mode (9.36 and 10.0 kHz) such that a target is illuminated by one PRF for the first half of a beam dwell and by the other PRF for the second half. This dual PRF mode eliminates "blind speeds" in the range of specified target speeds.

Two operating modes for the modified AN/VPS-2 system were considered. The first mode consisted of transmitting 1.0 kW, 2μs pulses and then summing returns from two contiguous range cells. The second mode consisted of transmitting 1.5 kW, 1 μs pulses and then summing returns from four contiguous range cells. The 1 kW, 2μs mode offers the superior detection performance because of greater average transmitter power, lower receiver bandwidth requirement, and lower range bin collapsing loss. The free space detection range for the recommended radar configuration is 7 kilometers. Based on multiple scan cumulative detection, the detection ranges are 14 kilometers and 12 kilometers, with all factors included, for a 2 square meter cross section aircraft flying at a constant altitude of 100 and 2,000 feet, respectively. Increasing the antenna tilt angle improves near range (high angle) coverage at the expense of maximum detection range. Although not shown graphically, detection of aircraft at 2,000 meters altitude is negligible due to lack of sufficient antenna gain at the necessary elevation angles.

Georgia Tech concludes that the recommended AN/VPS-2 configuration will technically fulfill General Electric's light DIVADS surveillance requirements with slight improvement in the antenna elevation angle coverage. Our calculations indicate that improved peak gain and higher angle gain of the Emtech cosecant squared elevation pattern should be possible through design refinements. Such improvements should result in the desired 15 kilometer range performance and 2,000 meter aircraft altitude detection.

Georgia Tech recommends that General Electric encourage Emtech to pursue these systems refinements to the point that specific parameter values for noise figure, antenna gain patterns, and signal processing response can be factored into a final detection performance evaluation. Georgia Tech can assist in antenna design and detailed signal processor design, working alongside Emtech personnel at the direction of General Electric.

Alternative radar systems to a modified AN/VPS-2 should be identified so that their surveillance capability can be expediently determined. Georgia Tech has performed radar surveys of similar nature and has search resources to quickly identify candidate systems, both American- and foreign-made. Georgia Tech then recommends that a detection performance evaluation be performed for each system identified, after approval by General Electric.

APPENDIX A
FAST FOURIER TRANSFORM MODULES

An industry search was conducted to locate FFT modules that could be bought off-the-shelf, routinely built, or configured by dedicating existing microprocessor modules. A number of potential vendors were contacted, but most proved unable to provide a module with the required processing speed (25 FFT's in 13 milliseconds). The baseline requirements specified for the module are summarized in Table A1.

TABLE A1. FFT REQUIREMENTS

FFT size	128-point, complex
Resolution	10 or more bits, in and out
Speed	25 FFT's/13 ms.
Power Consumption	~50 watts
I/O	Buffer in/out

Only four vendor sources were located that could provide modules to fit most of the stated criteria. The firms, their candidate processors, and some fundamental processor specs are given in Table A2. Apparently the requirement of 1 FFT/.5 msec, which translates to 1.16 μsec per butterfly, represents the limit of readily available, easily configured processor architectures. It was indicated to us by Mr. Schapp of Spectra Data Corporation that architectures which would allow speeds of 1 FFT/.1 ms. and even 1 FFT/.055 msec could be configured, but these would represent increased sophistication and complexity over the more standard 1 FFT/.5 msec configuration listed in Table A2.

Advanced Microwave Devices has recently come out with a new line of bipolar, microprogrammable chips that would allow for double our requisite processing speed in a relatively inexpensive custom built module. Since they would merely supply the parts, a manufacturer would have to be found to actually build the processor. The size of the module is, therefore, indeterminant, and the indicated cost is a rough estimate based on the cost of the major components.

TABLE A2. 128-POINT COMPLEX FFT MODULES

VENDOR	MODEL NO.	SPEED	PRECISION	SIZE	POWER	COST	COMMENTS
Spectra Data Corp. 18758G Bryant St. Northridge, CA 91324	Custom Built	1 FFT/.5 ms.	11-bits	12"x12"x2"	35W	$50-70K Prototype 8K/unit 100's 8K/unit 1000's	Faster device available
CNR, Inc. 220 Resevoir St. Needham, MA 02194	MARS 232	1 FFT/.5 ms.	16-bits	10-1/2" rack	250W	35K plus 2-6K in software	Multipurpose processor
Analogic, Inc. Audubon Road Wakefield, MA 01880	AP 400	1 FFT/.58 ms.	16-bits	(2) 10-1/2" racks	20W	34K plus software	"ruggedized" two units in parallel
Advanced Micro Devices 901 Thompson Place Sunnyvale, CA 94086	Custom Built	1 FFT/.25 ms.	16-bits	not known	11W	5K/Unit 1000's	Supplies components only

REFERENCES

1. Carlson, E., "Requirements, Radar for Light Armored Vehicle, Air Defense Variant," GE Control No. 793-82-RA01, Revision 1, March, 1982.

2. Blake, L. V., "A FORTRAN Computer Program to Calculate the Range of a Pulse Radar," NRL Report 7448, June, 1972.

3. Perry, B., et. al., "MERGE: An Analytical Radar Performance Model," Georgia Tech Final Report on Contract DAAK10-81-R-0006, March, 1982.

4. Muehe, C. E., "Digital Signal Processor for Air Traffic Control Radars," IEEE NEREM 74 Record, Part 4: Radar Systems and Components, pp. 73-82, Oct. 1974.

5. Levy, J. A., Shuhandler, M., and Logue, S., "Stand-Off Target Acquisition System (SOTAS)," Proceedings of the 23rd Tri-Service Radar Symposium, 1977, p. 251.

6. W. Fishbein, et al, "Clutter Attenuation Analysis," Tech Report ECOM-2808, March 1967, AD665 351.

7. N. C. Currie, F. B. Dyer, and R. D. Hayes - "Radar Land Clutter Measurements at Frequencies of 9.5, 16, 35 and 95 GHz," AD-A012709, April 1975.

ENGINEERING EXPERIMENT STATION
Georgia Institute of Technology
A Unit of the University System of Georgia
Atlanta, Georgia 30332

October 12, 1982

General Electric Company
Armament and Electrical Systems Department
Lakeside Avenue
Burlington, Vermont 05401

Attention: Mr. Freeman Perry

Subject: Letter Report Summarizing Activities on Georgia Tech Project A-3157-100, "Radar System for a Guided Projectile - Based ASMD System"

Dear Sir:

Georgia Tech reviewed and evaluated General Electric's preliminary anti-ship missile detection/track radar system concept. Analysis was based on radar parameter values selected by General Electric, representative of available technology, or thought to be available within three years. The radar concept includes an X-band system for initial target acquisition at 17 kilometer range and for initial target track. Since multipath interference effects can be expected to be for severe elevation plane track at X-band for all but very rough sea state conditions, the General Electric radar concept also includes a Ka-band system for closer range angle tracking.

This letter report summarizes the detection and angle tracking performance (noise component only) of both radar band system configurations against a Mach 2, $0.1m^2$ radar cross section incoming missile. Extrapolation to track and detection of outgoing projectiles can be made by appropriate increase or decrease of target cross section. In addition, Georgia Tech evaluated the projectile receiver/antenna concept for Ka-band implementation.

This investigation was performed by the Radar and Instrumentation Laboratory of the Georgia Tech Engineering Experiment Station. Dr. Robert Trebits of the Analysis Division was the Project Director, and his project team included Mr. Arch Nelson and Mr. Pete Britt, all of whom contributed to this letter report.

Radar Detection and Tracking

Initial acquisition of the approaching missile is made by the X-band radar. Figure 1 shows the radar system signal-to-noise (S/N) ratio as a function of range, based on a single coherent dwell time equivalent to a 1 kHz processed bandwidth. Clear air and two rainfall rate conditions are shown. Note that overall system probability of detection may be further enhanced by m-out-of-n selection or noncoherent integration of the coherent processor output. The S/N ratio may be related to probability of detection by modeling the missile as a Swerling 3 radar target (a single dominant scatterer whose reflection is correlated hit-to-hit but uncorrelated from coherent dwell-to-dwell). A 10 dB, single coherent dwell, S/N ratio then corresponds to a 50% probability of detection with a 10^{-4} false alarm rate, and a 20 dB S/N ratio corresponds to a 95% probability of detection with a 10^{-8} false alarm rate.(1)

Based on these S/N ratio value limits, maximum detection range values can be calculated. Thus detection in worst case rain is limited to approximately 16 kilometers. Note, however, that this rainfall scenario assumes rain conditions along the entire line of sight, a low probability event that results in a calculated maximum detection range that is unrealistically low.

The system noise contribution to the X-band angle tracking error is shown in Figure 2 as a function of range for clear air and the same two rainfall conditions. Furthermore, the RMS angle noise shown is that amount within an assumed 20 Hz system servo bandwidth. The angle noise does not exceed 1 mr for ranges out to 16 kilometers even in very heavy (25 mm/hr) rain. Note, however, that this angle noise does not include multipath interference effects.

Figure 3 shows single coherent dwell, S/N ratio curves as a function of range for a Ka-band radar with 300 W average power and other parameters as noted. For this radar configuration a 10 dB S/N ratio implies only 3 km detection range in very heavy (25 mm/hr) rain, 6 km range in heavy (10 mm/hr) rain, and 11 km in moderate (4 mm/hr) rain. The noise component of tracking error, shown in Figure 4, shows a 1 mr limit at 4 km in very heavy rain, 7-1/2 km in heavy rain, and 13-1/2 km in moderate rain. Figures 3 and 4 indicate that this Ka-band radar configuration is basically limited to 3 to 4 kilometers range by very heavy rain conditions.

Figure 5 depicts single coherent dwell S/N ratios versus range for a Ka-band radar with 5 kW average power, utilizing a tube that has been manufactured. Even with more than an order of magnitude more power than in the previous configuration, the detection for a 10 dB S/N ratio is only 4 km in very heavy rain, 8 km in heavy rain, or 14 km in moderate rain, other parameters being the same. Figure 6 shows the noise component of angle tracking error for this radar configuration. A limit of 1 mr angle error occurs at 4-1/2 km in very heavy rain, 9 km in heavy rain, and 17 km in moderate rain. Thus, under worst case weather conditions this Ka-band radar is, too, very range limited for an ASMD application.

Detection performance of an outgoing projectile may be estimated by calculating the radar cross section of a 40 mm diameter, flat circular plate at 35 GHz to be -5.7 dBsm as an upper bound. Probability of detection may then be estimated by modeling the projectile as a Swerling 1 target.

Reasonable conclusions from this limited radar system analysis are:

1. The postulated X-band system detection performance is adequate for this ASMD application.
2. The noise component of the angle tracking errors for the X-band system is adequate, except that multipath interference will degrade elevation angle tracking performance to unacceptable levels under any but higher than sea state 3 conditions.
3. Both Ka-band radar configurations are severely range limited in very heavy rain regarding maximum detection range and angle tracking error (noise component). The 10 mm/hr rainfall condition is a more realistic severe weather system requirement, in which case either Ka-band system represents an attractive system.
4. Increased Ka-band power does not appreciably increase radar detection performance and angle tracking performance for this application.
5. Multipath interference at Ka-band in the elevation plane will be negligible for any but sea state 0 or 1 conditions.

Guided Projectile Receiver Concepts

The determination of projectile roll attitude from radar beam polarization will result in a 180^{0} orientation angle ambiguity. Theoretically, the ambiguity can be resolved by detecting the difference in received signal amplitude, due to the radar antenna pattern gradient, between antennas distributed on the back of the projectile.

Assume that the phase center locations and polarizations of four antennas on the back of the projectile are as shown in Figure 7. (Each antenna may actually consist of an array of radiators, such as microstrip patches.) Also assume that a signal code synchronous with the conically scanning radar antenna is provided, permitting the projectile to derive relative beam directions.

Figure 8 shows four possible beam positions as the radar antenna is conically scanned about the nominal target direction. The signal differential induced between the antennas of either of the orthogonally polarized pairs of antennas for a particular beam position depends upon the projectile position in the beam and the roll attitude of the projectile. Therefore, the differential signal should be measured for both pairs of antennas and for the upper and lower beam positions. In this way, the signal differential need never by smaller than that which occurs at the crossover level of opposite beams. Also, the antenna pair that happens to most closely coincide with the polarization of the radar signal can be used to obtain the differential signal.

Figure 9 is a schematic diagram of a circuit that can be used to extract the normalized differential signal Δ/Σ, where Δ is the amplitude difference and Σ is the sum. For 100 m and 200 m ranges, plots of Δ/Σ as a function of the relative projectile and radar beam peak directions are given in Figure 10 for a 80 cm projectile aperture. If the crossover level of opposite beams (Figure 8) is 3 dB (6 mr), the minimum Δ/Σ level for the 100 m range is -39 dB. Since signal amplitudes are quite high, and only the sign of Δ/Σ is required, this level is probably a reasonable number. Because Δ/Σ drops off rapidly with range, the ambiguity resolution process must be completed within milliseconds after the projectile has been fired.

Once the 180 degree roll angle ambiguity has been resolved, the projectile roll attitude can be established by comparing the signals from the orthogonally polarized antennas. A circuit for performing this function is shown schmatically in Figure 11. The signs of the phase detector output voltages can be used to resolve potential ambiguities at the major or diagonal axes. Nulls at these same axes can be used to recalibrate the system.

With the projectile attitude established, projectile guidance can be achieved using conventional conical scan tracking concepts. The projectile senses the radar signal amplitude modulation that occurs when it is not in the proper trajectory and moves in the direction of minimum signal level.

Appendix

The single coherent dwell, signal-to-noise ratio was calculated from the equation (2):

$$S/N = \frac{P_t G^2 \lambda^2 \sigma}{(4\pi)^3 R^4 kTBFL(AR)} ,$$

where

P_t = Peak transmit power (W)
G = Antenna power gain (dimensionless)
λ = Wavelength (m)
σ = RCS (m^2)
R = Range (m)
k = Boltzmann's constant = 1.38×10^{-23} J/K
T = Effective antenna temperature = 290^{o} K
B = Receiver noise bandwidth (Hz)
F = Front end receiver noise factor (dimensionless)
L = System loss factor (dimensionless)
A = Atmospheric attenuation (1/meter)

The angle tracking error due to system noise was calculated from the equation (2):

$$\sigma_\theta = \frac{0.58\ \theta}{\left(\frac{(S/N)^2}{1 + S/N}\right)\left(\frac{prf}{B_s}\right)},$$

where

σ_θ = rms angle noise
θ = half power antenna beamwidth
S/N = single dwell signal-to-noise ratio
prf = pulse repetition rate
B_s = tracking bandwidth

Atmospheric absorption data were obtained from the following table (3):

ATMOSPHERIC ATTENUATION (dB/km) AS A
FUNCTION OF FREQUENCY AND RAIN RATE (mm/hr).

Frequency	Equation	
10 GHz	Loss $(\frac{dB}{km})$ A	= 2 0.013 + 0.00919 $RR^{(1.16)}$
16 GHz		= 2 0.045 + 0.039 $RR^{(1.124)}$
35 GHz		= 2 0.080 + 0.273 $RR^{(0.985)}$
95 GHz		= 2 0.22 + 1.60 $RR^{(0.640)}$
140 GHZ		= 2 0.30 + 1.60 $RR^{(0.70)}$

where RR is rain rate in mm/hr.

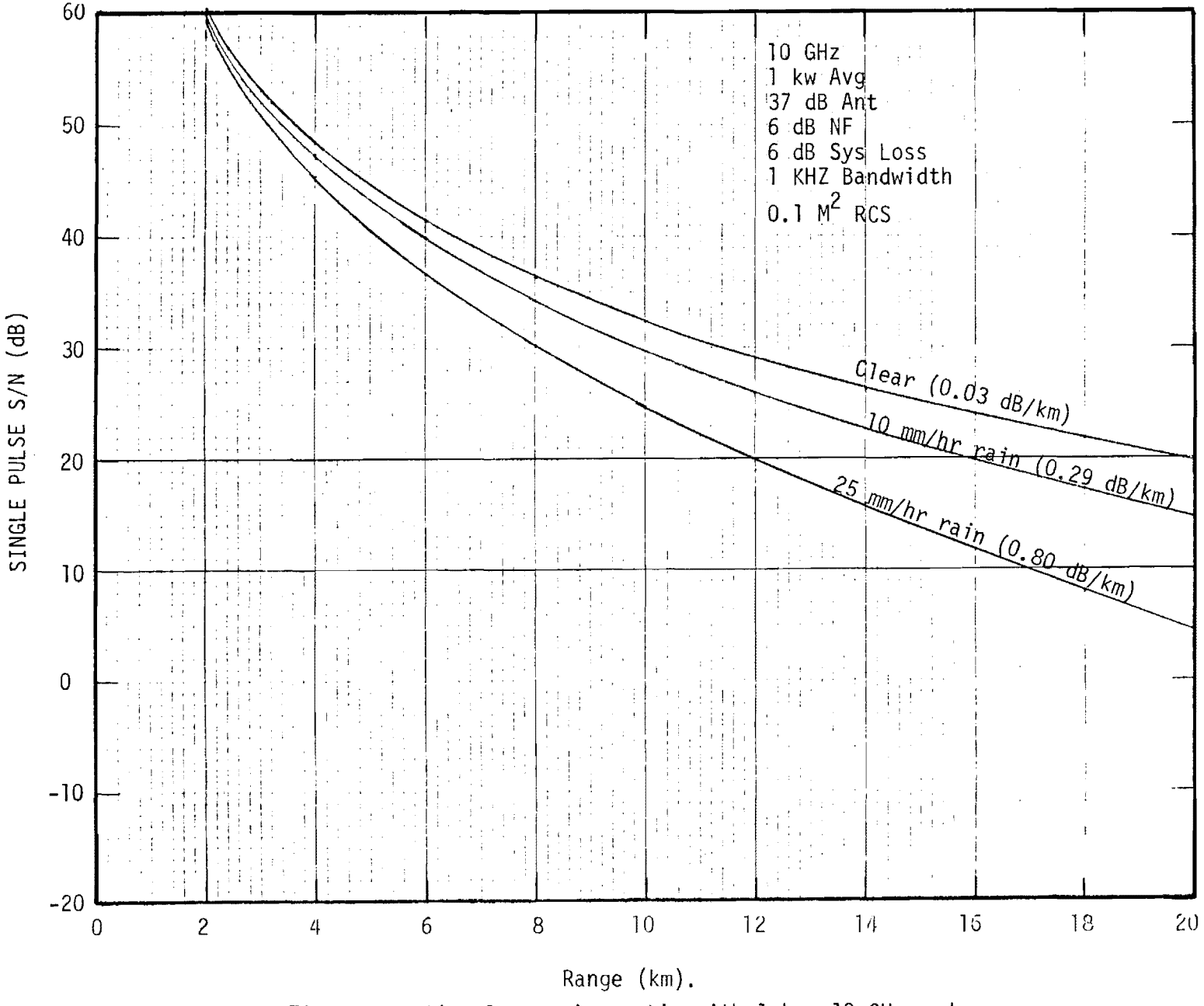

Figure 1. Signal to noise ratio with 1 kw, 10 GHz radar.

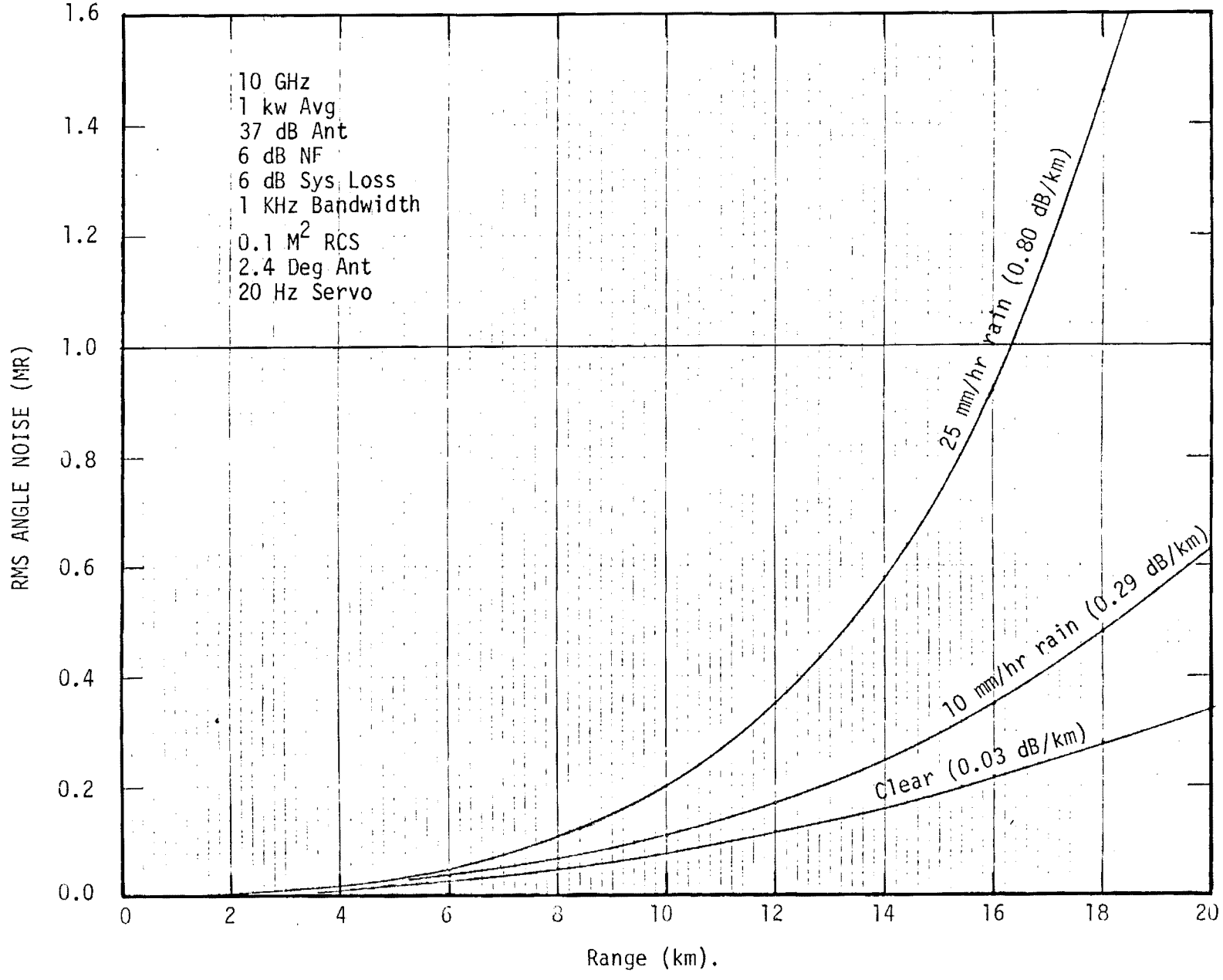

Figure 2. RMS angle error with 1 kw, 10 GHz radar.

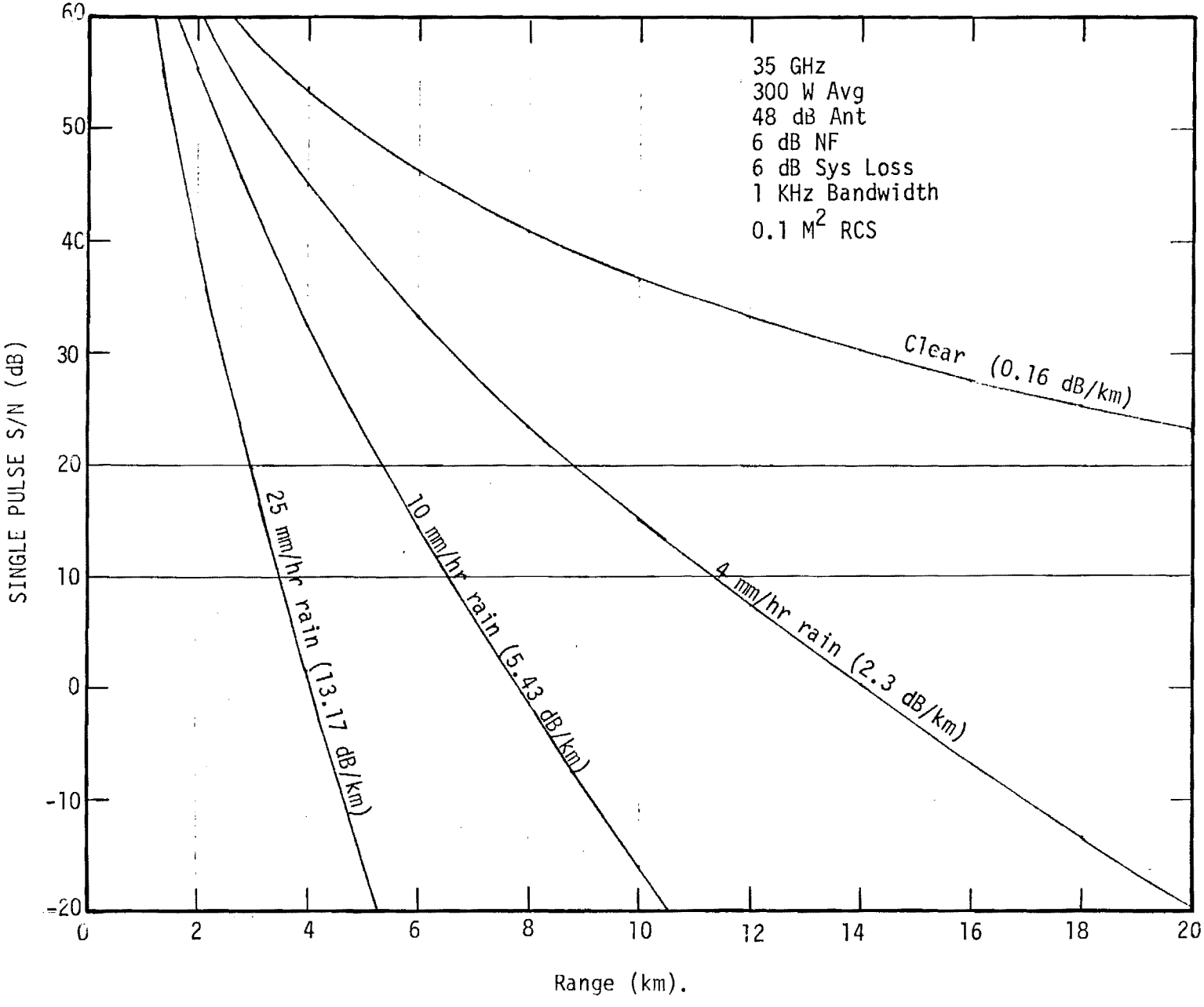

Figure 3. Signal to noise ratio with 300 W, 35 GHz radar.

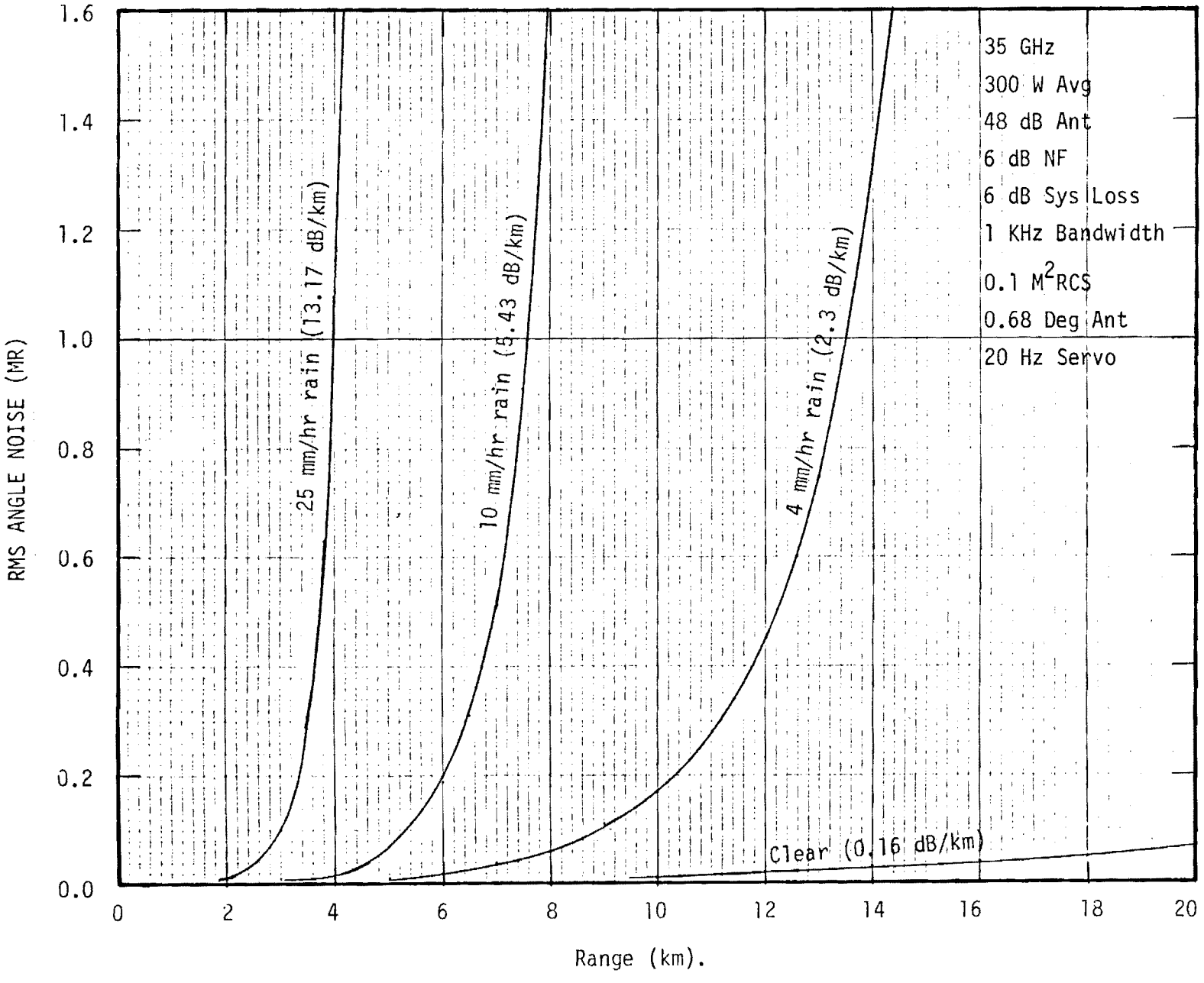

Figure 4. RMS angle error with 300 W, 35 GHz radar.

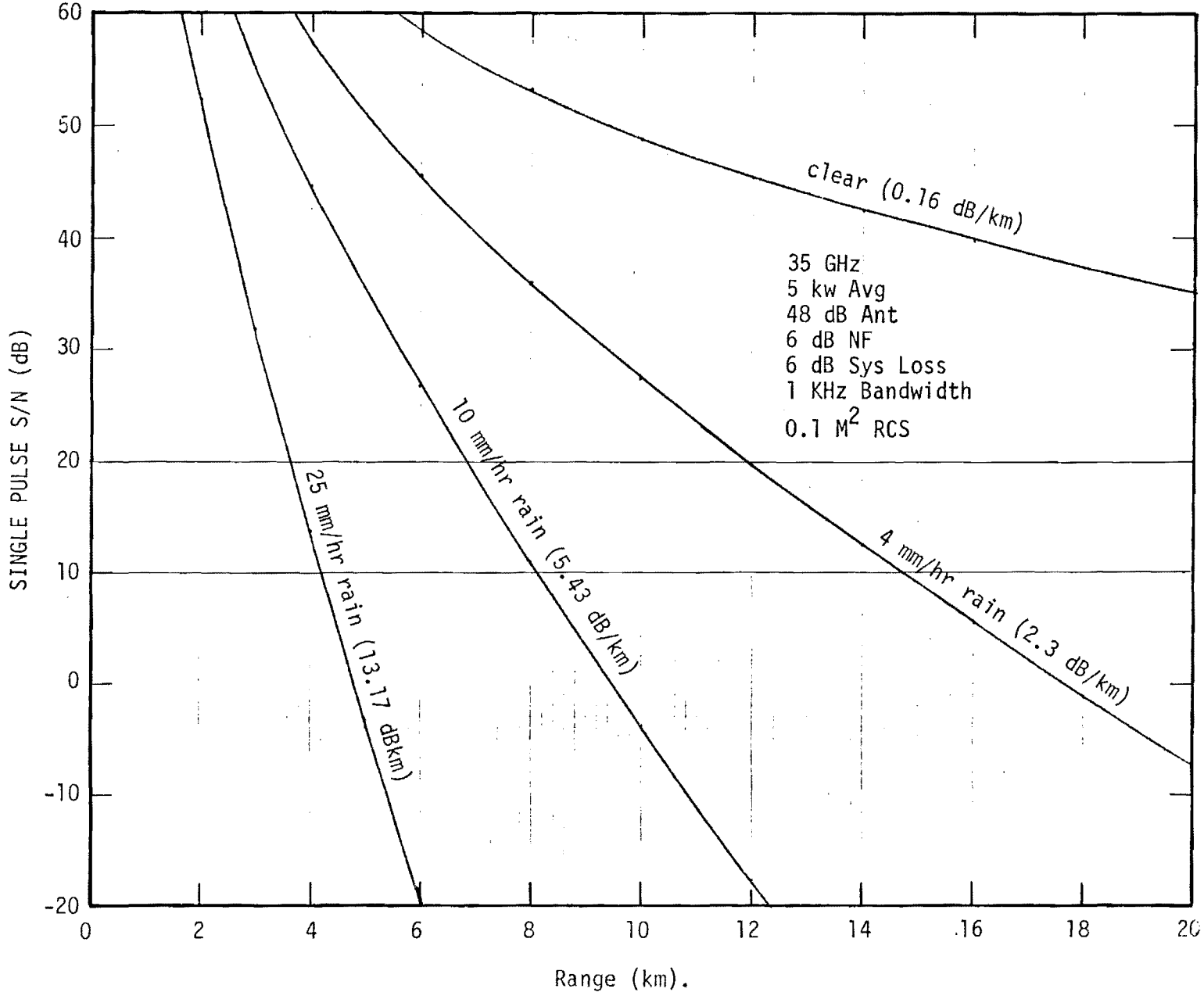

Figure 5. Signal to noise ratio with 5 kw, 35 GHz radar.

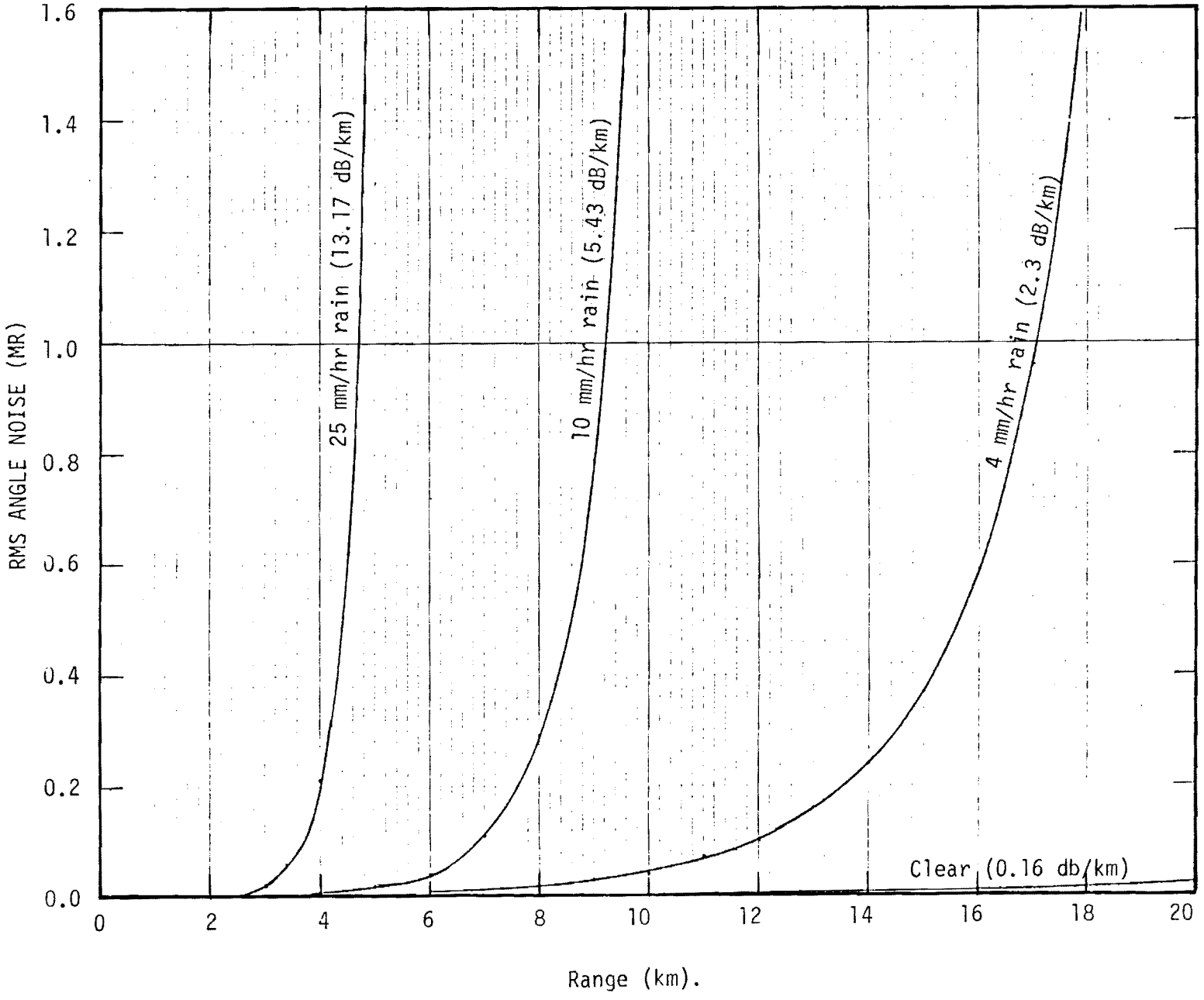

Figure 6. RMS angle error with 5 kw, 35 GHz radar.

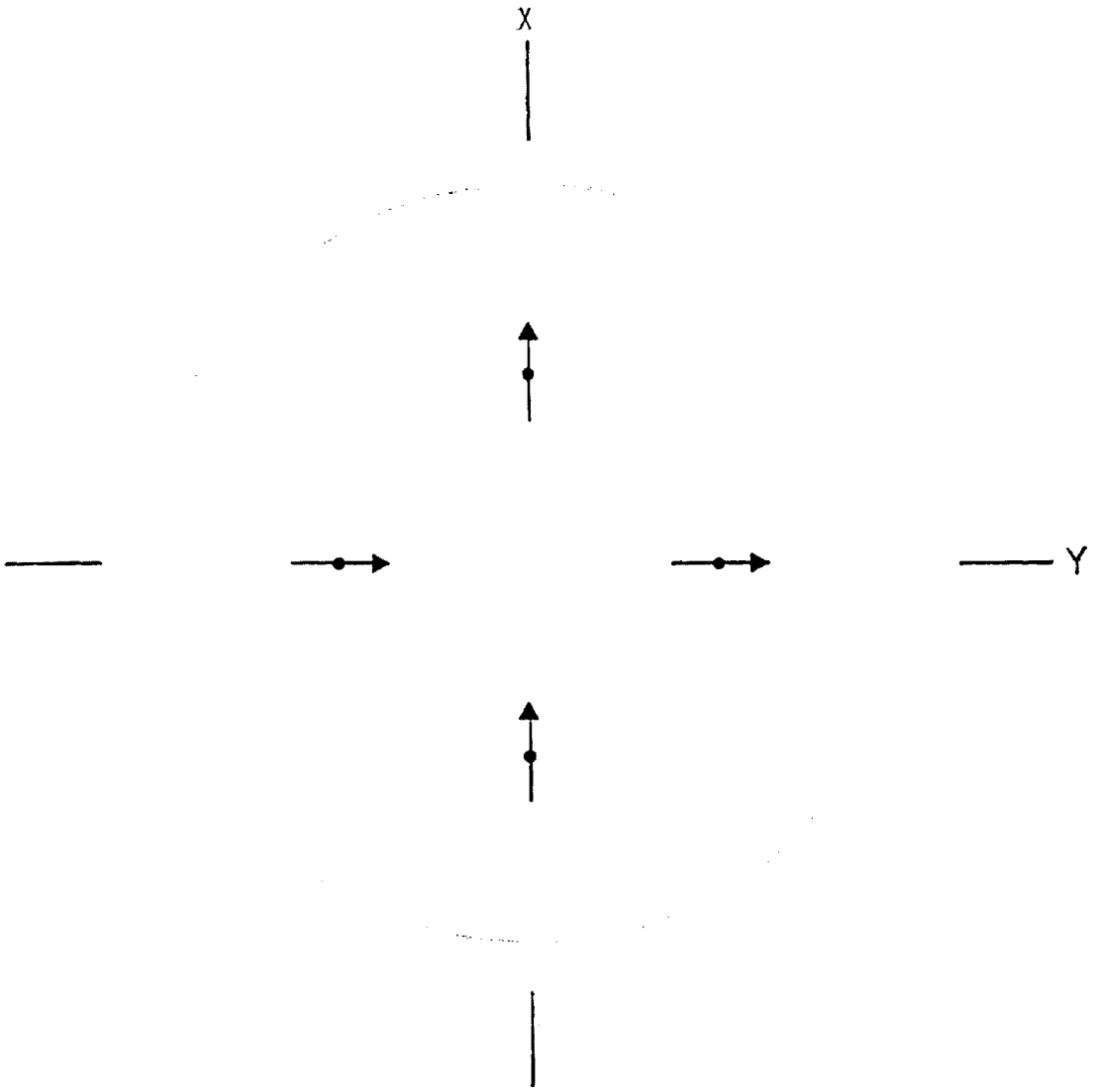

Figure 7. Projectile antennas.

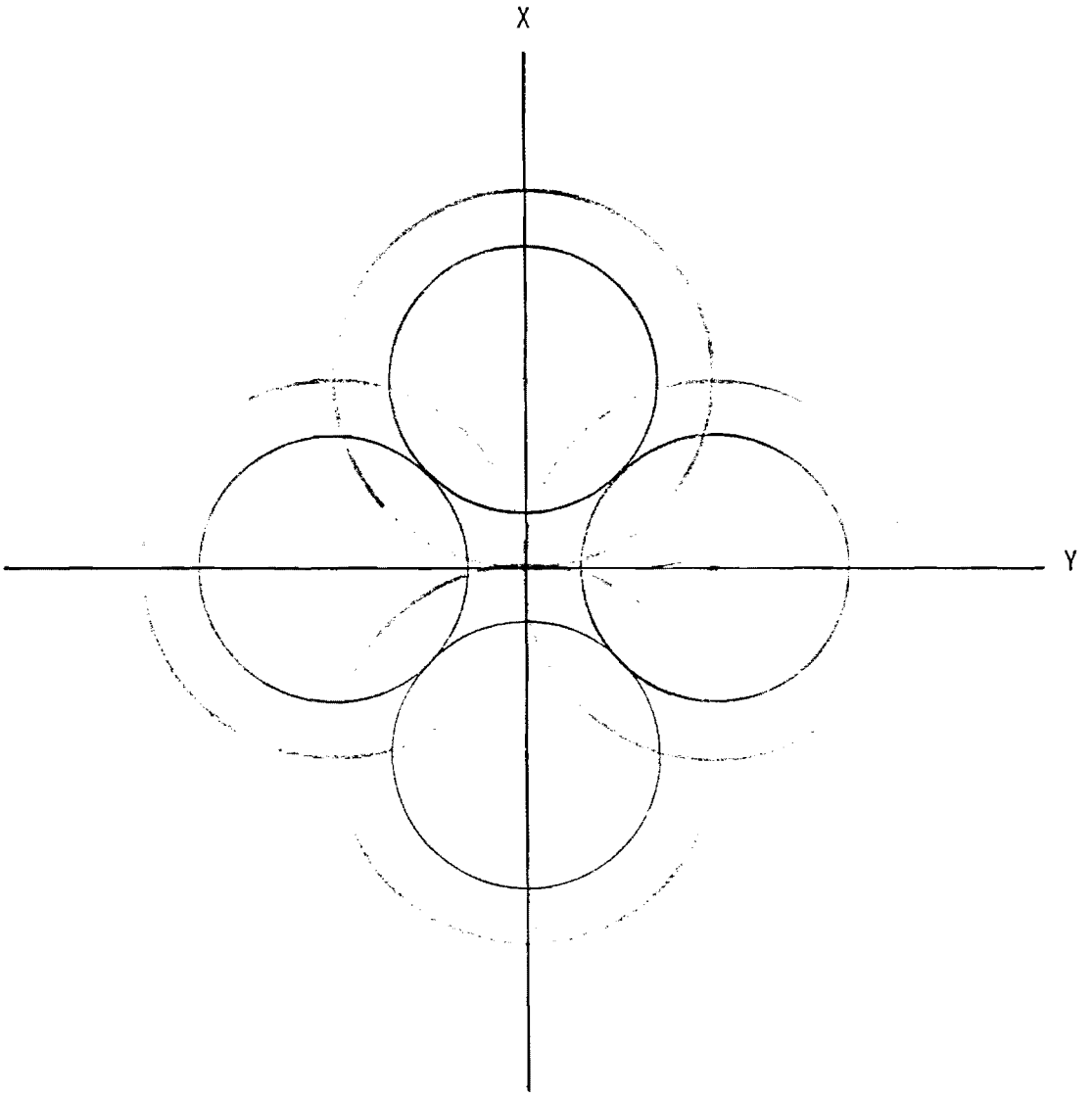

Figure 8. Con-scan beam positions.

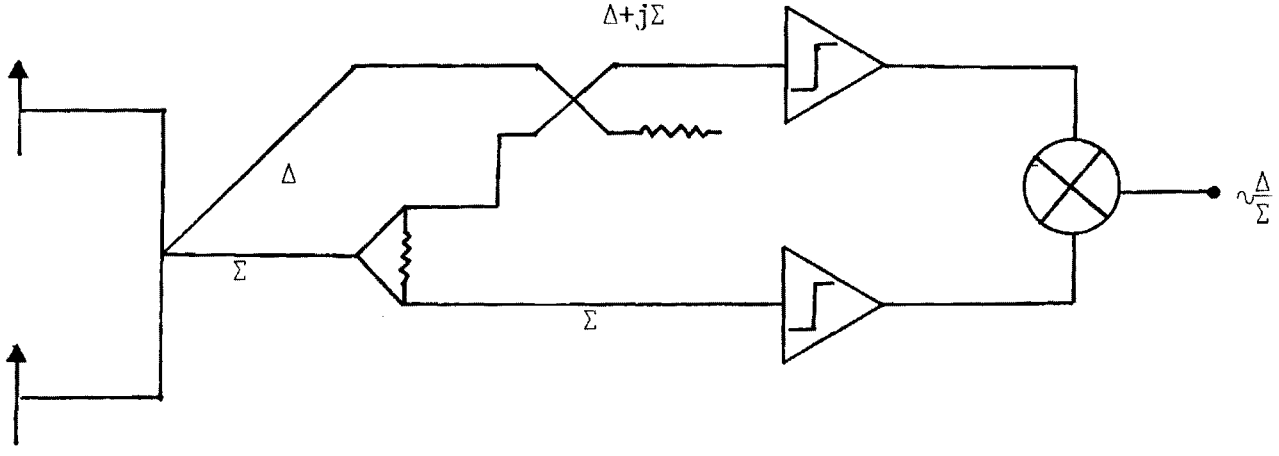

Figure 9. Normalized pattern differential circuit.

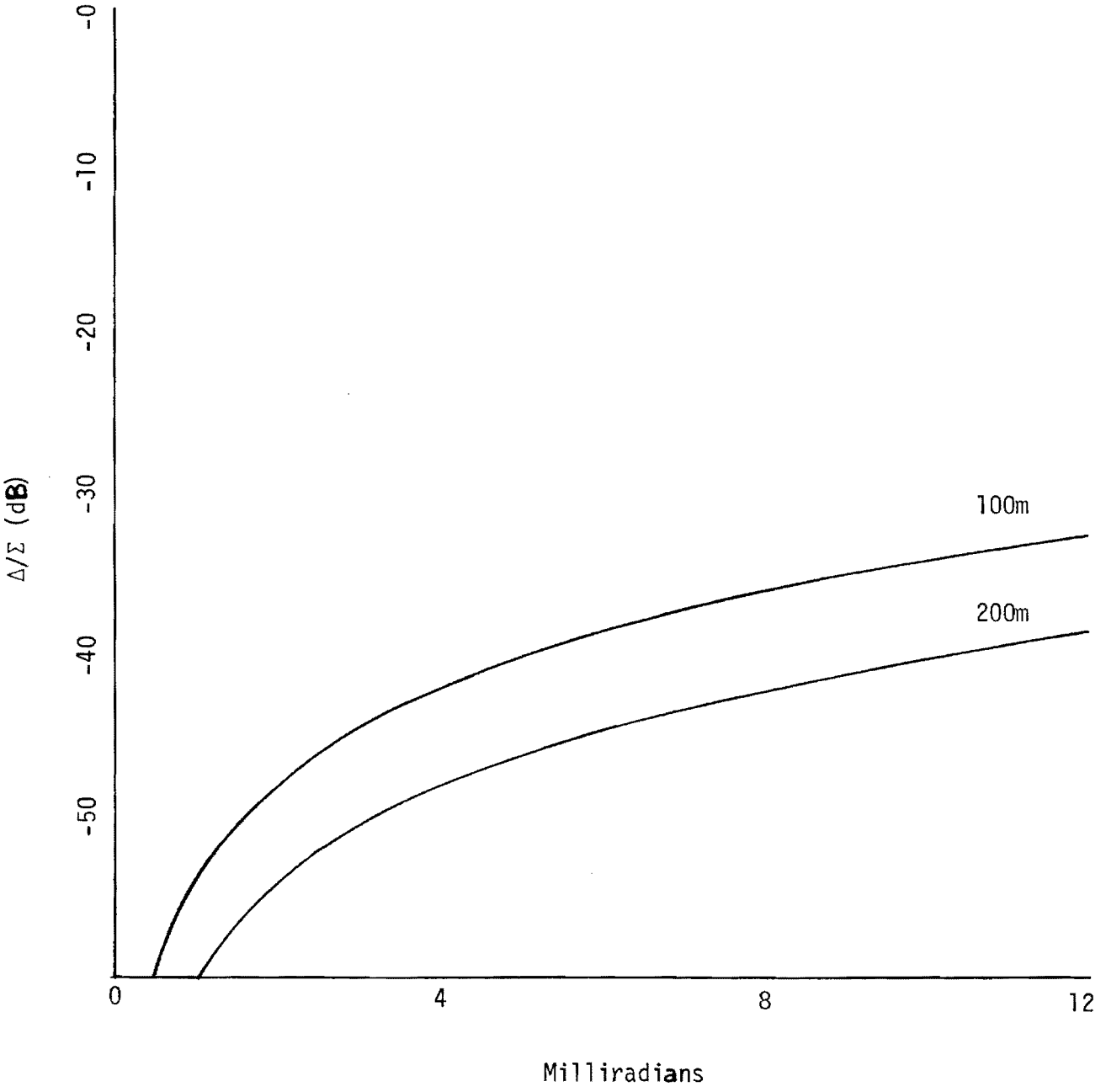

Figure 10. Normalized pattern differential.

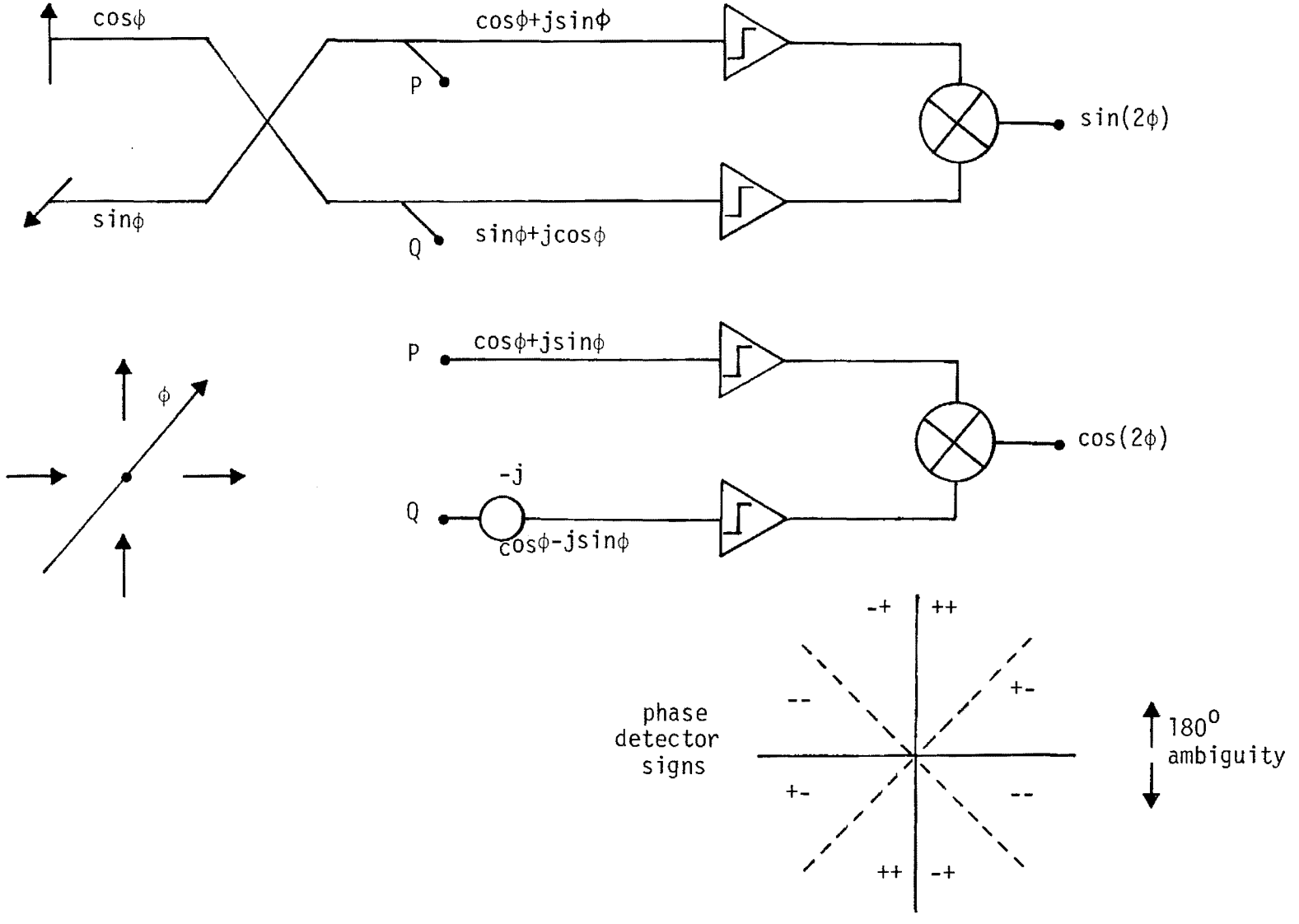

Figure 11. Roll angle circuit.

References

1. Merril I. Skolnik, "Radar Handbook," McGraw Hill, 1970.

2. David K. Barton, "Radar System Analysis," Artech House, 1976.

3. Frank R. Williams, et al., "Microwave Intervisibility System (MIS), Phase I - Concept Formulations", Georgia Institute of Technology, 1981.

Respectfully,

Robert N. Trebits
Project Director

Approved:

J. L. Eaves, Associate Director
Radar and Instrumentation Laboratory